

**STUDY ON THE TEMPERATURE EFFECT ON LAP SHEAR
ADHESIVE JOINTS IN LIGHTWEIGHT STEEL CONSTRUCTION**

A dissertation approved by
the Faculty of Architecture, Civil Engineering and Urban Planning,
Brandenburg University of Technology Cottbus-Senftenberg
to obtain the academic degree of DOCTOR-ENGINEER

by

M.Sc.-Eng. Samer Sahellie
from Damascus, Syria

Examiner: Prof. Dr.- Eng. habil. Hartmut Pasternak
Examiner: Prof. Dr.- Eng. Doncho Partov
Examiner: Prof. Markku Heinisuo

Date of the defense: April 29, 2015

„Printed with the support of the German Academic Exchange Service“
Series of Steel Construction (Stahlbau) 2015, Issue 9, ISSN 1611-5023

**STUDY ON THE TEMPERATURE EFFECT ON LAP SHEAR
ADHESIVE JOINTS IN LIGHTWEIGHT STEEL CONSTRUCTION**

Von der Fakultät für Architektur, Bauingenieurwesen und Stadtplanung
der Brandenburgischen Technischen Universität Cottbus-Senftenberg zur Erlangung
des akademischen Grades eines Doktor-Ingenieurs genehmigte Dissertation

vorgelegt von

M.Sc.-Ing. Samer Sahellie
aus Damaskus, Syrien

Gutachter: Prof. Dr.- Ing. habil. Hartmut Pasternak
Gutachter: Prof. Dr.- Ing. Doncho Partov
Gutachter: Prof. Markku Heinisuo

Tag der Disputation: 29. April 2015

„Gedruckt mit Unterstützung des Deutschen Akademischen Austauschdienstes“
Schriftenreihe Stahlbau 2015, Heft 9, ISSN 1611-5023

ACKNOWLEDGEMENT

I would like to express my deepest and sincerest gratitude to my supervisor, Professor Dr.-Eng. habil. Hartmut Pasternak. His logical way of thinking, guidance, understanding, and encouraging helped me overcome all circumstances that I confronted during the past four years. His wide knowledge has provided a good basis for the present thesis.

None of this would have been possible without the love, patience, and encouragement of my wonderful family: my wife Razan, my daughter Tala, and my son Zein Alabedien, to whom this dissertation is dedicated. They have been a constant source of love, concern, and support all these years.

My heartfelt gratitude with love goes to my father and mother, my brother and sisters. I warmly appreciate your help and encouragement throughout this endeavor.

I wish to express my warm and sincere thanks to the German Academic Exchange Service (DAAD) for their financial support. Special thank goes to Mrs. Birgit Klaes for her valuable advices and friendly help.

I am grateful to all my colleagues at the Department of Steel and Timber Structures at Brandenburg University of Technology Cottbus-Senftenberg for all kinds of support and help.

My gratitude is also to all people who have not been mentioned but helped in various ways to realizing the thesis.

Samer Sahellie

SUMMARY

In line with the developments in steel industry, the methods of joining steel members have been developed; therefore, the configuration of functional connections with economic and partly-aesthetic advantages has become possible by the use of the known joining methods, which are bolts, rivets and welding. However, these joining methods do not accompany the further developments and requirements needed to construct lightweight connections or to join dissimilar materials or composite constructions. Moreover, the traditional joining methods do not fulfill the increased requirements of the aesthetics of the joints.

In the field of steel constructions, structural engineers might use the bonding technique as an alternative method to join the lightweight steel members or as a helpful mean in the bolted or riveted joints in heavyweight steel structures.

Despite the advantages of the adhesive bonding technique, the structural designers in the field of steel constructions are still not able to use it in their practical applications because of the doubts regarding the verifiability of bonded steel joints. This is mainly because of the lack of standards for verifying such joints in steel constructions.

To facilitate using this technique in steel constructions, hard efforts have to be performed in order to find out the methods of verifications of bonded steel joints. This starts with understanding the behaviour of the adhesive materials as well as their cohesion ability to the steel surfaces over the whole lifetime of the structure and under all possible loading and environmental conditions. Afterward, the mechanical properties of the adhesives have to be presented by their reliable values that take into account all factors and conditions to which the bonded joint is subjected. These values have to be based on the reliability methods and consequently they are guaranteed for the intended lifetime of the designed structure.

It is well known that the adhesives, being viscoelastic materials, are very sensitive to several factors such as the environmental effects, mainly temperature and humidity, and the long-term loading. The loss of strength and durability of adhesives materials, due to the mentioned factors, is an essential aspect that has to be determined and to be taken into account of the structural designers during the design process.

For example, it is generally proven that the increase of temperature causes a decrease in the elastic (E) and (G) moduli, cohesive and adhesive forces within the joint and maximum stresses which can be carried by the joint. However, there is still a huge lack in describing the degradations of the mechanical properties quantitatively.

Similarly, the failure in the adhesives, loaded for long time by a constant stress even less than their short-term strengths, is probable due to the well-known rheological phenomenon of viscoelastic materials which is the creep phenomenon. Moreover, the adhesives will creep at high temperatures faster; hence the failure will happen in a shorter time. Describing the long-term behaviour of the structural adhesives is still modest; therefore, the time-to-failure of bonded steel joints under long-term loading cannot be exactly predicted. This is an essential

issue has to be dealt with to fulfill the requirements of employing the adhesive bonding technique in the structural fields including the steel constructions.

The efficiency of using adhesive-bonded joints in steel constructions is higher when the adhesives in these joints are loaded in shear. In such shear joints, the lightweight steel members (adherends) are likely to yield before the break within the adhesive layer happens, especially when large bonded areas are used because the developed shear stresses over the most of these areas will be very small.

This thesis deals with the temperature influence on the behaviour of two adhesive systems (acrylic and epoxy) and on the capacities of adhesively bonded lap shear joints. The temperature influence is quantitatively described for short-term loading over a service range of temperature from $-20\text{ }^{\circ}\text{C}$ to $+40\text{ }^{\circ}\text{C}$. The quantitative description is done by proposing the partial factors and the conversion factors that take the temperature effect into account. This influence is also dealt with for long-term loading to describe the shear creep behaviour of the adhesive materials used. Consequently, the time-to-failure of the bonded lap shear joints due to the creep phenomenon of the adhesives under three applied stresses at room temperature is predicted. Moreover, the estimation of time-to-failure is extended to be used for other shear stress levels. The temperature influence as well as the efficiency of using adhesive-bonded joints in lightweight galvanized steel constructions is also illustrated by giving a practical example of strengthening cold-formed “C” section girders. Comparisons between the two adhesive systems for all cases are given.

KEYWORDS: bonded steel joints; temperature effect; structural adhesives; short and long-term loading; shear strength.

ZUSAMMENFASSUNG

Im Einklang mit den Entwicklungen in der Stahlindustrie wurden die Methoden zum Verbinden von Stahlelementen entwickelt. Die Auslegung dieser funktionalen Verbindungen mit ihren ökonomischen und ästhetischen Vorteilen ist nur möglich geworden mit dem Einsatz des bereits vorhandenen Wissens über die Fügetechniken Schrauben, Nieten und Schweißen.

Trotzdem begleiten diese Verbindungstechniken die weiteren Entwicklungen und die nötigen Anforderungen an Verbindungen in Leichtbaukonstruktionen, an das Fügen artfremder Werkstoffe oder bei Mischbauweisen, nicht.

Im Bereich der Stahlkonstruktionen könnte die Klebtechnik, als eine alternative Methode zum Verbinden von Stahlleichtbauelementen oder als Hilfsmittel für Schraub- und Nietverbindungen im Falle von schweren Stahlkonstruktionen von Tragwerksplanern verwendet werden.

Trotz der Vorteile der Klebtechnik sind die Tragwerksplaner noch nicht in der Lage, sie in der Praxis zu nutzen. Vor allem aber aufgrund der fehlenden Normen zur Verifikation der geklebten Stahlverbindungen.

Um die Verwendung dieser Fügetechnologie im Stahlbau voranzutreiben, müssen große Bemühungen aufgewendet werden, Methoden zur Prüfung der geklebten Verbindungen zu finden. Dies beginnt mit dem Verständnis des Materialverhaltens von den Klebstoffen, sowie dessen Adhäsionsfähigkeit an Stahloberflächen über die gesamte Lebensdauer. Anschließend müssen zuverlässige Werte aller mechanischen Eigenschaften der Klebstoffe vorgelegt werden, die alle Einflüsse und Bedingungen berücksichtigen, die die Klebverbindung beanspruchen. Diese Werte müssen auf Zuverlässigkeitsmethoden beruhen und eine vorgesehene Lebensdauer der entworfenen Struktur garantieren.

Es ist bereits bekannt, dass Klebstoffe aufgrund ihrer Viskoelastizität sehr empfindlich auf verschiedene Faktoren, vor allem Temperatur und Feuchtigkeit, und die Dauerbeanspruchung reagieren. Der Verlust an Festigkeit und Gebrauchstauglichkeit des Klebstoffes aufgrund der genannten Faktoren, ist ein wesentlicher Aspekt, der festgelegt und der während des Entwurfsprozesses des Tragwerksplaners bereits berücksichtigt werden muss.

Zum Beispiel, ist im Allgemeinen nachgewiesen, dass die Erhöhung der Temperatur zur Abnahme des Elastizitäts- (E) und Schubmoduls (G) führt, sowie zur Abnahme der kohäsiven und adhäsiven Kräfte, die durch die Verbindung übertragen werden können. Es gibt immer noch eine große Wissenslücke in der allgemeinen Beschreibung der Abnahme von mechanischen Eigenschaften.

In ähnlicher Weise ist wahrscheinlich das Versagen der Klebstoffe, die unter Langzeitbelastung mit einem konstanten Spannungsniveau unterhalb der Spannungen bei Kurzzeitbelastung getestet sind durch das bereits bekannte rheologische Phänomen von viskoelastischen Materialien bedingt, nämlich das Kriechen. Ferner kriechen Klebstoffe bei

hohen Temperaturen schneller, somit tritt das Versagen in kürzerer Zeit auf. Das Langzeitverhalten von strukturellen Klebstoffen ist nach wie vor mäßig beschrieben, deshalb kann das Versagen über die Zeit von geklebten Stahlverbindungen unter Langzeitbelastung nicht exakt vorhergesagt werden. Dies ist ein wesentlicher Kernpunkt, welcher für die Anforderungen an strukturellen Klebungen, wie z.B. im Stahlbau, berücksichtigt werden muss.

Die Effizienz der Verwendung von Klebverbindungen im Stahlbau ist höher, wenn die Klebstoffe in diesen Verbindungen auf Schub beansprucht sind. In solchen auf Schub beanspruchten Verbindungen kann es früher zum Versagen der zusammenverbundenen Stahlteile (Fügeteile) als zum Versagen des Klebstoffes in der Klebfuge kommen. Vor allem, wenn große Klebflächen benutzt werden, da die auftretenden Scherspannungen über die meisten dieser Bereiche sehr klein sind.

Diese Arbeit beschäftigt sich mit dem Temperatureinfluss auf das Verhalten von zwei Klebstoffsystemen (Acrylat- und Epoxysystem) und mit der Kapazität der geklebten überlappten Klebverbindungen. Der Temperatureinfluss wird quantitativ für Kurzzeitbelastungen über einen Temperaturbereich von -20 °C bis $+40\text{ °C}$ beschrieben. Die quantitative Beschreibung wird mit Hilfe von Teilsicherheits- und Umrechnungskoeffizienten für Temperatureinflüsse durchgeführt, die den Temperatureinfluss in Betracht ziehen. Dieser Einfluss wird ebenfalls für die Dauerbeanspruchung behandelt, um das Kriechverhalten der verwendeten Klebstoffsysteme zu beschreiben. Infolgedessen wird die Zeit bis zum Versagen der überlappten Klebverbindung durch das "Kriechphänomen" des Klebstoffes, unter drei angelegten Spannungen und bei Raumtemperatur vorhergesagt. Darüber hinaus wird die Schätzung der Zeit bis zum Versagen auch für andere Scherspannungsniveaus erweitert. Der Einfluss der Temperatur sowie die Effizienz der Verwendung von Klebverbindungen auf verzinkte Stahlkonstruktionen im Stahlleichtbau wird ebenfalls mit einem praktischen Beispiel der Verstärkung von einem kaltgeformten C-Träger dargestellt. Schließlich werden Vergleiche zwischen beiden Klebstoffsystemen angegeben.

SCHLAGWORTE: Geklebte Stahlverbindungen; Temperatureffekt; Strukturelle Klebstoffe; Kurz- und Langzeitverhalten; Schubspannung.

TABLE OF CONTENTS

LIST OF FIGURES	VIII
LIST OF TABLES	XI
NOMENCLATURE.....	XIII
1 Introduction	1
1.1 Motivation	1
1.2 Structure of the thesis	2
2 Literature review	3
3 Background of adhesive bonding technology	8
3.1 Adhesive history.....	8
3.2 Polymers and adhesives classification	8
3.3 General types of structural adhesives.....	9
3.4 Selection of a proper adhesive for a particular application	10
3.5 Structural adhesives in engineering and industry.....	10
3.5.1 Structural adhesives in transportation	11
3.5.2 Structural adhesives in steel constructions.....	12
3.6 Advantages and disadvantages of adhesively bonded structural joints.....	12
3.7 Loading modes in adhesive-bonded joints	14
3.8 Failure modes of adhesive-bonded joints.....	15
3.9 Production of bonded joints	16
3.9.1 Processes serving the development of the adhesive forces (adhesion strength).....	17
3.9.1.1 Surface treatment.....	17
3.9.1.2 Adhesive application	19
3.9.2 Processes defining the cohesive strength of the adhesive layer	20
3.10 Factors affect the adhesive joint strength	21
3.10.1 Geometry-dependent factors	21
3.10.1.1 The influence of the adhesive thickness.....	21
3.10.1.2 The influence of the adherends thicknesses	22
3.10.1.3 The influence of the overlap length.....	23
3.10.2 Factors related with the process for preparing and producing the joint	24
3.10.2.1 The influence of the surface preparation.....	24
3.10.2.2 Elimination of the voids within the adhesive layer	25
3.10.3 The influence of the environmental conditions.....	25
3.10.4 The influence of the nature of the joint loading	26

4	Temperature effect on the adhesively bonded lap shear steel joints: Partial factors and conversion factors of the shear strength	28
4.1	Introduction	28
4.2	Materials description	29
4.2.1	Galvanized steel	29
4.2.1.1	Specimens preparation and test procedure	29
4.2.1.2	Mechanical properties	30
4.2.2	Structural adhesives.....	30
4.3	Double lap shear joints tests.....	32
4.3.1	Studied joints.....	33
4.3.2	Surface preparation	33
4.3.3	Bonding, conditioning and testing the joints.....	34
4.3.4	Shear behaviour and shear mechanical properties of the adhesives.....	35
4.3.5	Verification of the shear strength results.....	39
4.4	Reliability-based evaluation	40
4.4.1	General principles on reliability for structures.....	40
4.4.2	Probability distribution functions.....	41
4.4.3	Goodness of fit (GoF)	42
4.4.4	Checking of outliers	42
4.5	Direct evaluation of the maximum shear strength values	43
4.5.1	Determination of the partial factor	47
4.5.2	Determination of the conversion factor.....	48
4.6	Evaluation of the maximum shear strength values on the basis of an analysis model	48
4.6.1	Determination of the partial factor	51
4.6.2	Determination of the conversion factor.....	52
4.7	Conclusions	52
5	Shear creep behaviour of the adhesives used in the lap shear bonded steel joints.....	55
5.1	Introduction	55
5.2	Viscoelasticity of materials	56
5.3	Long-term behaviour of the bonded joints.....	56
5.4	Modelling of the creep behaviour of the adhesive	58
5.5	Creep tests of adhesively bonded joints	61
5.5.1	Studied joints.....	61
5.5.2	Test procedure at the room temperature.....	62
5.5.2.1	Observations and discussions.....	65

5.5.2.2	Creep results of adhesive-bonded joints.....	65
5.5.2.3	The lifetime expectancy of the bonded joints	69
5.5.3	Test procedure at 40 °C and 0 °C.....	75
5.5.4	Conclusions	79
6	A practical application of adhesively bonded joints (Strengthening cold-formed thin-gauged galvanized steel girders)	82
6.1	Introduction	82
6.2	Studied girders.....	83
6.3	Test set-up	85
6.4	Test results and observations.....	85
6.5	Stress distribution within the adhesive layers	88
6.5.1	FEM-models (at the room temperature).....	88
6.5.1.1	Models building.....	88
6.5.1.2	Materials description	91
6.5.1.3	Models validation	92
6.5.2	Investigations on the temperature effect	92
6.5.3	Observations and results of the numerical investigations	96
6.6	Conclusions	100
7	General conclusions.....	102
8	Future works.....	105
9	References	106
10	Appendices	111
10.1	Appendix A	111
10.2	Appendix B	113
10.2.1	Failure modes designations	113
10.2.2	Mean values and standard deviations of the mechanical properties of the acrylic and epoxy adhesives	115
10.2.3	Critical values ($D_{Critical}$) for discordance test.....	118
10.2.4	Critical values of Dixon's $r_{1,0}$	119
10.3	Appendix C	120
10.3.1	Chosen buckling modes obtained from buckling analysis of girders strengthened at the top flange AC-U and EP-U	120
10.3.2	Chosen buckling modes obtained from buckling analysis of girders strengthened at the bottom flange AC-B and EP-B	121
10.3.3	Chosen buckling modes obtained from buckling analysis of girders strengthened at the top and bottom flanges AC-U-B and EP-U-B	122

LIST OF FIGURES

Figure 3.1:	Temperature dependence of the polymer state of thermoplastic and thermosets (diagrammatic).....	9
Figure 3.2:	Structures with lightweight honeycomb sheets used in aircraft manufacture..	11
Figure 3.3:	Application of the adhesive technology in trains and care manufacture.....	12
Figure 3.4:	Adhesively bonded and bolted joints in the steel bridge in Marl-Hüls.....	13
Figure 3.5:	New bonded constructions of the bridge deck.	13
Figure 3.6:	Stress distribution in welded, bolted or riveted and adhesive-bonded joints ...	13
Figure 3.7:	Types of adhesive-bonded joints.....	14
Figure 3.8:	Connecting forces in an adhesive-bonded joint.	16
Figure 3.9:	Failure modes in bonded joints	16
Figure 3.10:	Treatments of the surfaces.....	17
Figure 3.11:	Wetting on poor degreased and perfect degreased surfaces.....	17
Figure 3.12:	Mixing process of the adhesive components.....	19
Figure 3.13:	Hand applicator to push two-components adhesive into the mixing nozzle.	20
Figure 3.14:	Methods of the adhesive application.....	20
Figure 3.15:	Curing temperature vs. curing time, schematic curve.....	21
Figure 3.16:	Stresses due to shear by tension loading in a single lap joint.	22
Figure 3.17:	The dependence of the shear strength on the adhesive thickness	22
Figure 3.18:	The influence of the adhesive thickness on the shear strength of single lap joints.....	23
Figure 3.19:	The influence of the adherend's thickness for two overlaps.....	23
Figure 3.20:	Comparison between the effects of the overlap length for both epoxy and acrylic.	24
Figure 3.21:	Average response for the interaction between the adherend yield strength and the overlap	24
Figure 3.22:	Influence of parameters studied by Hart-Smith on the shear strength of double lap joints	25
Figure 3.23:	Schematic temperature impact on the elastic modulus E , the strength σ_B and the fracture strain ε_B of an adhesive.....	26
Figure 3.24:	Environmental effects on the shear strength of paste adhesives.	27
Figure 3.25:	Environmental effects on the shear modulus of paste adhesives.	27
Figure 4.1:	Tensile specimen DIN 50125- H 20 × 80	29
Figure 4.2:	A tested specimen instrumented with a strain gage extensometer.....	30

Figure 4.3:	Engineering and true tensile stress-strain curves of the steel grade D × 51D + Z (275)- 2 mm thick	31
Figure 4.4:	Engineering and true tensile stress-strain curves of the steel grade D × 51D + Z (275)- 1 mm thick	31
Figure 4.5:	Double lap shear joints	33
Figure 4.6:	Test equipments.....	35
Figure 4.7:	Test set-up and the used extensometer	35
Figure 4.8:	Averaged shear stress-strain curves of the adhesives at the studied temperatures	36
Figure 4.9:	Failure modes	36
Figure 4.10:	Shear modulus G of the adhesives and its tendency	37
Figure 4.11:	Comparison of the rigidity of the materials over the temperature range	38
Figure 4.12:	Mean values of (τ_{max}) and $(\gamma_{at\ max})$ with their tendency.....	38
Figure 4.13:	Mean values of $(\tau_{at\ Break})$ and $(\gamma_{at\ Break})$	39
Figure 4.14:	Shear strength vs. temperature for AC-0.35(M) and AC-0.65(M).....	49
Figure 4.15:	Shear strength vs. temperature for EP-0.35(M) and EP-0.65(M)	49
Figure 4.16:	Comparison of test values with models values	50
Figure 5.1:	Combinations of mechanical analogues for creep behaviour.....	59
Figure 5.2:	Mechanical models for the creep of polymers	60
Figure 5.3:	Double lap shear joint designed for the creep test	61
Figure 5.4:	The efficiency of using the tapes during the tests	62
Figure 5.5:	Creep machine.....	63
Figure 5.6:	Tension sensor used to calibrate the applied loads	63
Figure 5.7:	Long-term shear strain measurement	64
Figure 5.8:	Three creep stages	64
Figure 5.9:	Shear creep strains of AC-0.35 at 20 °C.....	67
Figure 5.10:	Shear creep strains of AC-0.65 at 20 °C.....	67
Figure 5.11:	Shear creep strains of EP-0.35 at 20 °C	68
Figure 5.12:	Shear creep strains of EP-0.65 at 20 °C	68
Figure 5.13:	Determination of the steady-state creep rate at 20 °C	73
Figure 5.14:	Normalized shear stress vs. $\ln(t_f)$	74
Figure 5.15:	The creep machine and the calibration of the weights inside the climate chamber	75
Figure 5.16:	Shear creep strains of AC-0.65 and EP-0.65 at 40 °C	77
Figure 5.17:	Fitted Findley's and Burger's models for shear creep strains at 40 °C.....	79

Figure 6.1:	Geometries and types of the girders	84
Figure 6.2:	Strengthened girders manufacturing	84
Figure 6.3:	Test set-up	86
Figure 6.4:	Deformation of the non-strengthened girder	86
Figure 6.5:	Deformations of AC-U and EP-U	87
Figure 6.6:	Deformations of AC-B and EP-B.....	88
Figure 6.7:	Deformations of AC-U-B and EP-U-B	89
Figure 6.8:	The mesh and the boundary conditions used in the models.....	90
Figure 6.9:	The rigid body under the angle and the contacting surfaces definitions.....	90
Figure 6.10:	Quantitative comparisons between test results and FEM results	94
Figure 6.11:	Qualitative validation of the models	95
Figure 6.12:	Von Mises stress distributions over the adhesive layers in AC-bonded girders.....	97
Figure 6.13:	Von Mises stress distributions over the adhesive layers in EP-bonded girders.....	98
Figure 6.14:	Absolute stress values in [MPa] for AC-bonded girders.....	99
Figure 6.15:	Absolute stress values in [MPa] for EP-bonded girders	99
Figure 10.1:	Failure modes of (RTD) specimens	111
Figure 10.2:	Failure modes of (ETD) specimens.....	111
Figure 10.3:	Failure modes of (ETW) specimens.....	112
Figure 10.4:	Designations of the failure patterns acc. to EN ISO 10365:1995	113
Figure 10.5:	Examples of (a) the mixed failure and (b) the oscillating rupture acc. to EN ISO 10365:1995	114
Figure 10.6:	Sketches representing the failure modes acc. to ASTM 5573-99	114
Figure 10.7:	Buckling modes used for AC-U and EP-U girders	120
Figure 10.8:	Buckling mode used for AC-B and EP-B girders	121
Figure 10.9:	Buckling modes used for AC-U-B and EP-U-B girders	122

LIST OF TABLES

Table 3.1:	Most common classifications of the adhesives	9
Table 4.1:	Typical uncured physical properties of the used adhesives as reported by 3M Scotch-Weld™.....	32
Table 4.2:	Comparison of the shear strength results	40
Table 4.3:	Statistical and critical values of Z-test and discordance test.....	43
Table 4.4:	Statistical and critical values of Dixon’s test for a sample size of $3 \leq n \leq 7$..	43
Table 4.5:	Coefficients of the Student distribution	44
Table 4.6:	Statistical calculations of the data set of AC-0.35	45
Table 4.7:	Statistical calculations of the data set of AC-0.65	45
Table 4.8:	Statistical calculations of the data set of EP-0.35	46
Table 4.9:	Statistical calculations of the data set of EP-0.65	46
Table 4.10 :	Characteristic and design values R_k, R_d at each temperature for AC-0.35 and AC-0.65	47
Table 4.11:	Characteristic and design values R_k, R_d at each temperature for EP-0.35 and EP-0.65	47
Table 4.12:	Partial factors of the shear strength of the studied adhesives.....	48
Table 4.13:	Values of the conversion factor (η)	48
Table 4.14:	Statistical calculations of the data sets of K_i	51
Table 4.15:	Characteristic and design values of K_i	51
Table 4.16:	Characteristic and design values R_k, R_d at each temperature for AC-0.35, AC-0.65, EP-0.35, and EP-0.65	52
Table 4.17:	Partial factors of the shear strength by calibrating the proposed models.....	52
Table 4.18:	Values of the conversion factor η	52
Table 5.1:	Experimental setup of the shear creep tests	64
Table 5.2:	Burger’s model parameters of the shear creep strains.....	66
Table 5.3:	Findley’s model parameters of the shear creep strains	66
Table 5.4:	Parameters of the steady-state creep rate approach.....	70
Table 5.5:	Short-term mechanical properties and predicted time-to-failure	71
Table 5.6:	Relative errors of the time-to-failure comparing with the steady-state creep rate approach	71
Table 5.7:	Parameters of the normalized shear stress- $\ln(t_f)$ correlation.....	72
Table 5.8:	Normalized shear stress for 1, 5, 10, and 25 years.....	72

LIST OF TABLES

Table 5.9:	Applied shear stresses in tests at 40 °C and 0 °C.....	76
Table 5.10:	Shear strains recorded at the end of the test for 40 °C.....	77
Table 5.11:	Degradation of the shear strength of the studied adhesives	77
Table 5.12:	Findley’s model parameters for the shear creep strains at 40 °C.....	78
Table 5.13:	Burger’s model parameters for the shear creep strains at 40 °C	78
Table 6.1:	Combinations of the chosen modes obtained from the buckling analysis	91
Table 6.2:	Material properties of the adhesives used in Abaqus.....	92
Table 6.3:	Material properties of the adhesives used in Abaqus for -20 °C and +40 °C ..	95

NOMENCLATURE

E	Elasticity modulus
G	Shear modulus
ν	Poisson's ratio
E^*	Apparent elasticity modulus
T	Temperature
T_g	Glass transition temperature
σ_t	True stress
ε_t	True strain
σ	Engineering stress
ε	Engineering strain
AC	Cold-cure toughened acrylic adhesive
EP	Cold-cure epoxy adhesive
σ_y	Yield strength of the steel
σ_u	Ultimate strength of the steel
$\sigma_{u,t}$	True ultimate strength of the steel
CF	Cohesive failure
SCF	Special cohesive failure
τ_{max}	Maximum shear strength
$\tau_{at\ Break}$	Shear stress at break
$\gamma_{at\ \tau_{max}}$	Shear strain corresponding to τ_{max}
$\gamma_{at\ Break}$	Shear strain corresponding to $\tau_{at\ Break}$
Z	The limit state
R	the resistance
E	the action effect
E_d, E_k	Design and characteristic values of the action effect
R_d, R_k	Design and characteristic values of the resistance
γ_E	Partial factors of the action effect
γ_R	Partial factors of the resistance
η	Conversion factor

$P(.)$	Probability of (.)
Φ	Standard normal distribution function
α_E, α_R	Sensitivity factors of the first order reliability method (FORM)
β	Target reliability index
$f_X(x)$	Density of the random variable x
$F_X(x)$	Cumulative probability function of x
μ, σ	Mean and standard deviation
n	Sample size
z	Standardized value of x
AD	Anderson-Darling value
AD^*	Critical Anderson-Darling value
$r_{i,j}$	Statistical value of Dixon's test
$t_{v,k}$ and $t_{v,d}$	Coefficients of the Student distribution
ν	Degree of freedom
COV	Coefficient of variation
K_i	Multiplication factor
$\varepsilon(t)$	Creep strain at the time t
ε_0	Instantaneous strain
$E_{t(0)}$	Initial Young's modulus
E_M, E_K	Elasticity of the spring of Maxwell and Kelvin elements
η_M, η_K	Viscosity of the dashpot of Maxwell and Kelvin elements
$\gamma(t)$	Shear creep strain at the time t
$\gamma(0)$	Instantaneous shear strain
G_M, G_K	Elasticity of the spring of Maxwell and Kelvin elements in shear
λ_M, λ_K	the viscosity of the dashpot of Maxwell and Kelvin elements in shear
R^2	Coefficient of determination
γ_s	Shear strain of the adhesive at the steady-state stage
γ^*	Creep rate
τ_{app}	Applied shear stress
t_f	Time-to-failure
σ_y	Yield strength of the adhesive in tension

NOMENCLATURE

τ_y	Yield strength of the adhesive in shear
F	External load applied to the girder
u	Deflection of the girder

1 Introduction

1.1 Motivation

The motivation of this research is that in lightweight steel constructions, traditional joining methods are associated with essential problems such as the stress concentration at the edges of the holes (in riveted and bolted joints) and the disability of thin steel members to resist the thermal effects due to welding process. The increasing application of the adhesives as joining techniques in the industrial world aroused the interest of engineers to use bonding technique in their structural applications. This is mainly due to their advantages and applicability to join dissimilar materials in several fields.

In lightweight steel constructions, using bonding technique with the improved material properties of the available structural adhesives may become an alternative method to be applied in not only joining but also strengthening such constructions.

However, despite the advantages of the adhesive bonding technique, the structural designers, in the field of steel constructions are still not able to use it in their practical applications because of the doubts regarding the verifiability of bonded steel joints. This is mainly because of the lack of standards for verifying such joints in steel constructions and also because of the lack of describing the loss of strength and durability of adhesive materials due to the environmental effects, mainly temperature and humidity, and the long-term loading.

The contribution presented by this thesis mainly aims to investigate the temperature influence on the lap shear adhesively bonded joints used basically to strengthen lightweight galvanized steel constructions. The temperature influence will be investigated by:

1. Giving a general overview of the change in the behaviour and the mechanical properties of two different kinds of the structural adhesives, loaded in shear, due to the change of temperature (from $-20\text{ }^{\circ}\text{C}$ to $40\text{ }^{\circ}\text{C}$). A quantitative description of the strength of the adhesives will also be given.
2. Determining the partial factors and conversion factors based on the specifications of EN 1990:2002 and ISO 2394:1998 to express the temperature effect on the short-term strength of the adhesives.
3. Describing the long-term behaviour of the adhesives (the creep behaviour) at particular temperatures using two creep models.
4. Predicting the lifetime (time-to-failure) of the bonded joints due to the creep phenomenon.
5. Estimating the applied shear stress limits for particular lifetimes of the bonded joints subjected to the shear creep.
6. Showing the efficiency of the bonded joints in strengthening lightweight galvanized steel girders and presenting the temperature effect on these joints.

1.2 Structure of the thesis

The thesis is structured presenting in the next chapter, chapter 2, a literature review of the recent researches conducted about the adhesive bonding technology and its applications in many fields, especially in the structural field.

The third chapter gives a general background of adhesive bonding technology, classifications of adhesives, advantages and disadvantages of bonding systems, factors affect the capacities of bonded joints and procedures of producing a bonded joint.

The investigations, presented in the fourth chapter, focus on describing the change in the behaviour of two different structural adhesive systems widely used for assembling metals (acrylic and epoxy) due to the temperature change within a service range of temperature valid for internal uses (-20 °C to +40 °C).

The representative values for the shear strengths of the adhesive materials are found based on reliability methods according to EN EN 1990:2002 and to ISO 2394:1998 specifications as well as to the systematic approach developed by Van Straalen in his PhD thesis. Consequently, the partial factors for these materials and the conversion factors that take the temperature effect into account are proposed.

The fifth chapter is assigned for the long-term loading experiments to describe the creep behaviour of the adhesives loaded in shear. Well-known rheological models (Burger's and Findley's models) together with the steady-state creep rate approach are used for predicting the time-to-failure of the bonded joints loaded by different shear stresses. The applied shear stress limits for particular lifetimes of the bonded joints is estimated. Long-term tests are also done at 0 °C and 40 °C.

A practical example of applying the adhesive bonding technology in lightweight galvanized steel constructions is given in the sixth chapter in which strengthening the flanges of cold-formed "C" section girders by externally bonded galvanized steel plates is presented. Investigations on the strengthened girders are experimentally done at room temperature. The temperature effect is numerically investigated using the finite element method (ABAQUS software) at the minimum and maximum temperatures (-20 °C and +40 °C) of the service range considered as well as at room temperature. The stress distributions over the bondlines are shown and the efficiency of using adhesive bonding technology in joints loaded mainly in shear is illustrated.

The main conclusions from the results obtained in the previous three chapters are summarized in chapter 7.

Chapter 8 gives some recommendations for the future research activities and works.

2 Literature review

Lap shear adhesive-bonded joints have been and are still the interest of bonding technologists and researchers. Intensive analytical, experimental, and numerical investigations have been carried out over the past decades in order to develop methods and solutions regarding the behaviour of such joints as well as material properties of the used adhesives.

The first analytical method for the stress analysis of bonded joints known in literature was proposed by Volkersen (1938). Volkersen's method, "shear-lag model", was based on the assumption of one-dimensional bar-like adherends with only shear deformation in the adhesive layer, the bending effect due to the eccentric load path is not considered. The consideration of the effects due to the rotation of the adherends has been taken into account by Goland & Reissner (1944). They assumed that the joint is consisting of tow beams bonded with an elastic adhesive layer. The Goland & Reissner model was later, in 1973, extended by Hart-Smith to consider the plasticity of the adhesive layer. Elastic-plastic behaviour of the adhesive was assumed for the solutions of single and double lap joints [1]. All models mentioned above were improved later by Tasi *et al.* [2] who assumed linear shear stress distributions through the thickness of the adherends in the analysis. Hence, the adherends shear deformations was involved.

In 2001, Kim H. and Kedward K. [3] addressed an analysis methodology for designing joints loaded in both tension and in-plane shear. A two-dimensional solution that predicts a multi-component adhesive shear stress state was proposed for an adhesive bonded lap joint as well as for a finite-sized doubler where tension and shear loads are simultaneously applied; and hence, a combined biaxial shear stress state in the adhesive is resulted. The range of the combined loading conditions within which the joint is expected to behave elastically, the elastic limit of the joint, is predicted by using the von Mises yield criterion. The solutions proposed were validated by comparing them with numerical analyses of examples and applications to real structures.

A detailed analysis of adhesive-bonded joints used in reinforcement of steel structures was carried out by [4]. Experimental investigation of a reinforced box girder was conducted. Numerical calculations based on the experimental results were used to realize the stress state within the bonded joint. The results of numerical calculations of the reinforced girder stay in a good adequacy with the analytical ones proposed by [3].

Da Silva, L.F.M. *et al.* [5] proposed a simple predictive equation for the design of single lap joints. This predictive equation takes into account the influence of eight variables affecting the strength of single lap joints. The variables considered are the adhesive (toughness and thickness), the adherend (yield strength and thickness), the overlap, the test speed, the surface preparation and durability. It was found experimentally and statistically that the main effect is from the overlap length whereas the other variables have less influence. Negligible effects for the surface treatment, durability and test speed was also reported.

Similarly, Eskandarian M. *et al.* [6] have experimentally reported significant influence of adhesive hardness and thickness, adherend thickness and overlap length on single lap joints (SLS) made of aluminum substrates bonded by relatively brittle and ductile adhesives. The effects of plastic deformation in adherends were investigated by using double lap joints (DLS). It was also observed that the brittle adhesive performed better in short overlaps while a better performance was corresponded to the ductile adhesive at larger overlaps.

The optimum overlapping design which secure the reliability and which do not increase the joint production costs was studied by [7], who mainly investigated the influence of the length of the bonded lap joints on the joint capacity experimentally.

The mechanical properties of adhesives materials, which are of great importance, have to be determined and well described. Adhesives may behave ductilely or rigidly depending on the materials, from which the adhesive is made. It is known that the behaviour of epoxy adhesives is rigid and adhesives of polyurethane have ductile behaviour whereas acrylics can be in-between. The suitability of the adhesive with the adherends materials, for getting better adhesion and durability, is also fundamental. Theoretical details on differences among adhesives and on practical testing methods can be found in literature, for instance in ([8], [9]) whereas [10], [11], and [12] provide experimental comparison among some adhesives.

The environmental conditions that the adhesive joint is subjected to, strongly affect the mechanical behaviour of the adhesives. Tests were carried out by [13] to determine the shear stress-strain relation of polyurethane and epoxy adhesives at three different temperatures. Comparison among studied cases was explained as well as simplified diagrams were found suitable to be used for describing the shear moduli at each temperature. The effect of both heat and humidity on the shear responses of twelve structural adhesives was experimentally investigated by [14] in order to make obtained data available for use in design and modelling processes.

Similarly, in 2011, [15] studied the effect of temperature changes and adherends materials on the strength and modulus of seven adhesives commonly used in aerospace bonded structures. Dynamic Mechanical Analysis (DMA) was used to study the adhesive modulus with temperature. Comparison among the adhesive performances over a wide range of temperatures was therefore provided in order to facilitate the adhesive selection process.

A reasonable correlations between the tensile and the shear properties of three adhesives were reported by [16] in terms of stiffness and strength and poor correlations were found in terms of ductility. Changes in the performance of the studied adhesives over a wide range of temperatures were also recorded.

Geometry and temperature effects were studied on single lap joints bonded by an epoxy adhesive [17]. Results of these tests showed that applying the investigated adhesive in situations, where temperatures are higher than 40 °C, is not advisable, as the strength losses of the adhesive were over 60% at this temperature. It was also found that increasing the

overlap length could be a good way to produce more resistant joints with lower losses of strength and that the rates of the strength loss decreased after 50 °C.

Short and long-term shear tests were performed on specimens composed of galvanized steel sheets assembled by using epoxy and acrylic adhesives, [18]. Tests carried out at four temperatures (-20 °C, 0 °C, 20 °C, and 40 °C) for the short-term tests and for the long-term tests only 40 °C was used. The investigations showed that the increase of the temperature changes the mechanical behaviour from brittle to ductile and decreases both the shear modulus and shear strength. Furthermore, failure modes may change as temperature increases. In addition to that, long-term tests showed that a higher temperature can lead to failure in shorter period, even when a joint loaded by constant shear stresses much less than the short-term ultimate shear strength.

The long-term strength of bonded joints is of great importance for optimizing the design process of the joint. Experiments examined the combined effect of constant load and environmental exposure (heating and heating/humidity) on time-to-failure of adhesively bonded joints of different configurations was reported by [19]. However, the results of the creep tests were relatively doubtful as more data points were needed. In 1998, Boyes R. [20] conducted room temperature creep tests on AISI 304L stainless steel standard single lap shear joints and single lap box specimens, bonded with toughened epoxy DP 490. Shear stress levels from 20% to 80% of the short-term strength were applied to the specimens, the time to failure was recorded for each studied case. Results showed a lot of scatter and were almost inconclusive. Single lap shear joints could withstand low loads (20% to 40% of the mean static failure load) for considerable periods of time without fracture. Whereas the box type specimens did exhibit a room temperature creep endurance limit at approximately 40% of the static failure load in tensile shear.

[21] covers various aspects related to the process of maximizing the long-term strength and performance of a joint under static, cyclic and creep loading, and hostile environments.

Tests on long-term strength, also called the durability, are time consuming. However, their results can be predicted by performing shortened tests that can simulate the application of the conditions for longer time. Shortening the test period is done by subjecting the joint to elevated temperature for subsequent periods of time so that time-temperature superposition concept, [22], can be applied, more details can be found in [23].

The long-term creep is a rheological phenomenon that can be described by many rheological or mathematical models such as Maxwell model, Kelvin-Voigt model, Burger model, or Findley's model, detailed information on these models as well as other modified models are addressed in, for example [24].

Detailed information on Findley model and power-law models that are used to describe the creep behaviour of polymeric and non-polymeric composite materials are given in [25].

(Dean, G. D.; Broughton, W. R., [26]) modeled the creep behaviour of toughened adhesives and thermoplastics. It is found that the creep behaviour of the adhesives, as being viscoelastic

materials, is not only dependent on time but also on stress level. Moreover, a new model was developed for describing the creep behaviour of glassy adhesives by a generalized model for time-dependent plasticity in the finite element analysis (FEA) package ABAQUS. Hence, changes in the stress and strain distributions with time under load are able to be calculated for the adhesive layer of bonded joints.

The creep behaviour of hardened-adhesive epoxy samples was experimentally investigated at room temperature by [27]. The results obtained by experimental investigations were analyzed and mathematically treated. Thus, a modified Burger's model was developed. The developed model is for the studied adhesive with a constant modulus of elasticity and can describe the instant elastic strain, and the tensile stress-dependent variables. A very good consistency between the creep deformations calculated by the model and the results of experimental investigations was recorded.

A methodology for predicting the long-term creep behaviour of epoxy adhesives was proposed by Feng *et al.* [28] who used the time-temperature superposition method to produce the master curve by which the long-term creep compliances of the investigated adhesive can be estimated. The temperature and moisture effects were also investigated by means of mechanical responses and were found to have equivalent effect on the mechanical responses.

Both Burger's model and the adapted Burger's model proposed by Feng *et al.* were used by Costa *et al.* [29], [30] to describe the tensile creep behaviour of structural adhesives, being used in flexural strengthening technique with CFRP laminates, a high accuracy was reported. It is also found that the parameters of the models strongly depend on the applied stress level.

Structural reliability methods were implemented in a systematic approach to develop design rules for adhesive-bonded joints. The approach is given in [31]. To illustrate the potential of this approach, examples of design rules for overlap joints were worked out. The introduction of the conversion factor additional to the partial factor to incorporate the effect of the resistance degradation of the aged joints was found to be a practical method. Probabilistic techniques were used to calibrate the values of partial factor and conversion factor, more details and other examples of using this systematic approach are also provided in [32].

The technique of providing additional steel reinforcement for concrete structures by externally bonded plates dates back to the 1960's, [33]. Recently, reinforcing steel structures by bonding additional steel plates were investigated by (Pasternak and Mainz, [34]). The test results on frames with knee joints, which had been reinforced by adhesive bonded plates, showed that reinforcement applications using the technique of adhesive bonding brought a significant increase of knee joint's stiffness. Same conclusion was derived by the tests performed on cold-formed light gauge members, which had been strengthened by adhesive bonded plates to avoid stability problems. In [4], a box girder strengthened by bonding additional steel plates on its slender web was investigated. An increase in the local buckling load and carrying capacity in comparison with non-reinforced girder amounted 340% and 60% respectively was reported.

The effect of reinforcement of additional bonded metallic sheets on a cold-formed light gauge member, a lipped channel section (“C” section) under bending stress, was examined by [35]. An increase of the ultimate load of approximately 22% was achieved by hindering the local buckling of the upper chord. Interestingly, the failure of the bondline due to the stress during the test was not to be noticed.

Additional information and other applications in strengthening and/or connecting steel members by adhesively bonding technique can be found in ([33], [36], [37], and [38]).

3 Background of adhesive bonding technology

3.1 Adhesive history

Adhesives are defined as the materials that are capable of joining two or more other materials and are generally categorized as natural or synthetic.

The oldest known adhesive is dated to 4000 B.C. When archaeologists found broken pottery vessels, buried with the deceased. These vessels had been repaired with sticky resins from tree sap.

Many art objects and furnishings from the tombs of Egyptian pharaohs, date back to the period between 1500 B.C. and 1000 B.C, were bonded or laminated with some type of animal products. This discovery gave another evidence of that glue had become a method of joining [39].

The first references concerning glue and its usage were set about the year of 200 B.C., when simple procedures were written about how to make and use animal glue.

The art of veneering, which is the bonding of thin sections or layers of wood, was developed by the Romans and Greeks in the period between 1 and 500 A.D. From this art, the making of animal and fish glues were refined and other types of adhesives were developed, such as an adhesive from egg whites to decorate parchments with gold leaf.

During the 19th century, the natural adhesives have been synthetically developed and improved. The first steps of manufacturing fully synthetic adhesives were around the Second World War [32].

3.2 Polymers and adhesives classification

Adhesives are made of many combined molecules and chains; therefore, they can be classified as polymeric materials.

Polymers are categorized into four basic types in accordance with the forms of the chains:

When chains of molecules are connected in a linear form, then the polymer is linear. Branched Polymers are formed, as the name indicates, in branched configurations or irregular arrays. If the chains are connected to aside ones by crossing links, the crossed-linked polymer is formed. A network polymer is when the molecules chains are connected together in the form of a net. The nature of the connections of the polymers chains in all previous mentioned categories can be either physical or chemical bonds.

According to their behaviour, polymers are classified as elastomer, thermoset, and thermoplastic groups, [40].

- Elastomer: is a cross-linked polymer that is capable to stretch and recover without permanent deformations.
- Thermoset: is a strong cross-linked polymer forming a complete network polymer. It is better suited to higher temperature applications and is more rigid than the elastomer.

- Thermoplastic: is a linear or branched polymer which physical properties change drastically between its glass transition temperature, T_g , and its melting point, T_m .

The behaviour of thermoplastics and thermoset materials is temperature-dependent and is schematically shown in Figure 3.1, [40].

Adhesives can generally be classified according to: their components and ingredients that they made from, to the physical nature of the adhesives, before or after curing, as well as to the function of them and the way of formation or curing.

Hot melt adhesive, for example, needs applying heating to activate it to form the bond with the adherend while pressure sensitive adhesive forms the bond when only pressure is applied. The curing method of other adhesives may need applying other motivators like moisture or UV radiation. Some of the adhesives can also be cured by chemical reactions between two parts one of them is the adhesive and the other is an accelerator. However, no motivators are needed for the curing of some kinds of adhesives. The most common of these classifications can be illustrated as shown in Table 3.1.

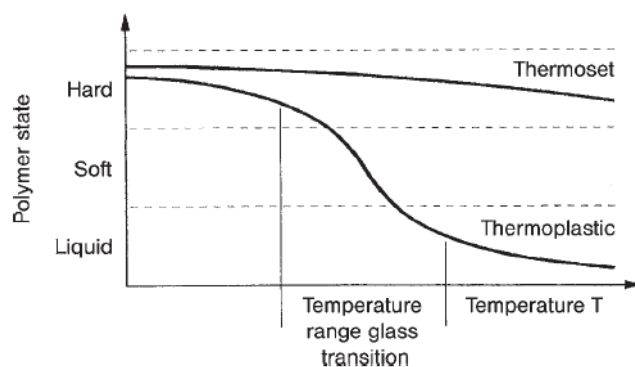


Figure 3.1: Temperature dependence of the polymer state of thermoplastic and thermosets (diagrammatic), [40].

Table 3.1: Most common classifications of the adhesives

Adhesive class	Examples
Chemical group	epoxy, phenolic, urethane, anaerobic, acrylic, cyanoacrylate, silicone and polysulphide
Physical form before curing	one or two part, liquid, solid, film, paste
Physical form after curing	rigid or flexible
Functional group	structural, hot melt, pressure sensitive etc
Curing process	cross-linking, polymerization
Curing method	heat, UV light, moisture etc

3.3 General types of structural adhesives

There are three main groups of structural adhesives commonly used in the structural applications: epoxy, polyurethane, and acrylic adhesives.

Epoxy adhesives generally have the highest strength properties of the other adhesives. An intensive surface preparation and/or treatment are necessary to guarantee the durability. The two-component epoxies can cure at the room temperature but need longer time unless they have been heated. The one-component epoxies mostly need heating to cure. After curing they

become rigid and the failure of epoxies is rather brittle. They can be applied for a wide variety of materials, however, bonding to thermoplastics and rubbers can be difficult.

The strength properties of polyurethane adhesives are relatively low or medium. The durability is mostly good even with a simple surface preparation and/or treatment. The two-component polyurethane adhesives, which one of them is the hardener, can easily cure at the room temperature while the one-component polyurethanes cure by a reaction with the moisture. After curing they become highly flexible with ductile behaviour. They are mostly used for structural applications with a wide range of materials including metals, plastics, rubbers, and glass. They can be used for both bonding and sealing applications and where large gaps between materials being bonded exist. Polyurethane adhesives compensate for contraction and expansion between bonded surfaces such as concrete and metal.

Good strength properties with flexible form and ductile behaviour after relatively fast curing are what acrylic adhesives characterized by. The durability is guaranteed with a moderate surface preparation and/or treatment. They are mostly available in a two-component and capable to bond most materials well, in particular metals. But they are not good for rubbers or low friction polymers.

3.4 Selection of a proper adhesive for a particular application

Considerable effort is required for choosing the adhesive that will be used to bond two or more materials together. Generally, it is desirable that the strength of the bond must be not less than that of the weaker material being bonded. The ability of the adhesive to resist the hostile environments is also an important criterion that must be taken into account.

Furthermore, the adhesives adversely affect the physical properties of the materials being bonded; therefore, the physical and chemical requirements of the adhesive are very exacting.

Other considerations have to be taken into account for choosing the adhesive which are the surface preparation of the adherends as well as the possible ageing effects, which lead to the degradation of the mechanical properties of the adhesive over the time.

Because of the availability of the various adhesives in the market which fulfill all requirements and conditions mentioned above, suitable prices have to be considered as well.

3.5 Structural adhesives in engineering and industry

Synthetic adhesives invention and their properties motivated the engineers to employ them for engineering fields. The rapid development of these adhesives and improving their properties over the years to fit some conditions and specifications that are requested to be used in the engineering applications, increase the interest of the engineers to use the adhesive bonding technique as a new way of joining structures.

The viewpoint of engineers is that a lot of disadvantages of the traditional methods of assembling structures might be avoided by using either a new technique of joining or together with the classical methods.

The disability of the traditional joining methods to assemble new materials which have been created in the recent years as well as the new requirements that have to be fulfilled for the modern designs, made engineers to pay attention to employ the advantages of adhesive bonding in their applications. For example, plastic structures, fiber-reinforced plastic or polymer laminated panels (FRP), carbon fiber reinforced polymer laminates (CFRP), glass fiber reinforced polymer (GFRP laminates) and glass structures cannot be joined to other materials by using the traditional ways like bolts or welding. Moreover, the requirements of reducing the weight and costs of a structure as well as the necessity of sealing a joint or increasing the damping feature of it are able to be fulfilled by bonding technique.

3.5.1 Structural adhesives in transportation

Structural adhesives are durable synthetic adhesives that are designed to resist heavy loads over the duration of the application.

For more than several decades now, structural adhesives have been used for bonding in the aircraft industry. Bonding by these adhesives was introduced to aircraft manufacture due to features that this way of bonding is characterized by, such as having long lifetime of up to 30 years, high endurance to static and dynamic loads, as well as high resistance to temperature changes. Weight reduction is an economically beneficial aspect and is done by offering the ability of using and joining very lightweight metal alloys, sandwich panels, and fiber-reinforced plastic laminates. An example of applying bonding technique in aircraft manufacture is given in Figure 3.2, [41].

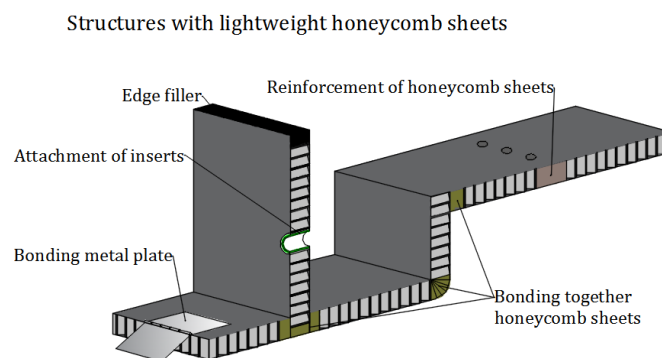


Figure 3.2: Structures with lightweight honeycomb sheets used in aircraft manufacture, [41].

In car manufacturing field, bonding by structural adhesives was introduced about forty years ago. It offered a suitable solution of the problem of that car bodies comprise steel sheets having a thickness of 0.6 to 0.8 mm which have to be used for weight reduction purpose and therefore less fuel-consuming cars can be fabricated. For example, 10 meters of adhesive were used in BMW-7 body in 2001, today a car contains about 150 meters (approximately 18 Kg) of adhesive with better safety than the welded cars.

In trains manufacturing, ready painted outer skin made of glass fiber-reinforced plastics (GFRP elements) is connected to the supporting metal structure by structural adhesives. Hence, a weight-reduced train with modern aesthetic appearance is produced, [41].

Examples of the adhesives applications in trains and care manufacture are shown in Figure 3.3.

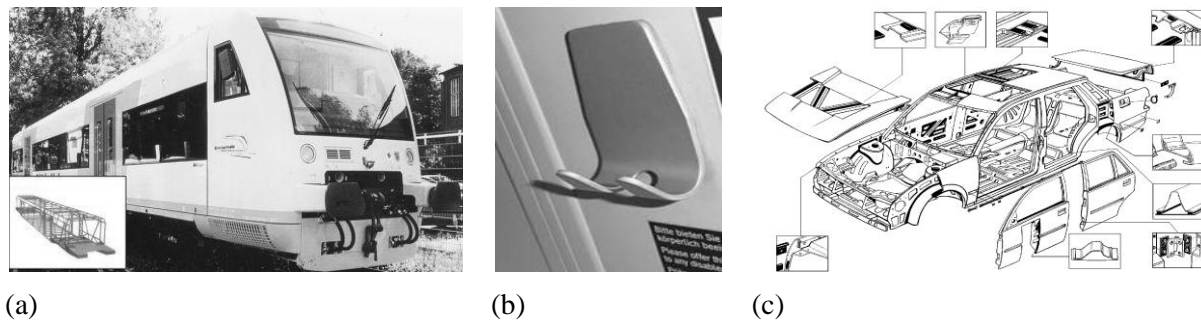


Figure 3.3: Application of the adhesive technology in trains and care manufacture

(a) In trains cladding, [41] (b) Coat hook of DB (c) Application of adhesives in car manufacturing, [37].

3.5.2 Structural adhesives in steel constructions

The great advance in the field of structural adhesive at the end of the 20th century aroused the interest of steel industry to employ this technology in the steel constructions, [37].

In 1956, the steel bridge in Marl-Hüls across the Lippe-Seitenkanal (Figure 3.4, [42]) was built with adhesively bonded joints. In these joints, bolts were used as well for disaster cases. The bridge is still working giving a good proof of the ability of using this technology in steel structures. Since at that time no sufficient experience was available, the need to use bolts in joining beside the adhesives was justified.

Recently, new rectangular and triangular hollow sections were fabricated by adhesively bonded steel plates to be used as new bridge deck constructions. Pictures of these designs are given in Figure 3.5, [43].

3.6 Advantages and disadvantages of adhesively bonded structural joints

Structural adhesives are durable synthetic adhesives, generally designed to carry heavy loads which must be transferred from one part to the other of the substrates bonded together. They are powerful enough to replace the convenient and traditional methods used for this purpose.

As the other joining methods, adhesive bonding technique has beside its advantages some disadvantages that have to be known by the structural engineers. Essential advantages of adhesive bonding can be summarized as following [32], [37]:

- The material structure will not be affected by thermal influence; hence no thermal distortion of the adherends due to heating stress is possible.
- No changes in the geometric properties of the adherends like the cross section area and straightness, as well as the material behaviour.
- Stress distribution, vertical to load direction, is regular. Figure 3.6 demonstrates the stress distribution in welded, bolted or riveted, adhesive-bonded joints.
- Joining very thin adherends is possible.

- Similar and dissimilar adherends and materials are able to be adhesively joined.
- The possibility of joining metals with different electrochemical properties.
- Adhesives have high dynamic strength and vibration damping.
- The ability to form almost invisible connections (aesthetic demand).
- The ability to produce more complex connection forms.
- A sealing function.
- The possibility of minimizing weights.

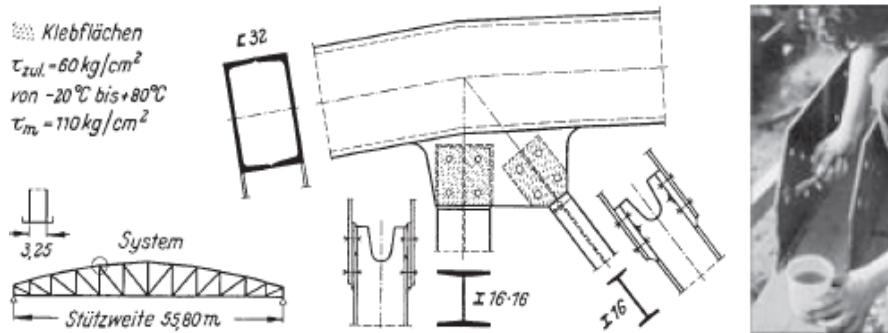


Figure 3.4: Adhesively bonded and bolted joints in the steel bridge in Marl-Hüls, [42].

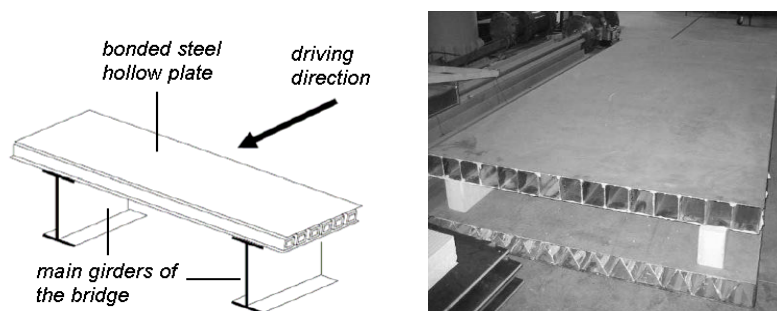


Figure 3.5: New bonded constructions of the bridge deck, [43].

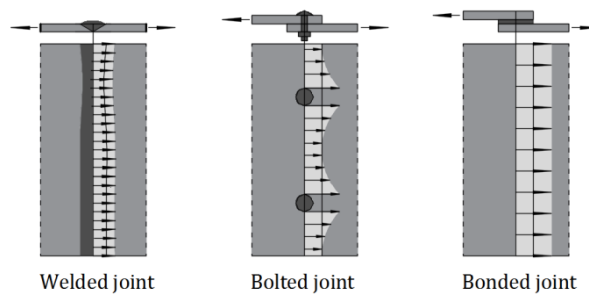


Figure 3.6: Stress distribution in welded, bolted or riveted and adhesive-bonded joints (Modified figure from [44]).

The disadvantages that the bonding technique is suffering from can be presented as [37], [32]:

- Significant skills will be required to manufacture adhesively bonded connections.
- Application conditions of the adhesives have to be accurately met, like the need of pre-processes prior to bonding such as pre-treatment and preparation of the surfaces being bonded.
- Long time of usage will probably change the properties of the adhesives.
- The sensitivity of these materials to the environmental conditions.
- Compared with the other joining ways, more time will be needed to reach the desirable strength.
- Heat resistance is Limited.
- The difficulty to dismantle the joint for repair or re-use of the materials.
- For quality-testing purposes, non-destructive testing is not always possible.

3.7 Loading modes in adhesive-bonded joints

The types of the adhesive-bonded joints can be mainly categorized according to the loading behaviour over the bondline into five types, as shown in Figure 3.7 (modified figure from [38]), these types are:

- Joints loaded in peel.
- Joints subjected to tension loading.
- Joints loaded in shear.
- Joints confront the cleavage.
- Joints subjected to torsion load.

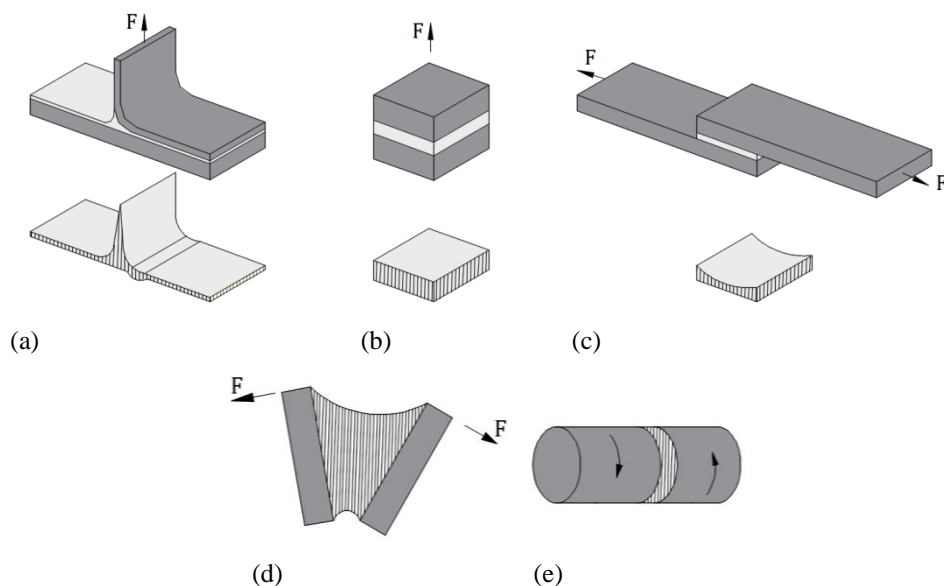


Figure 3.7: Types of adhesive-bonded joints

Joints loaded in: (a) peel, (b) tension, (c) shear, (d) cleavage, (e) torsion.

In joints loaded in peel, high concentrated tensile stresses will appear because of the load that has to be transferred in the joint, which lead to premature failure of the joint, therefore, this type of joints is the most unfavorable one.

Since the tensile strength of the adhesive is much lower than the corresponding strength of the adherends, in steel applications for example it equals to approximately 10 up to 20 percent [38], joints loaded in tension are very rarely used.

Similar to the joints loaded in peel, joints with thick adherends may experience the cleavage; therefore, they are not favorable as well.

Joints loaded in shear, either shear by tension load, Figure 3.7(c), or shear by torsion, Figure 3.7(e), are the most favorite type because they have the best properties of the carrying capacities, However, in the shear by tension joints, the peel stress existence is probable due to the eccentricity of the load transferred through the adhesive layer and should be avoided as much as possible to achieve the highest carrying capacity of the joint.

The nature of the load acting on the adhesive-bonded joints can be variant. It can be one or more (combined effects) of short-term or long-term (static or dynamic) load and environmental effects such as temperature, humidity, etc.

3.8 Failure modes of adhesive-bonded joints

Failure in adhesive-bonded joints might be resulted from mechanical or environmental loads acting on it. Once the affecting external load is greater than the internal forces in the joint, the failure will be occurred.

To illustrate the expected failure modes in adhesively bonded joints, necessary information about the configuration of these joints (Figure 3.8, [40]) as well as the adhesion and cohesion phenomena must be understood.

Adhesion phenomenon

Adhesion is the force by which the surfaces of two materials are connected together. This force opposes the stresses exerted to pull the materials apart. Therefore, adhesion is the attractive force between the connected surfaces.

The attraction between surfaces may be due to the molecular attraction between the contacting surfaces, or resulted from the flow of the one material into the microstructure of the surface of the other one. The optimum adhesion strength occurs when both of them are combined.

The most effective factor on the strength of the adhesion is the pre-treatment and preparation of the surfaces being bonded.

Cohesion phenomenon

Cohesion can be defined as the attraction forces among the particles of the adhesive (or other material) by which the adhesive mass is held together.

Thus, an adhesively bonded joint fails if a separation occurs between the adhesive and the substrate, adhesion failure, or within the adhesive layer, cohesion failure. The failure can also be in the adherends (Figure 3.9).

The best bonding quality is achieved by providing best combination of adhesion and cohesion strengths. If this combination of both strengths is great enough to resist the applied stress, and is greater than the carrying capacity of the substrate itself, then the expected failure, either yielding or breaking in the substrate, is inevitable. It is worth mentioning that the failure mode in an adhesively bonded joint may change because of aging or its exposure to environmental effects. In engineering, the cohesive failure within the adhesive is the most preferable one; however, designers have to take into account all possible failure modes.

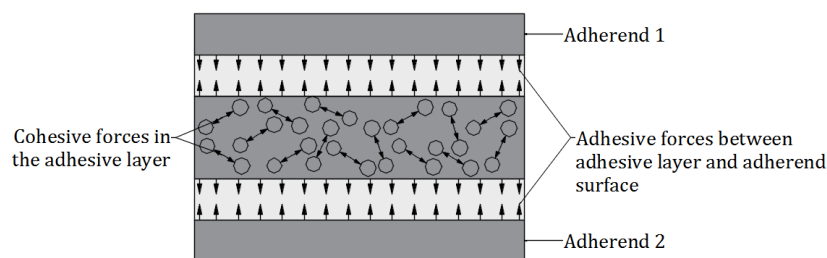


Figure 3.8: Connecting forces in an adhesive-bonded joint, [40].

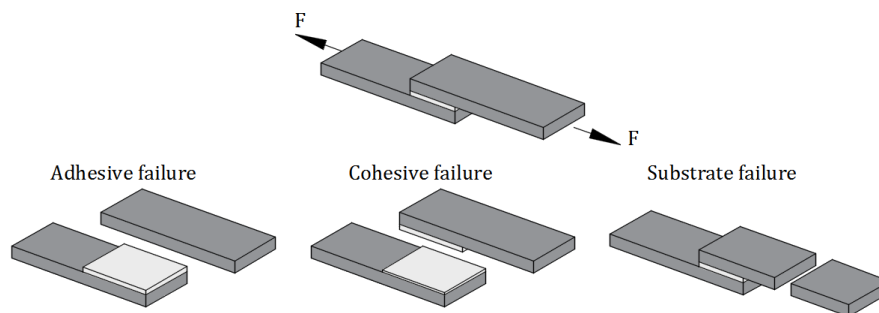


Figure 3.9: Failure modes in bonded joints

3.9 Production of bonded joints

Following the understanding of the description of different kinds of adhesives and the structure of the bonded joint, the most important processes for producing a bonded joint can be subdivided into two groups, [40]:

- Processes serving the development of the adhesive forces. They include surface treatment of the adherend and adhesive application.
- Processes defining the cohesive strength of the adhesive layer. In this case, the conditions in respect of time, temperature and pressure during adhesive curing have to be taken into account.

The increase of the joint strength will be achieved when proper adhesive, good design and accurate manufacturing process are utilized. The processes needed for producing an

adhesively bonded joint with metal adherends are here explained while for other materials can be found in literatures (see for example [40], [44]).

3.9.1 Processes serving the development of the adhesive forces (adhesion strength)

3.9.1.1 Surface treatment

Treatments on the surfaces that are to be bonded can be generally divided into three groups [40], Figure 3.10:

Surface preparation during which, cleaning and degreasing the surface have to be carried out. By the cleaning the adherend surfaces, the removal of adhesive solid layers like dirt, rust, paint, and so on is served. Mechanical cleaning by means of grinding or brushing is preferred. The cleaner the adherend surfaces, the more guaranteed the aspired joint strength is expected. Organic solvents or hot distilled water (approximately 60 °C – 80 °C) added with liquid cleaning agents are used for degreasing adherend surfaces. Degreasing is one of the most important necessities for perfect wetting; therefore it should be carried out in any case regardless whether or not further surface pretreatment will follow. For this reason, attention should be paid to the fact that the agents used for degreasing and cleansing may contain small fractions of silicone components that will complicate wetting if remained on a surface, see Figure 3.11, [40].

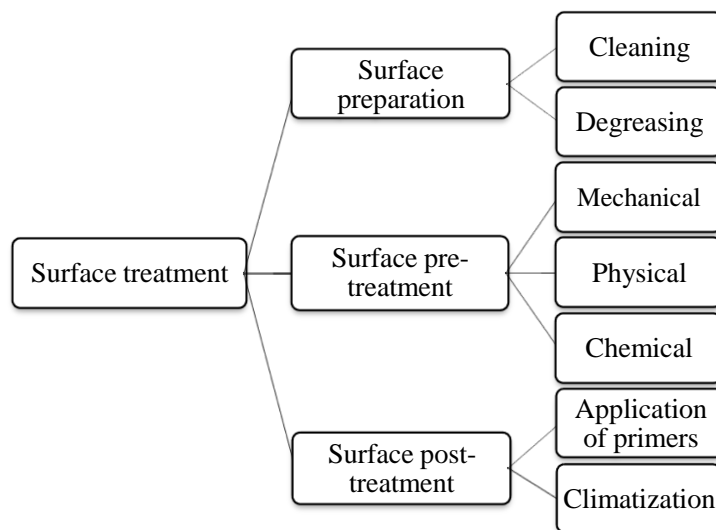


Figure 3.10: Treatments of the surfaces.

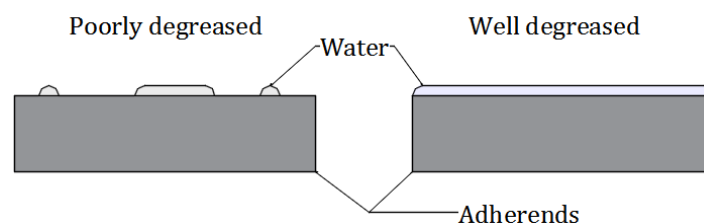


Figure 3.11: Wetting on poor degreased and perfect degreased surfaces, [40].

There are various agents well known as grease killer. Due to their relatively moderate price as well as the low effect on the environment, acetone, methylethylketone (MEK), thylacetate or also methyl- and isopropylalcohol are used with good degreasing properties.

Surface pre-treatment is the second group of the treatments needed for achieving highest adhesive forces between the surface and the adhesive. This treatment can be done mechanically by grinding, brushing, sanding or blasting and/or physically or chemically. Grinding or brushing the surfaces is done by the use of low dust load in comparison to blasting or a steel brush. When they are used repeatedly with different angles, the effect of this pre-treatment will be enhanced. More effective than grinding and brushing is sanding (grit blasting) with shot solids in different kinds and forms (aluminum oxide abrasive, steel grit, lass pearls). However, none of these prescribed pre-treatments is capable to fully remove the grease; therefore cleaning and degreasing the surfaces before and after these treatments are essential demand.

Great care has to be given when dealing with special surfaces that are coated or covered by additional layers for some necessary reasons. In the case of zinc-plated steels, the only mechanical surface pretreatment method to be recommended is careful grinding (sponge with household cleaning powder or using acetone agent), because of possible zinc layer damage. In the case of a damaged zinc layer, the bonded area should be protected against corrosion creep by suitable primers or by sealing of the edges of the bonded area.

When chemical modifications are needed to improve the adhesive forces for extremely high demands on bonded joints, physical and chemical pretreatment methods are used on the surfaces of materials that are poorly bondable. The name “physical method” refers to the fact that they utilize physical effects in the form of electrical or thermal energy to improve the bondability of the surfaces to be bonded. The physical methods are mainly used in bonding of plastics; more details are found in [40]. All chemical methods have the disadvantage of containing aggressive chemicals that are strongly harmful; therefore, their application is subjected to legal obligations, and thus to strong safety regulations. For this reason in industry they are only applied in exceptional cases such as a bonded joint that is supposed to resist high stress for a long time. An example of this is the aerospace industry with service lives of aircrafts of up to 30 years.

Pickling is one of chemical surface pretreatment methods, which are commonly used. The principle of using such a method is to apply thinned acids, which remove layers on the metal surfaces via chemical reactions resulting in metallicity clean surfaces.

The last group of treatments on surfaces is the post-treatment. This group includes applying primers and climatization process.

Primers consist of solutions of polymers that are related to the adhesive and applied on the surface in a thin layer to improve the adhesion forces after drying. Applying the primers can be done to the material either after manufacturing or after the surface pre-treatment. An

adjustment and compatibility between the primer and the adhesive is necessary for creating the strongest bonded joint.

To maintain or improve the adhesion conditions resulting from the respective pretreatments, climatization process is performed. Climatization serves for getting rid of the possible limiting of the adhesive properties due to the water condensation on the adherend because of the change in temperature and humidity.

3.9.1.2 Adhesive application

Adhesives can be applied after they have been prepared in terms of adjusting the required viscosity, which is important for achieving a desirable layer thickness of a solvent-containing adhesive, and in terms of getting the best homogenization to avoid the existence of air bubbles. Climatization is sometimes necessary for providing the temperature needed for a required viscosity of the applied adhesive.

Mixing process is important to guarantee a very good-prepared adhesive with the described ratios of the components. This process can be done manually, industrially, dynamically, or statically. The manual mixing is well known but is used less than the other methods of mixing because the ease of using them with no danger of skin contact with the adhesive and the accuracy of ratios of the components being mixed and the dosing amount required for bonding a specific area; thus it serves in saving the adhesive material.

When the adhesive consists of components with large differences of their viscosities as well as in their ratios, it is preferable to use a dynamic mixer. Extreme ratios are, for example, when a few percent of the hardener component has to be mixed with the resin component.

If the adhesive components are of approximate viscosities or their ratios are not extreme, a static mixer can be used. This device has a mixing helix, which is fixed in a tube and offset by angles of 90°. The dynamic mixer and the static mixer are shown in Figure 3.12.

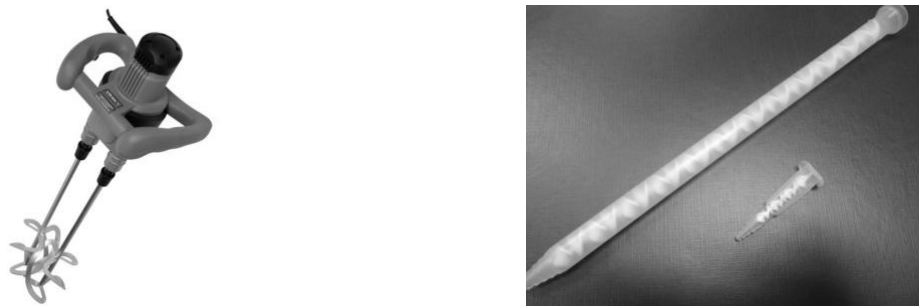


Figure 3.12: Mixing process of the adhesive components
Dynamic mixer (left), Static mixer (mixing nozzle) (right).

Providing specific ratios of the components of an adhesive is done by either the weights of them (weight ratio) or by volume (volume ratio). Weight ratio is carried out by weighing the components using a suitable scale. On the other hand, special components cartridges are designed in different sizes that are equal to the required mixing ratio (volume ratio). The two components of the adhesive, A and B, are pushed into the mixing nozzle by the use of hand

applicator (Figure 3.13) which is sufficient for the cartridges of small sizes or by air pressure-aided applicator for large sizes.

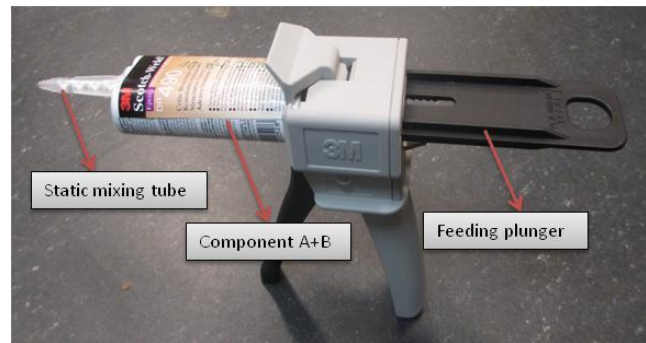


Figure 3.13: Hand applicator to push two-components adhesive into the mixing nozzle.

Adhesives can also be applied in several methods, depending on the viscosity of them; spraying, immersing, and dripping are suitable methods for low viscosity-adhesives. For applying the moderate viscosity-adhesives rolling, pouring and brushing can be used. While for high viscosity-adhesives it is easier to distribute them on the surface in coating-like layer by a proper knife, Figure 3.14, [40].

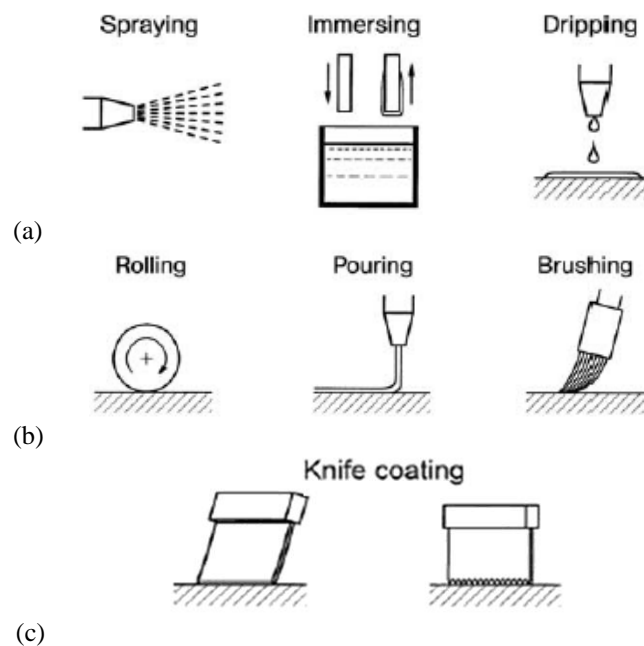


Figure 3.14: Methods of the adhesive application
Suitable for (a) low, (b) moderate, (c) high viscosity-adhesives, [40].

3.9.2 Processes defining the cohesive strength of the adhesive layer

Adherends to be bonded must be fixed to each other in a correct way to prevent them from shifting during the curing period which leads to a destruction of the adhesive layer and thus to a destruction of the cohesive strength. Applying a uniformly distributed sufficient pressure on the bonded adherends over the curing process will serve to have equal adhesive layer thicknesses.

Adhesive curing

Curing is defined as the transition of the state of a reactive adhesive layer from liquid to solid adhesive through chemical reaction. Although some adhesives can be cured at room temperature but heating is necessary for the curing of the other adhesives, which cannot cure at room temperature. On the other hand, temperature accelerates the curing process of those which can cure at room temperature. It is mandatory that both temperatures and times have to be observed. The temperature–time curve, shown in Figure 3.15, [40] depends on the properties of the adhesive as well as the adherends. Most important parameter is the thermal conductivity; materials with high thermal conductivity (e.g., metals) need shorter heating times than low thermal conductivity materials such as plastics, wood, and glasses.

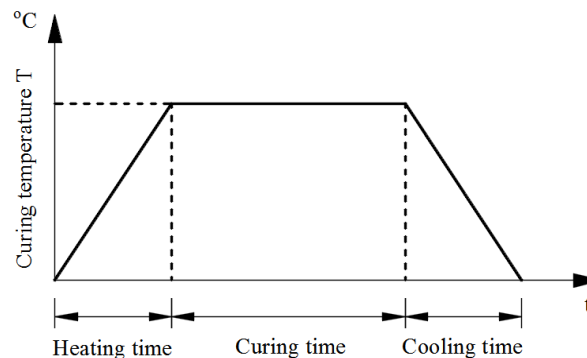


Figure 3.15: Curing temperature vs. curing time, schematic curve, [40].

3.10 Factors affect the adhesive joint strength

The strength of adhesively bonded joints can be affected by several factors that can be grouped as:

- Factors depend on the geometry of the joint including the dimensions of both adhesive and adherends used in it.
- Factors related with the process for preparing and producing the joint.
- Environmental factors.
- Impact of the nature of loading

3.10.1 Geometry-dependent factors

Lap shear bonded joints are good examples for illustrating these factors:

3.10.1.1 The influence of the adhesive thickness

It is likely that the joint strength decreases when thicker adhesive layer is applied, i.e. the thicker the adhesive thickness is, the less the joint strength will be. This is attributed to some facts, which are [5]:

- In thicker adhesive layers, the existence of the defects, such as voids and microcracks, is more probable.

- Plastic spreading of the adhesive along the overlap occurs more rapidly when the adhesive gets thicker.
- Higher interface stresses will result from the increased bondline thickness. In adhesively bonded single lap joints that are loaded in shear by tension, for example, an increase in the bending moment due to a thicker bondline is inevitable; thus the resultant stress of both peeling and shear stresses will be increased over the bondline, Figure 3.16, [40].

The dependence of the shear strength on the adhesive thickness is schematically presented in [44] and shown in Figure 3.17.

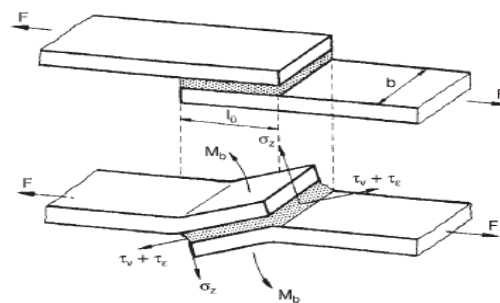


Figure 3.16: Stresses due to shear by tension loading in a single lap joint, [40].

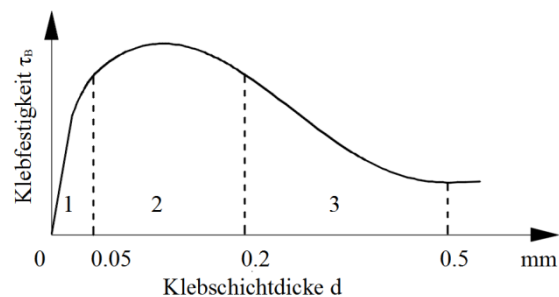


Figure 3.17: The dependence of the shear strength on the adhesive thickness, [44].

Experimentally curves on the effect of the adhesive thickness on the shear stress of lap shear aluminium (6061-T6) joints bonded by epoxy and acrylic adhesives are shown in Figure 3.18, [6]. In these curves, thicknesses greater than 0.5 mm (up to approximately 2.5 mm) are investigated. The same conclusion can be derived for both adhesives within the studied range of the thicknesses.

3.10.1.2 The influence of the adherends thicknesses

The adherend thickness affects the strength of a bonded joint. It is important to distinguish between these two cases [5]:

- For low strength adherends, an increase in thickness is beneficial because the adherend becomes stronger and less likely to deform plastically. In other words, in thinner adherends there is a higher concentration of bondline peel stresses at the

overlap edges due to the deformation of the adherends. This is clear in (Figure 3.19, [6]), where epoxy adhesive was used for bonding aluminum adherends with different thicknesses and for two overlap lengths.

- On the other hand, for high strength adherends, a higher thickness can decrease the joint strength. In lap joints for example, higher thicknesses will also increase the bending moment; and thus additional peel stress will be added.

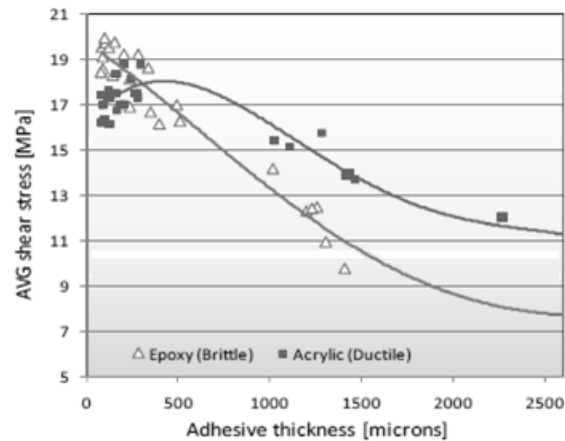


Figure 3.18: The influence of the adhesive thickness on the shear strength of single lap joints, [6].

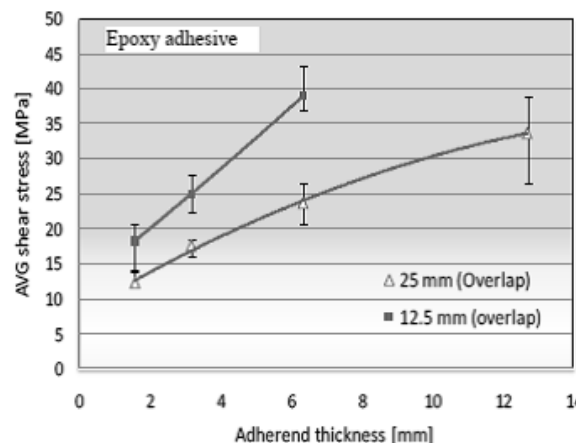


Figure 3.19: The influence of the adherend's thickness for two overlaps, [6].

3.10.1.3 The influence of the overlap length

The joint strength is an overlap length–dependent regardless the adhesive or adherends types used in the bonded joint. From Figure 3.20, [6], one can see that for both rigid and ductile adhesives used, the joint strength increases as the overlap length increases. Another interesting result can be derived here, that is for shorter overlaps, the performance of epoxy adhesive is better than ductile acrylic adhesive while it becomes the opposite for longer lengths.

Same conclusion was reported by Da Silva *et al.* [5] for high and low strength of steel adherends as graphed in Figure 3.21.

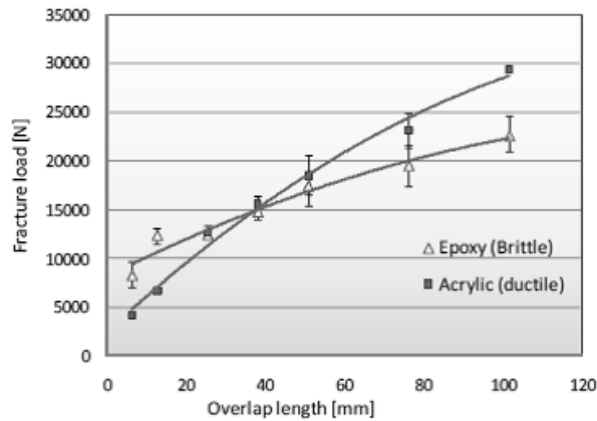


Figure 3.20: Comparison between the effects of the overlap length for both epoxy and acrylic, [6].

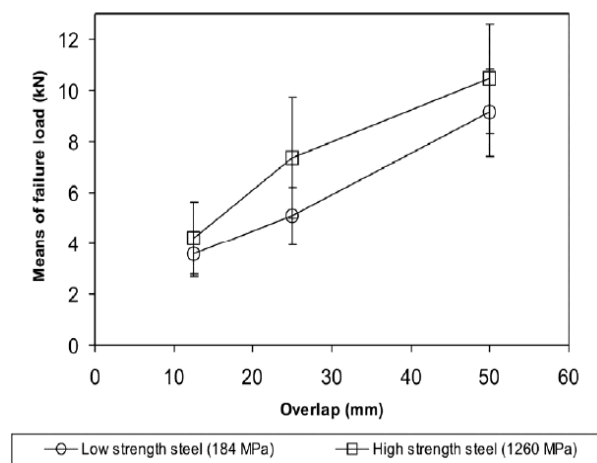


Figure 3.21: Average response for the interaction between the adherend yield strength and the overlap, [5].

Hart-Smith [1] showed that for very short overlaps only the average bond stress is the appropriate basis for design while the joint strength is for longer overlaps because the joint strength becomes independent of overlap rapidly as the overlap increases. It is clear in Figure 3.22 that the load capacity increases when the overlap length increases up to a defined value. Beyond that overlap, no greater load transfer can be affected.

3.10.2 Factors related with the process for preparing and producing the joint

3.10.2.1 The influence of the surface preparation

Surface preparation is recognized as the most critical step in the adhesive bonding process. Depending on the required strength and durability of the joint, the selection of surface treatment has to be made.

The purpose of surface pre-treatments is to remove contaminations and the weak surfaces for the sake of getting better bonding.

When the surface is prepared correctly and all respective requirements are fulfilled, a better joint strength can be achieved and maintaining the long-term structural integrity of bonded

joints has a greater chance. As a result of unsatisfactory surface preparation, the bond fails adhesively and unpredictably at the adhesive/adherend interface might be occurred.

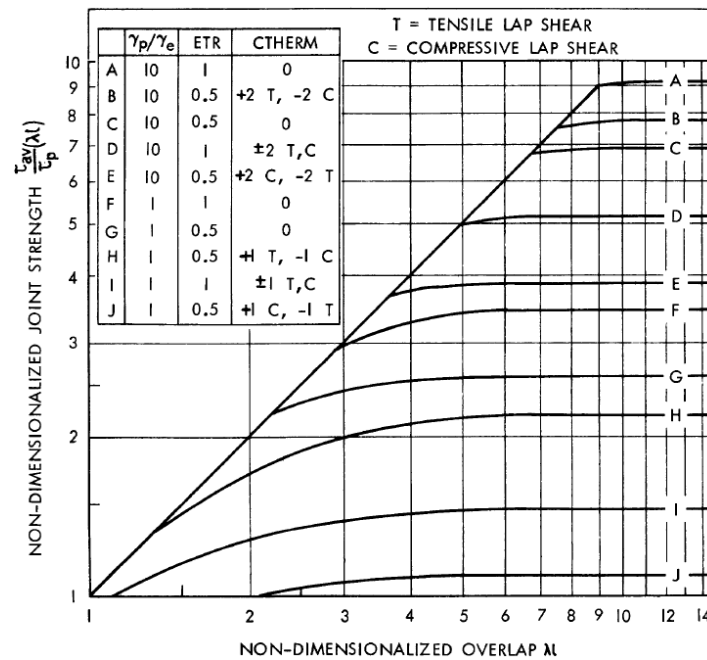


Figure 3.22: Influence of parameters studied by Hart-Smith [1] on the shear strength of double lap joints

3.10.2.2 Elimination of the voids within the adhesive layer

Voids must not be existed in the adhesive layer; otherwise the adhesive bonding will be weaker. The existence of the voids in the areas, where the concentrated stresses are, will lead to a premature failure. In overlap joints, attention should be given to the ends of the bonded area at which no voids must exist.

Introducing voids within the adhesive layer takes place when stirring the adhesive or when controlling the adhesive layer thickness. Stirring process is more preferable to be in a vacuum to ensure that no air is stirred into the adhesive.

If adhesives are applied with specific glass balls for determining a desired thickness of the adhesive layer or with fillers added to achieve a greater thickness, then these fillers or balls have to be stirred to enable equal distribution.

The application of a thick thickness must be carefully done, because the risk of inserting a high level of voids is increased when using thicker thickness.

3.10.3 The influence of the environmental conditions

Adhesively bonded joint strength is strongly affected by environmental conditions that it is likely exposed to them over the lifetime. Due to these conditions, mainly temperature, humidity, and hostile atmospheres, the adhesive layers and boundary layers towards the adherends surfaces may be damaged; and therefore a reduction of the joint strength is inevitable and a premature failure is to be expected.

Figure 3.23, ([44]) schematically shows how the mechanical properties of adhesives such as the elastic modulus and the strength degrade as the temperature increases while the fracture strain increases simultaneously.

The resistance of environmental effects varies among the adhesives kinds; generally, epoxies have the best resistance of the environmental effects.

Experimental investigations on the effect of both heat and moisture on film and paste adhesives used to bond aluminum lap shear joints were conducted by [14]. The specimens were subjected to three different environments, RTD (room temperature dry), ETD (elevated temperature dry), and ETW (elevated temperature wet). The apparent shear strength, Figure 3.24, and the shear modulus, Figure 3.25, of the paste adhesives tested, indicate a significant decrease as the adhesives were exposed to heat and moisture. The same conclusion was found for the film adhesives as well. The reported failure modes with respect to the environmental conditions are changeable as shown in Figure 10.1, Figure 10.2, and Figure 10.3 (in appendix A).

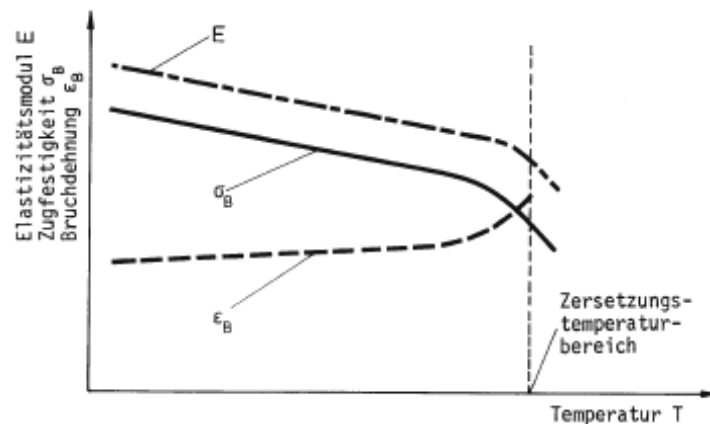


Figure 3.23: Schematic temperature impact on the elastic modulus E , the strength σ_B and the fracture strain ϵ_B of an adhesive, [44].

3.10.4 The influence of the nature of the joint loading

The strength of an adhesive joint loaded, either mechanically or environmentally, for short time is surely higher than when loaded for long time or frequently (cyclic loading). It is thought for adhesively bonded joint that the so-called “endurance limit”, which defines the remaining strength of an adhesive joint, indicates that only about 40% of the short-term strength is kept after long-term loading [20]; however, a big lack of information regarding this fact and the long-term behaviour of adhesive joints is still existed; therefore, intensive investigations on this regard are of great importance.

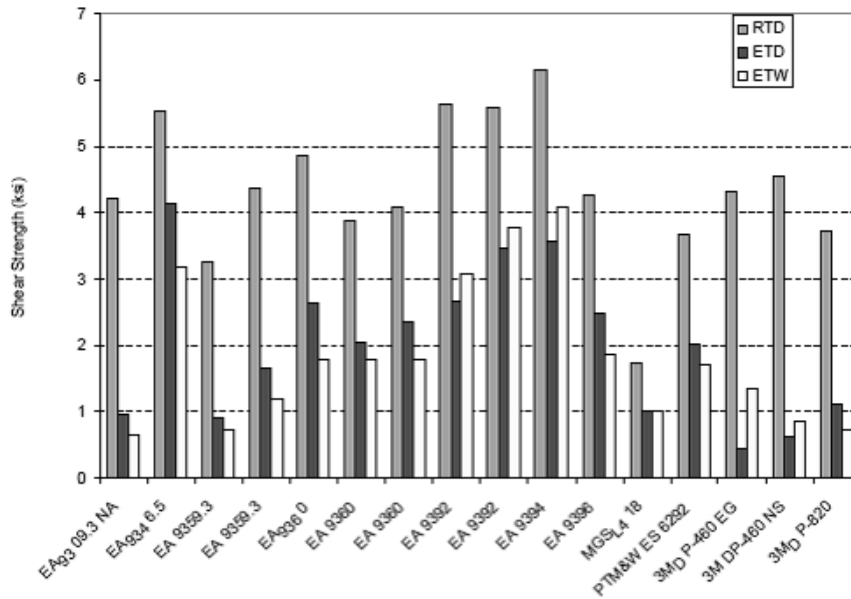


Figure 3.24: Environmental effects on the shear strength of paste adhesives, [14].

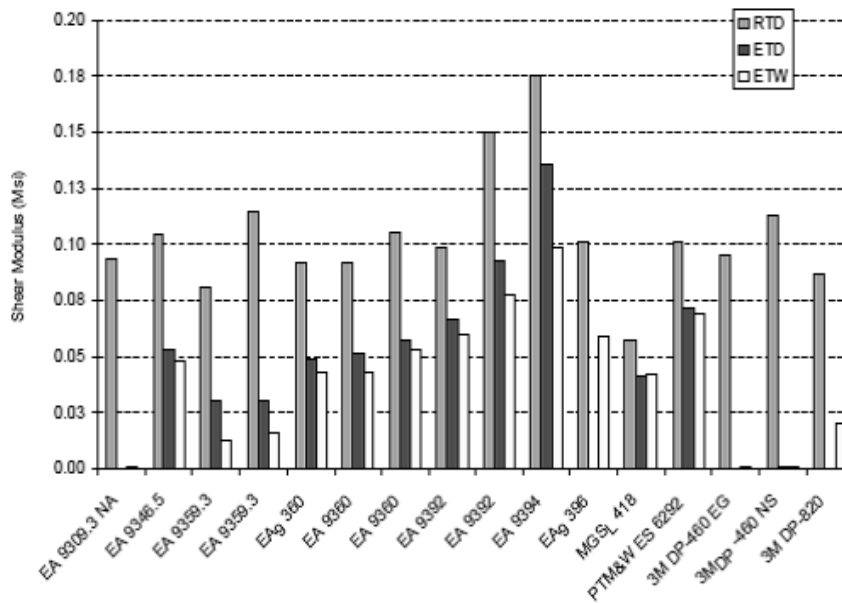


Figure 3.25: Environmental effects on the shear modulus of paste adhesives, [14].

4 Temperature effect on the adhesively bonded lap shear steel joints: Partial factors and conversion factors of the shear strength

4.1 Introduction

Adhesively bonded lap shear joints are considered as the most efficient among the other types of bonded joints. When peel stresses developing in these joints are avoided, the highest shear strength of the adhesive (or the carrying capacity of the joint) can be reached. This type of joints can be usually found in strengthening joints by bonding additional plates on the region of the structural member which is to be strengthened. The adhesive layer, therefore, will transfer the force from the strengthened member to the additional plates (the strengthening plates) in a way similar to the work principle of the lap joints.

The carrying capacity of lap shear bonded joints as well as the understanding of the mechanical behaviour has been the interest of many researches over the past years. The effect of using different adhesive materials, thicknesses, and overlap lengths on the carrying capacity of these joints was approved experimentally. Furthermore, the effect of the environmental conditions and the loading nature was also investigated and shown to be of great effective; however the limited experience with the selection of adhesive bonding systems and the lack of knowledge about the stochastic nature of the strength of the bonded joints, failure mechanisms, and ageing are still existed [31].

Conducting extensive test plans to validate the use of the adhesive bonding technique and its design rules in structural engineering will not be afforded because of the high costs and the time-consuming. The structural reliability method is proposed to be used to guarantee the structure reliability taking into account the stochastic nature of the strengths. This method can also be used to validate a prediction model that describes the structural behaviour of the bonded joints under prescribed conditions [31] and [32].

In this chapter, the focus will be on the investigation of lap shear galvanized steel joints bonded by structural adhesives. The effect of the temperature on the mechanical behaviour and shear properties of the adhesives when the joints are short-term-loaded is the main objective of the investigations. The partial factors of the limit states as well as the conversion factors that cover the use conditions and circumstances, particularly the temperature influence within a defined temperature range, are proposed for the shear strengths of the adhesives. These factors are derived from the representative values (characteristic and design values) of the shear strength. The representative values are determined by evaluating the test results data at each temperature using the direct evaluation method according to ISO 2394:1998 and by using analysis models (prediction models) that describe the change of the shear strength of the studied adhesives due to the temperature change according to the standard procedure of EN 1990:2002 together with the systematic approach developed by Van Straalen [32].

4.2 Materials description

4.2.1 Galvanized steel

Galvanized steel is a component which is essential in fabrication. It is used widely in the fields which require a good resistance to the exposure to corrosive environmental conditions; therefore it is often used for constructions and building materials as well as in industry applications such as marine, automotive, and aircraft industries. Furthermore, galvanized steel has also significant strength and fulfill the aesthetic requirements. For all these advantages, its use in the steel structures is increasing.

For cold forming, the continuously hot-dip zinc coated sheets of low carbon steels are commonly used in the field of building materials, cladding, roofing, and facades. These sheets have been submerged in a molten bath containing a zinc content of at least 99%.

The steel grades covered by (DIN EN 10327, [45]) are classified as follows: $D \times 51D + Z$, $D \times 52D + Z$ up to $D \times 57D + Z$. The available coating masses (expressed in grams per square meter) are in the range of Z100 and Z600. It was decided to use the steel grade $D \times 51D + Z$ (275) because it is widely used in the building claddings and facades.

Galvanized steel testing

4.2.1.1 Specimens preparation and test procedure

The galvanized steel used is available in sheets of different thicknesses. The thicknesses used here are 1 and 2 mm. Three sheets of 2 mm thick and one sheet of 1 mm thick were brought.

Thirty samples were cut from the three sheets of 2 mm thick while for the samples of 1 mm thick, ten samples were cut from the sheet. The samples were equally cut in both longitudinal and transverse directions. Dimensions and type of test pieces were selected according to DIN 50125 [46] as shown in Figure 4.1.

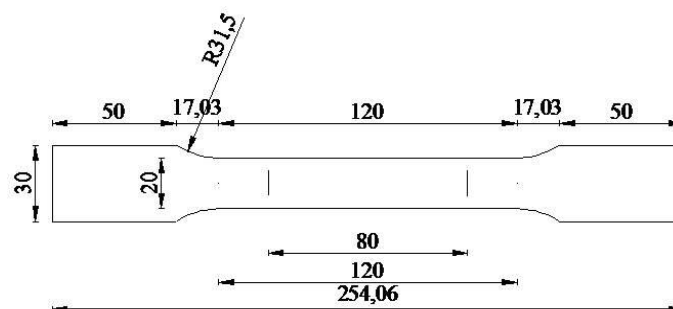


Figure 4.1: Tensile specimen DIN 50125- H 20 × 80

Tensile tests were done to determine the mechanical properties, (E modulus, yield strength, and ultimate tensile strength) for this grade of steel. The specimens were instrumented with a strain gage extensometer, Figure 4.2, and installed in the clamps of the tensile test machine. The tests were carried out at room temperature of 22 °C.

4.2.1.2 Mechanical properties

Elasticity modulus E , yield strength σ_y , and ultimate tensile strength σ_u for the steel grade D × 51D + Z (275) were determined according to ISO 6892-1[47].

The stress/strain curves were recorded and then for each thickness they were averaged by the use of the software techniques of Findgraph. Scattered points were excluded. True stress and strain were also calculated for the sake of using these curves later in FEM-simulations, they were calculated by the following equations:

$$\sigma_t = \sigma(1 + \varepsilon)$$

$$\varepsilon_t = \ln(1 + \varepsilon)$$

in which σ_t and ε_t are the true stress and strain respectively while σ and ε are the engineering stress and strain.

The modulus of elasticity, (E) was calculated as the slope of the linear part of the curve. The yield stress was taken as the stress corresponding to the maximum value prior to the first decrease in the stress in stress/strain curves, while the ultimate tensile strength was taken as the maximum value after the yielding extension. Results are presented in Figure 4.3 for 2 mm thick sheets and in Figure 4.4 for 1 mm thick sheets.



Figure 4.2: A tested specimen instrumented with a strain gage extensometer

4.2.2 Structural adhesives

Two systems of adhesives, epoxy and acrylic, were chosen for bonding the joints. The criterion preliminarily adopted for the selection of the adhesives was the highest shear strength with cohesive failure at room conditions, i.e. (20 °C and 50% R.H.); therefore, polyurethane adhesive was completely excluded due to its little shear strength [48]. Another candidate acrylic adhesive SkiaFast[®] 5241, tested by the author, was also excluded because it failed adhesively.

The succeeded two kinds were:

- 3M Scotch-Weld™ DP 490: Two-component, cold-cure epoxy, denoted later by EP.
- 3M Scotch-Weld™ DP 810: Two-component, cold-cure toughened acrylic, low-odor Acrylic, denoted later by AC.

More details about the adhesives as reported by the manufacturer are presented in Table 4.1. Both the DP 490 and DP 810 adhesives are supplied in double-tube cartridges, incorporating the adhesive and the hardener. The adhesives can be applied using a special gun applicator which pushes the adhesive and the hardener through a pre-mixing nozzle attached to the cartridge (3M EPX applicator), Figure 3.13.

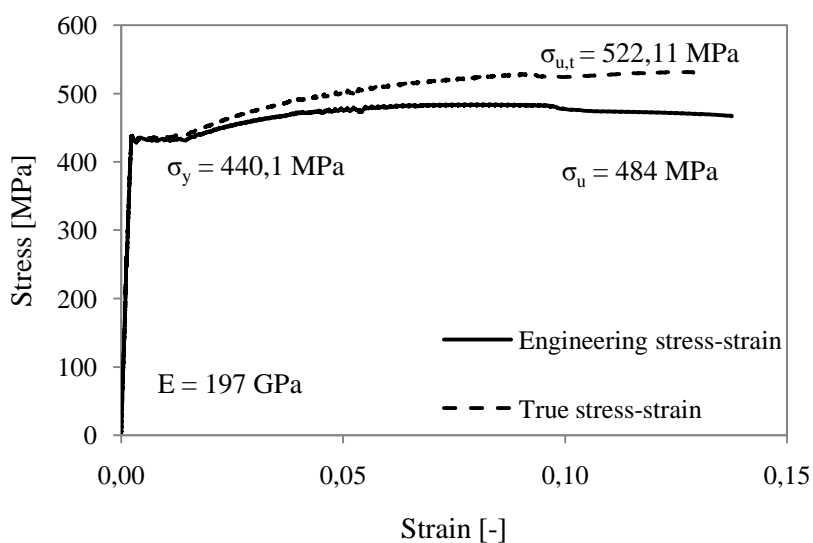


Figure 4.3: Engineering and true tensile stress-strain curves of the steel grade D x 51D + Z (275)- 2 mm thick

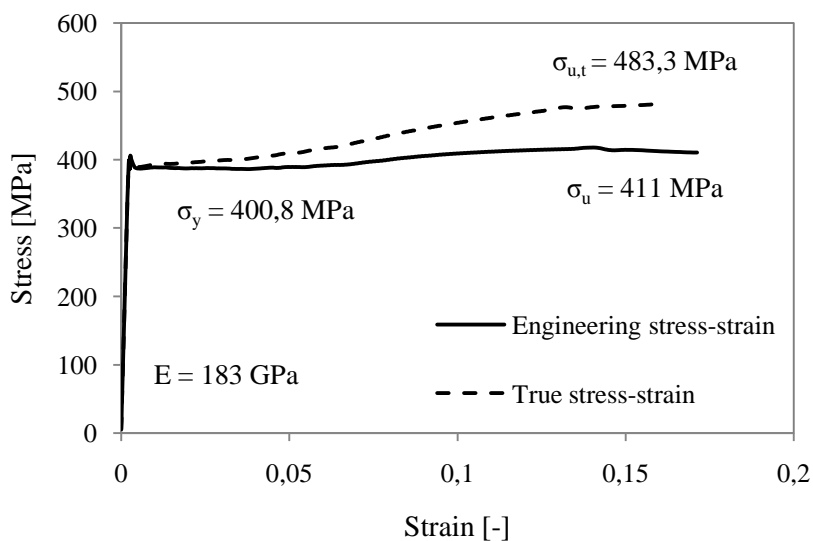


Figure 4.4: Engineering and true tensile stress-strain curves of the steel grade D x 51D + Z (275)- 1 mm thick

Table 4.1: Typical uncured physical properties of the used adhesives as reported by 3M Scotch-Weld™

	DP 490		DP 810	
	Base	Accelerator	Base	Accelerator
Color	Black	Off-white	Green	White
Mix ratio by (weight or volume)	100:50		1:1	
Time to handling strength	4 to 6 h at 23°C		10 minutes	
Full cure at 23°C	7 days		8-24 h	
Worklife at 23°C	1.5 h minimum at 23°C		10 minutes	

4.3 Double lap shear joints tests

According to the respective codes ([49], [50], and [51]), the shear behaviour of the adhesives in shear by tension loading for bonding metals can be determined by the thick adherends shear tests while the shear strength properties can be determined by double lap shear joints. Double lap galvanized steel joints were preferred to be used to investigate the effect of temperature on the mechanical behaviour and the shear properties of the structural adhesives (epoxy and acrylic, respectively). The selection of this kind of joints was made due to the following reasons:

- The ease of manufacturing and bonding them as well as the relatively cheap costs comparing with the thick adherends samples, especially when a large number of samples needs to be tested.
- Installing the double lap joints into the testing machine after conditioning (heating or cooling) them in a separate climate chamber located near to the testing machine is easier and faster than for the thick adherends specimens. This is an important point to guarantee that the temperature will not be lost during the installing and testing processes.
- No special or expensive equipments and devices are required as it is in the case of the thick adherends shear tests.
- Both double lap and thick adherends shear tests are mainly used as typical low-peel production-type structural joints [49]. Moreover, the relatively high strength of the steel adherends that are used can also help to reduce the peel stresses.
- The manufacturing and preparing thick adherends from galvanized steel, which is selected to be the adherends, is more difficult and expensive. Another advantage is that the failure modes of these adhesively bonded joints can therefore be seen and described for the galvanized steel used.
- The bonded area recommended for the thick adherends test is very small (the overlap length is only 5 mm) which needs a special skill, not only in manufacturing but also in bonding process to avoid the existence of the voids within the adhesive layer, which could result in reducing the shear strength.

4.3.1 Studied joints

Double lap shear joints shown in Figure 4.5 were proposed. The external and internal galvanized steel plates are 1 mm and 2 mm thick respectively. Two thicknesses of the adhesive layer to be studied were 0.35 and 0.65 mm. These thicknesses were achieved by the use of one-sided adhesive strips of 12 mm wide. Using such strips were preferred more than the other methods such as glass balls or fine wires, which are usually used for this target, because the bonded area will not be reduced or affected by adding the glass balls or wires. To accommodate these strips, the width of the adherends had to be increased to 40 mm (25.4 mm is the recommended value in the standard [49]) and the width of the bonded area was reduced to 16 mm. This reduction was also decided in order to account for adjusting the bonded area here to be as similar as the ones which will be used later for the long-term loading tests, see chapter 5. The reduction of the width of the bonded area has to be taken into account because it will result in concentrating the normal stresses at the edge of it. To verify that there is no fear with using such a width, i.e. the steel will not yield before the adhesive fails, a numerical study (FEM simulation) by the use of the commercial software ABAQUS was done by the author [52].

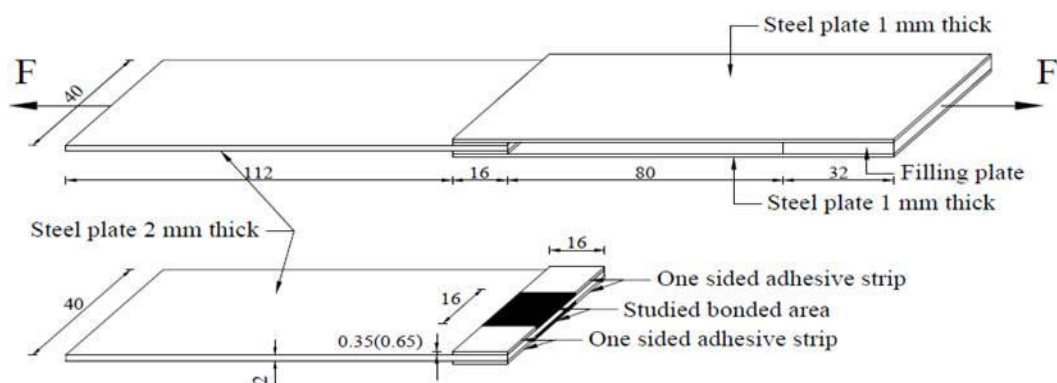


Figure 4.5: Double lap shear joints (black areas represent bonded areas)

The length of the bonded area was chosen to be also 16 mm; hence a bonded area of 16 mm × 16 mm for each side was obtained.

To prevent the squeeze-out adhesive from participating in carrying a part of the shear stresses, transparent tapes after the overlap region on each side were used. Small pieces of 32 × 40 mm of 2 mm thick steel were used as fillers which bonded in between the external plates at the other side as shown in Figure 4.5. To provide the straightness of these external plates, pieces of the same strips were put on the fillers on both sides before being bonded.

4.3.2 Surface preparation

Great care has to be given to the surface preparation process. It is known that the best bond strength required and the highest environmental resistance desired need the surfaces to be sufficiently prepared. This means that substrates should be clean, dry and free of paint, oxide

films, dust, mold release agents and all other surface contaminants. The degree of surface preparation varies from one adhesive to the other. 3M Scotch-Weld™ low-odor acrylic adhesives can bond oily metal and other substrates with very little surface preparation. More surface preparation is needed for the epoxy. Usually for bonding metals, it is recommended to follow special procedure to prepare the surfaces of the substrates, one of the steps of this procedure is to sandblast or to abrade the surface by the use of clean fine grit abrasives; however, for galvanized steel, this procedure cannot be used to keep the galvanized layer safe. Therefore, the surfaces of the plates were prepared by wiping them with acetone as an oil-free solvent. The wiping process was repeated for three times using clean tissues. After each time the surface was left to dry for enough time. Removing the particles of the tissues was done by blowing air to the cleaned surfaces before applying the adhesive.

4.3.3 Bonding, conditioning and testing the joints

After the areas of the adherends, areas between two parallel strips (see Figure 4.5), were prepared to be bonded, the adhesives were applied using a special gun applicator which pushes the adhesive and the hardener in the correct proportions through a pre-mixing nozzle. The adherends, then, were aligned and pressed by a sufficient weight, amounts to 0.5 Kg, on the upper adherend during the time to handling strength recommended for each adhesive. Thereafter, the specimens were left (7 days for EP and 5 days for AC) at room temperature to be cured.

Similar to the procedure followed by [53], fully cured bonded specimens were put in a climate chamber for 24 h at the desired temperature for conditioning. Then specimens were tested by means of a tensile testing machine. The installation of a specimen up to the end of the test was done within 2 minutes. Temperature was measured using a laser thermometer at the surface of the specimen and only changed with a maximum of 2 °C after being installed in the testing machine out of the climate chamber. Figure 4.6 shows the climate chamber beside the testing machine and the laser thermometer used. Some primary tests were conducted at temperatures of 50 °C and 60 °C; however most specimens failed adhesively, i.e. the separation occurred between the adhesive layer and the steel surface; therefore, the temperature range was decided not to exceed 40 °C below and at which the failure was mostly cohesive (within the adhesive layer) [54]. The tests, after that, were performed at seven temperatures in the range from -20 °C up to 40 °C with a step of 10 °C, this range of temperature can be for the internal use or for conditioned structures. Seven specimens for each temperature were tested.

The speed rate of the crosshead was set to 1.27 mm/min. The longitudinal strain was recorded by the use of an extensometer (MFA 2/ 350 Ohm) which has a range of measurement of 1.8 mm as shown in Figure 4.7.



Figure 4.6: Test equipments
Left: the climate chamber and the testing machine. Right: the laser thermometer used for measuring the temperature at the surface of the specimen



Figure 4.7: Test set-up and the used extensometer

4.3.4 Shear behaviour and shear mechanical properties of the adhesives

The recorded strain was used to calculate the shear strain by dividing it by the bondline thickness. However, this strain does not represent the real shear strain of the adhesive material because it includes the normal strain of the adherends; therefore, a further calculation had to be done to correct the measured strain by excluding the normal strain of the steel adherends.

The shear stress was considered regularly distributed over the bondline and calculated by dividing the recorded applied force by the two-sided bonded areas, i.e. $2 \times 16 \times 16 = 512 \text{ mm}^2$.

The shear stress-strain curves were plotted for each case studied, every seven curves that represent the seven samples tested at one temperature was averaged using the built-in techniques available in Excel. These curves are presented in Figure 4.8, in which EP/AC

represents the epoxy/acrylic adhesives respectively and 0.35/0.65 indicates the thicknesses (in mm) of the adhesive layer tested.

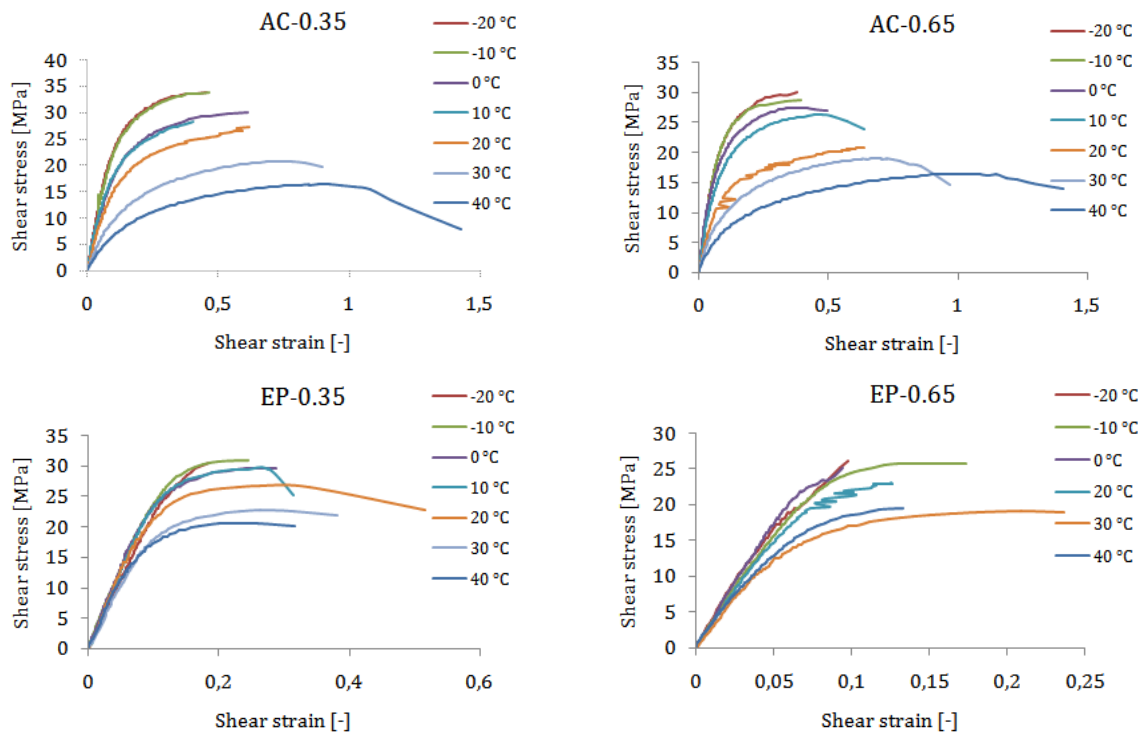


Figure 4.8: Averaged shear stress-strain curves of the adhesives at the studied temperatures

These curves generally show that the shear strength of the adhesives is higher when the thickness is less and it decreases with the increase of the temperature. For the acrylic adhesive, it is clear that it becomes more ductile when the temperature increases; however, it is not the case of the epoxy. This is attributed to the fact that it failed in brittle in many cases. It is worthwhile to mention that all specimens failed either cohesively (CF) or special cohesively (SCF) [54], [55] (see section 10.2.1 in appendix B). Types of the observed failure modes of the samples are seen in Figure 4.9.

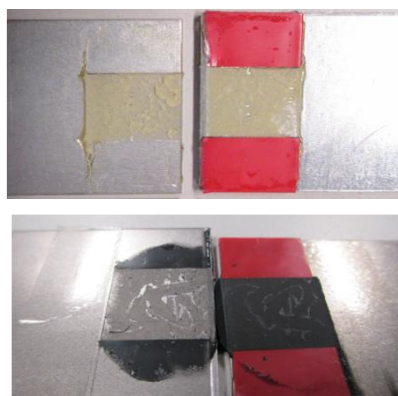


Figure 4.9: Failure modes: AC (above) and EP (below)

To clarify the effect of the temperature on the shear mechanical behaviour of the studied adhesives, mechanical properties of the materials have to be reported as functions of the temperature.

The shear modulus G was estimated by taking the slope of the linear portion of the curve at the shear strain interval up to 0.03.

The maximum shear strength (τ_{max}) and its corresponding strain ($\gamma_{at \tau_{max}}$), as well as the shear stress at break ($\tau_{at Break}$) with its corresponding strain ($\gamma_{at Break}$) were determined. The mean values of the mentioned mechanical properties and their standard deviations are available in (section 10.2.2, appendix B).

Figure 4.10 presents the mean values of the shear modulus G with the standard deviations at each temperature. A linear trend line was assigned here in order to give good understanding about the tendency of this property with the temperature.

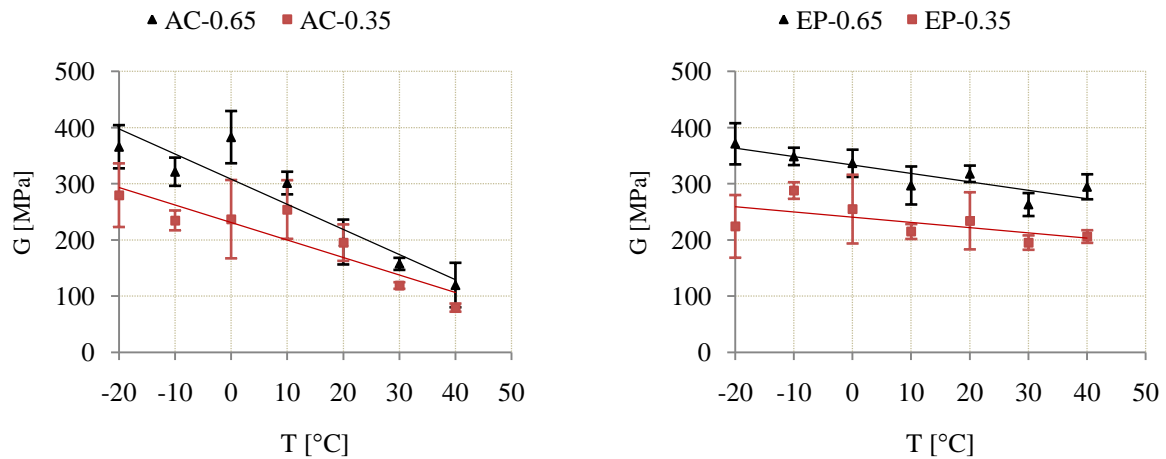


Figure 4.10: Shear modulus G of the adhesives and its tendency

It is shown in Figure 4.10 for all cases, the shear modulus tends to decrease with the increase of the temperature. Moreover, in case of greater thicknesses, higher rigidity of the material is expected. For the comparability purpose, G values of the materials of the same thickness were plotted together in Figure 4.11 to highlight the difference between the rigidity of epoxy adhesive and acrylic adhesive over the range of temperature studied.

Similarly, Figure 4.12 represents the tendency of the maximum shear strength (τ_{max}) and its corresponding strain ($\gamma_{at \tau_{max}}$), while the shear stress at break ($\tau_{at Break}$) with its corresponding strain ($\gamma_{at Break}$) are shown in Figure 4.13.

From Figure 4.12, it can be seen that the maximum shear strength values (τ_{max}) are also higher for the greater thicknesses and that they decrease as the temperature increases. While the shear strain values corresponded to (τ_{max}), i.e. ($\gamma_{at \tau_{max}}$), have ascending tendency with the increase of the temperature. This proves the fact that the materials become more ductile when they are heated. It is noticeable that the values of ($\gamma_{at \tau_{max}}$) for the thickness of 0.35 mm are in most cases, except the acrylic adhesive at 40 °C, higher than those of 0.65 mm, it

can indicate that adhesives of smaller thicknesses behave in a ductile manner more than those of the higher thicknesses.

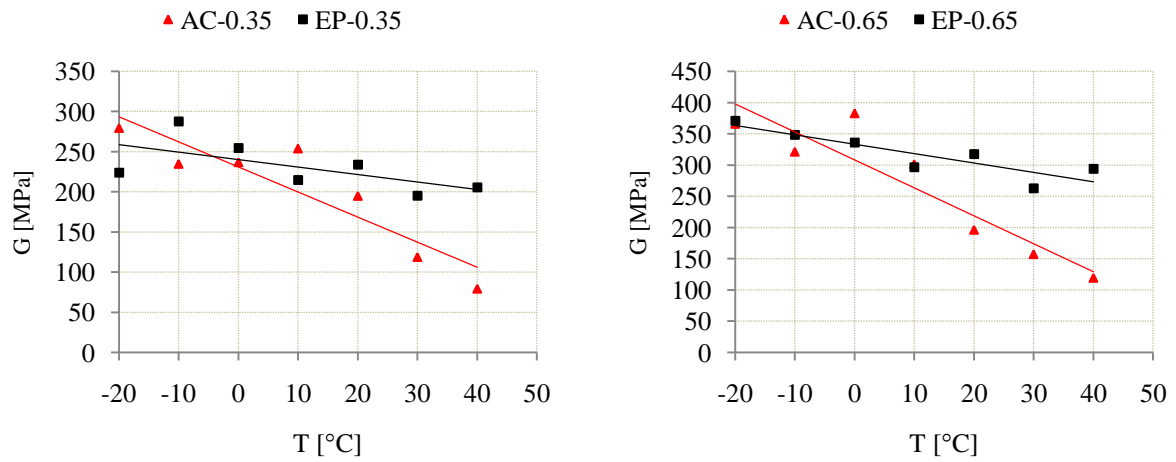


Figure 4.11: Comparison of the rigidity of the materials over the temperature range

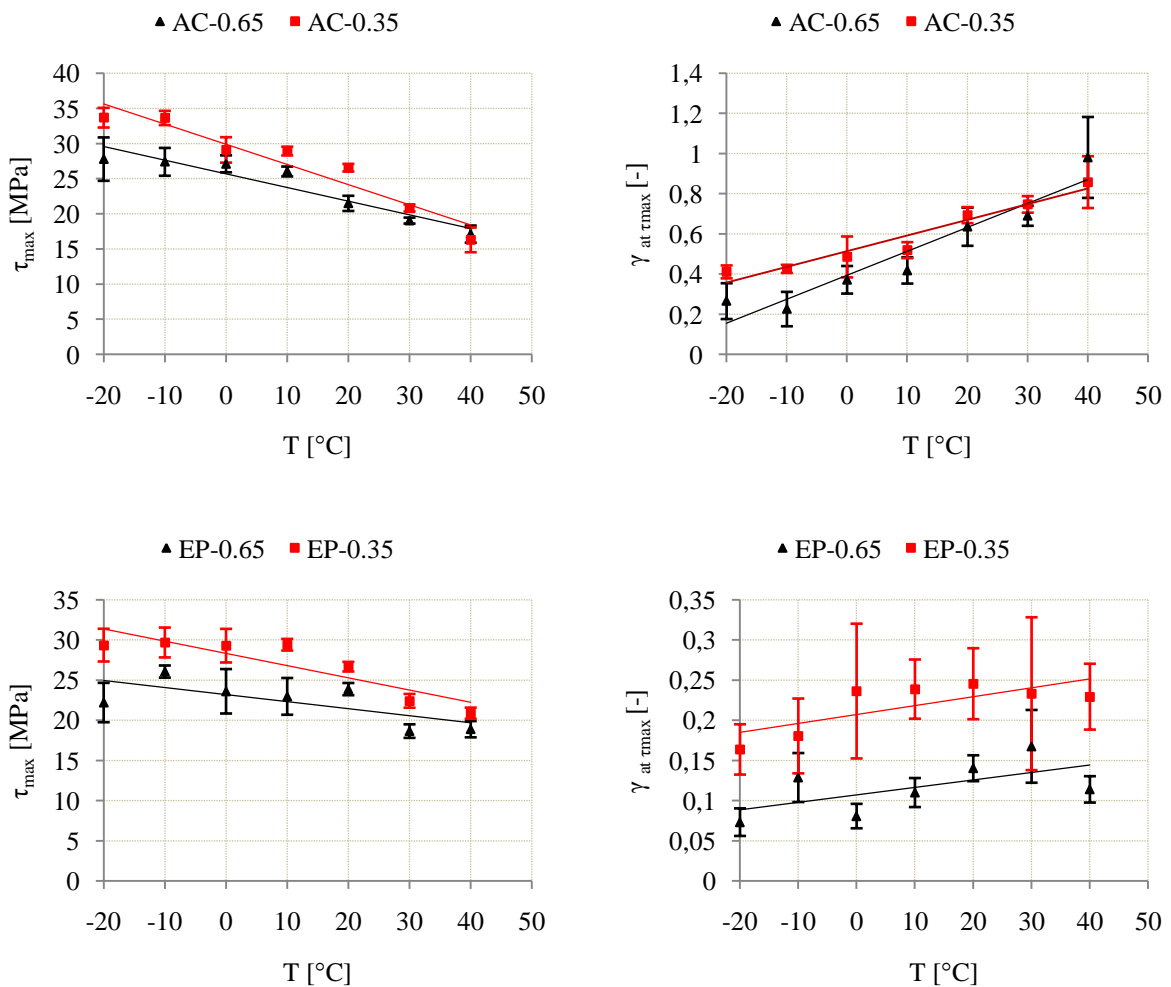


Figure 4.12: Mean values of (τ_{max}) and ($\gamma_{at \tau_{max}}$) with their tendency

Almost the same conclusions can be derived from Figure 4.13 for the shear stress values at break ($\tau_{at\ Break}$) with their corresponding strain values ($\gamma_{at\ Break}$); however, ($\gamma_{at\ Break}$) for acrylic adhesive at temperatures higher than 20 °C is greater for the thickness of 0.65 mm. Furthermore, the strain at break values ($\gamma_{at\ Break}$) for epoxy adhesive is much scattered. This is because epoxy fails in brittle. The difference in the behaviour of both adhesives is clear when the values of all shear strains of epoxy adhesive and the matching values of the acrylic are compared to each other; one can conclude how brittle the epoxy adhesive is; while the acrylic is ductile.

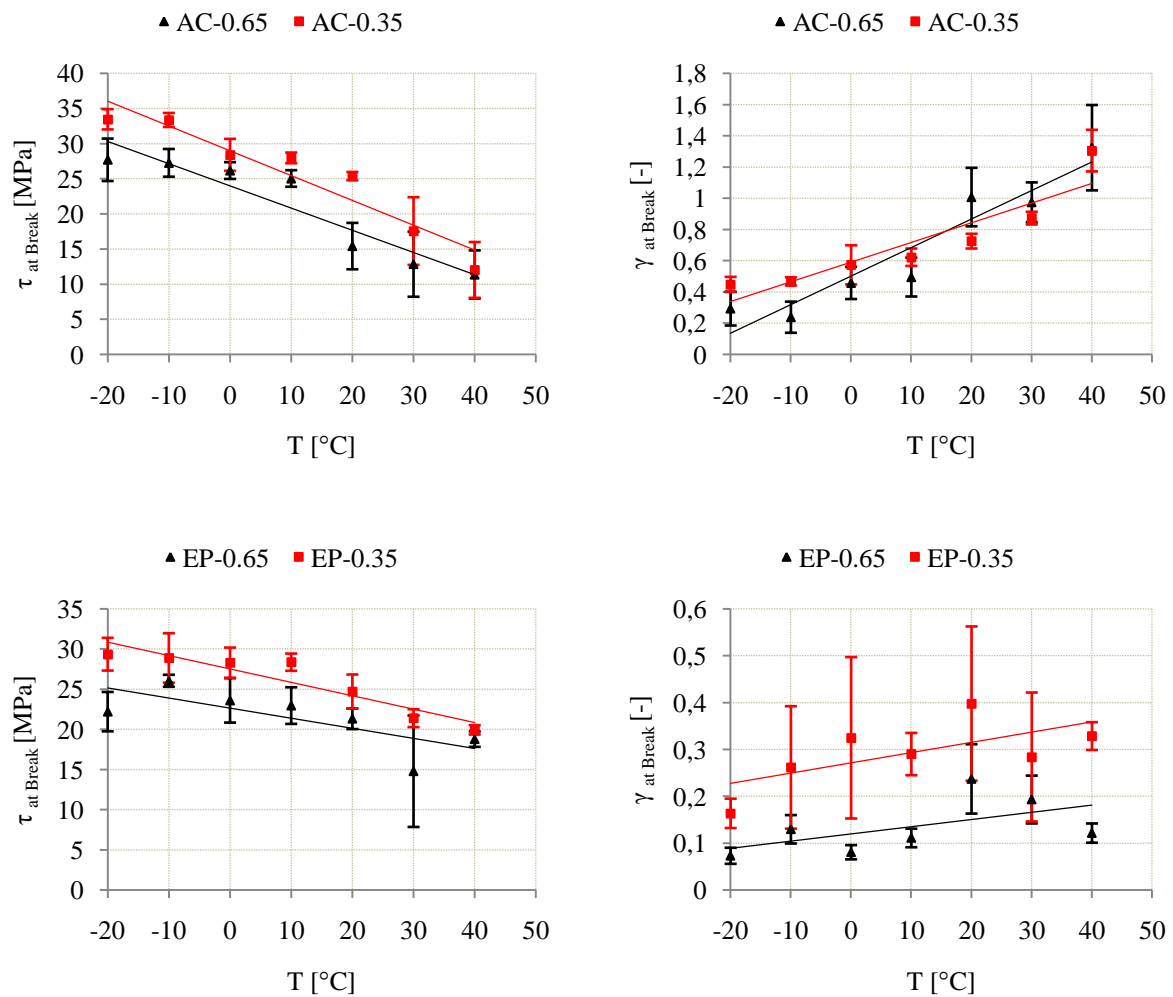


Figure 4.13: Mean values of ($\tau_{at\ Break}$) and ($\gamma_{at\ Break}$)

4.3.5 Verification of the shear strength results

The shear strength results are compared to those available in the final report of [56] and to the data reported by the manufacturer, as shown in Table 4.2. It is known that if the thickness of the adhesive layer is greater, then the strength is likely lower. Here, by taking this fact into account, the differences between the comparable shear strength values (for 0.2 mm with 0.35

mm and for 0.5 mm with 0.65 mm) are therefore justified. However, for the acrylic adhesive DP 810 the difference is attributed to the curing period which is longer in this research (see notes ^(*) and ^(**)).

Table 4.2: Comparison of the shear strength results

Shear strength in [MPa] at room temperature ($\approx 23^\circ\text{C}$)	Results of [56]		3M- Scotch-Weld TM	Research results	
	0.2	0.5		0.35	0.65
Thickness [mm]					
DP 490	31.17±0.97	26.41±1.58	26-30.2	26.68±0.59	23.89±0.76
DP 810	-	-	24.82 ^(*)	26.58±0.54 ^(**)	21.5±1.08 ^(**)

^(*) Adhesive is cured only for 24 h, ^(**) Adhesive is cured for 5 days.

4.4 Reliability-based evaluation

4.4.1 General principles on reliability for structures

Partial factors are used in the limit state-based design. The limit state defines the condition beyond which the structure is no longer safe. It is mathematically expressed by:

$$Z = R - E \quad (4.1)$$

in which R is the resistance and E is the action effect.

If $Z > 0$ or $R > E$, then the structure is safe and no failure occurs. The reliability of the structure is validated when the highest predicted action effect is still equal to (or less than) the smallest predicted resistance over the intended lifetime of the structure. This can be expressed by the design and characteristic values of the action effect E_d , E_k and the resistance R_d , R_k :

$$E_d \leq R_d \text{ or } \gamma_E \cdot E_k \leq \frac{\eta \cdot R_k}{\gamma_R} \quad (4.2)$$

where γ_E and γ_R are the partial factors of the action effect and the resistance respectively which take the stochastic nature of the action effect and the resistance into account, while η is the conversion factor that takes into account the change of the resistance over the lifetime intended.

The design values of the action effect and resistance should be defined such that the probability of having a more unfavorable value is as follows [57]:

$$P(E > E_d) = \Phi(+\alpha_E \beta) \quad (4.3)$$

$$P(R \leq R_d) = \Phi(-\alpha_R \beta) \quad (4.4)$$

where:

Φ is the standard normal distribution function. β is the target reliability index, and α_E and α_R (with $|\alpha| \leq 1$) are the sensitivity factors of the first order reliability method (FORM). For the ultimate limit state and an intended lifetime of 50 years a target value $\beta = 3.8$ is defined;

this value corresponds to a failure probability ($P_f = 0.00007$). The value of α is negative for unfavorable actions and action effects and it is positive for resistances. α_E and α_R may be taken as -0.7 and 0.8 respectively.

4.4.2 Probability distribution functions

Random variables should be described by probability distributions, which often should be considered as conditional. In many cases these distributions are characterized by main parameters such as mean, standard deviation, skewness and coefficient of correlation in the case of multi-dimensional distribution.

The most common distribution functions used in the structural reliability are normal, lognormal, and Weibull.

In this work, only normal and lognormal distributions will be explained while detailed information about Weibull distribution can be found in [32].

When the density of the random variable (x) is given by equation (4.5), it can be considered normally distributed.

$$f_X(x) = \frac{1}{\sqrt{2\pi}\sigma} e^{-\frac{(x-\mu)^2}{2\sigma^2}} \quad (4.5)$$

Integrating $f_X(x)$ from $-\infty$ up to X determines the cumulative probability function $F_X(x)$ which expresses the probability of being $x \leq \text{specified } X$, equation (4.6):

$$F_X(x) = \int_{-\infty}^X f_X(x) dx = P(x \leq X) \quad (4.6)$$

The parameters μ and σ are the mean and the standard deviation respectively, and can be calculated by equations (4.7) and (4.8) for a sample of n values:

$$\mu = \frac{\sum_{i=1}^n x_i}{n} \quad (4.7)$$

$$\sigma = \sqrt{\frac{\sum_{i=1}^n (x_i - \mu)^2}{n - 1}} \quad (4.8)$$

When μ and σ are equal to 0 and 1 respectively, the distribution will become standard and its probability density function (P.D.F) will become as given in (4.9):

$$f_X(x) = \frac{1}{\sqrt{2\pi}} e^{-\frac{x^2}{2}} \quad (4.9)$$

While the probability $P(x \leq X)$ becomes as presented in equation (4.10):

$$F_X(x) = P(x \leq X) = \Phi\left(\frac{x - \mu}{\sigma}\right) = \Phi(z) \quad (4.10)$$

$\Phi(\cdot)$ is the standard normal distribution function, and $z = \frac{x-\mu}{\sigma}$ is the standardized value of x .

The lognormal distribution function is the normal distribution of the natural logarithmic values of the random variable (x_i).

4.4.3 Goodness of fit (GoF)

In order to obtain valid results, it is necessary to verify that a data set follows a proper distribution. One of the most common tests used in practice to test normality of the distribution of a data set is Anderson–Darling test, which also can be applied for Log-normality assumption after Log-transferring the original data [58].

The Anderson-Darling test (AD test) for normality has the functional form given by the equation (4.11) [58]:

$$AD = \sum_{i=1}^n \frac{1-2i}{n} \{\ln(F_0[z_i]) + \ln(1 - F_0[z_{n+1-i}])\} - n \quad (4.11)$$

where (n) is the sample size and the subscript (i) runs from 1 to n , $F_0[\cdot]$ is the assumed (Normal) distribution with the estimated parameters of the sample (μ and σ), z_i is the i^{th} sorted standardized sample value. Calculated AD value must be compared with the critical value AD^* , equation (4.12), for a confidence level equals to 95%. If $AD \leq AD^*$, then the distribution of the data set is Normal, otherwise it is not Normal distributed.

$$AD^* = \frac{0,752}{\left(1 + \frac{0,75}{n} + \frac{2,25}{n^2}\right)} \quad (4.12)$$

4.4.4 Checking of outliers

The normal and lognormal distributions are two parameters functions. These parameters are the mean value and the standard deviation μ and σ . Since these parameters are strongly affected by the extreme values, it would be very convenient to exclude the values that do not appear to represent the population they were sampled from [59]. To check if there are any of these values, which are called outliers, statistical outliers tests have to be used. Three common statistical outliers tests are commonly used for this purpose: Z-test, discordance test, and Dixon extreme value test [59]. The concept of these tests is, if the calculated value (the statistical value from Table 4.3 and Table 4.4) is less than or equal to the critical value of each test, then no outlier exists. The all mentioned tests are valid to be used only when the data without the suspected values (outliers) are normally distributed.

In Dixon's test, the statistical value or ratio ($r_{i,j}$) has to be determined according to the sample size which has to be ($n \leq 30$). The first digit in the subscript of each ratio, $r_{i,j}$, refers to the number of possible suspected outliers on the same end of the data as the value being tested, while the second digit indicates the number of possible outliers on the opposite end of the data from the suspected value. The suspected outliers have to be checked at both ends of the

data set individually. Here, the statistical ratio ($r_{i,j}$) for a sample size of $3 \leq n \leq 7$ is given in Table 4.4 while for other sizes, they are found in [60] and [61].

Dixon's critical values, which were developed and corrected with accuracy of $\pm 0,002$ by [61], are used here.

Table 4.3: Statistical and critical values of Z-test and discordance test

Statistical value		Critical value
Z test	$Z_{Statistic} = \frac{ Mean - outlier }{\sigma}$	$Z_{Critical} = 2 \sim 3$
Discordance test	$D_{Statistic} = \frac{ Mean - outlier }{\sigma}$	$D_{Critical}$ From (section 10.2.3, appendix B)

Table 4.4: Statistical and critical values of Dixon's test for a sample size of $3 \leq n \leq 7$

Dixon's test	Statistical value*	Critical value** acc. to the sample size (n)	
Considering that $X_{(1)}$ is a potential outlier, statistical $r_{i,j}$ is computed by:	$r_{1,0} = \frac{X_{(2)} - X_{(1)}}{X_{(n)} - X_{(1)}}$	n	$r_{1,0}$
		3	0.941
		4	0.765
Considering that $X_{(n)}$ is a potential outlier, statistical $r_{i,j}$ is computed by:	$r_{1,0} = \frac{X_{(n)} - X_{(n-1)}}{X_{(n)} - X_{(1)}}$	5	0.642
		6	0.56
		7	0.507

* $X_{(1)}$ to $X_{(n)}$ refer to the data set in ascending order.

** Critical values are at a confidence level of 90% (see section 10.2.4 in Appendix B).

4.5 Direct evaluation of the maximum shear strength values

The resistance of the adhesively bonded joints or the shear strength of the adhesives can directly be evaluated from the tests.

If the partial factor format is used, either the classical method, or the Bayesian method may be applied. A mixture of both methods is sometimes used [62]. Here, the determination of the characteristic and design values of the maximum shear strength results and then the corresponding partial factors are based on the Bayesian method. This procedure was also followed by [32]. The characteristic and design values R_k, R_d can be determined by Bayesian method as follows:

$$R_k = \mu - t_{v,k} \cdot \sigma_R \sqrt{\left(1 + \frac{1}{n}\right)} \quad (4.13)$$

$$R_d = \mu - t_{v,d} \cdot \sigma_R \sqrt{\left(1 + \frac{1}{n}\right)} \quad (4.14)$$

in which:

μ and σ_R are the mean value and the standard deviation of the shear strength of the adhesive.

$t_{v,k}$ and $t_{v,d}$ represent the coefficients of the Student distribution to be used for estimating the characteristic and design values respectively. They depend on the target probability and the degree of freedom (ν). In the absence of other information, the characteristic value is assumed to be at the target probability of 0.05, [62]. While the design value has to be taken at the target probability corresponds to $\alpha_R\beta = 0.8 * 3.8 = 3.04$.

The degree of freedom (ν) equals to $n-1$, where n is the number of tests or the sample size.

The coefficients of the Student distribution for the desired degree of freedom (ν) and the probability target can be determined by the use of Excel software. Table 4.5 lists $t_{v,k}$ and $t_{v,d}$ values at some specific values of (ν).

Table 4.5: Coefficients of the Student distribution

ν	4	5	6	7	15	25	35	45	46	47	48	49
$t_{v,k}$	2.13	2.02	1.94	1.89	1.75	1.71	1.69	1.68	1.68	1.68	1.68	1.68
$t_{v,d}$	6.86	5.67	5.04	4.64	3.65	3.38	3.28	3.22	3.22	3.21	3.21	3.21

Since this quantity, the shear strength of the adhesive, is a random variable and considered as continuous, it has to be described by a probability distribution. Although Van Straalen [32] had found that Weibull distribution fits the data well for adhesively bonded joints, the normal and lognormal distribution functions will only be used here due to the fact that they are commonly used and recommend by the related standards [57], [62].

According to the previously mentioned procedures, sections from 4.4.2 to 4.4.4, the Anderson-Darling test (AD test) for normality as well as excluding the outliers were done on the experimental results of the maximum shear strength at the studied temperatures. The mean value and the standard value were calculated by equations (4.7) and (4.8). The results of all statistical calculations are shown in (Table 4.6 to Table 4.9) for AC-0.35, AC-0.65, EP-0.35, and EP-0.65 respectively.

The characteristic and design values R_k, R_d of the maximum shear strength of the adhesives can now be determined by applying the equations (4.13) and (4.14). The coefficients $t_{v,k}$ and $t_{v,d}$ should be taken from Table 4.5 considering the degree of freedom ($\nu = n-1$).

For AC-0.35, AC-0.65, EP-0.35, and EP-0.65 the characteristic and design values R_k, R_d at each temperature are listed in Table 4.10 and Table 4.11.

4 Temperature effect on the adhesively bonded lap shear steel joints: Partial factors and conversion factors of the shear strength

Table 4.6: Statistical calculations of the data set of AC-0.35

Temperature [°C]	Distribution	Checking for outliers		Distribution parameters			Anderson-Darling test ^(c)	
		Outliers	Sample size (<i>n</i>)	μ [MPa]	σ_R [MPa]	COV [%]	AD	AD*
-20	Normal	1	6	34.17	0.72	2.09	0.24	0.63
	Log-normal	1	6	3.53	0.02	0.57	0.24	0.63
-10	Normal	0	7	33.66	1.01	3.00	0.25	0.65
	Log-normal	0	7	3.52	0.03	0.85	0.25	0.65
0	Normal	1	6	29.70	1.00	3.37	0.31	0.63
	Log-normal	1	6	3.39	0.03	0.88	0.30	0.63
10	Normal	0	7	28.95	0.62	2.14	0.47	0.65
	Log-normal	0	7	3.37	0.02	0.59	0.46	0.65
20	Normal	0	7	26.58	0.54	2.03	0.20	0.65
	Log-normal	0	7	3.28	0.02	0.61	0.20	0.65
30	Normal	0	7	20.85	0.50	2.40	0.28	0.65
	Log-normal	0	7	3.04	0.02	0.66	0.28	0.65
40	Normal	0	7	16.31	1.75	10.73	0.42	0.65
	Log-normal	0	7	2.79	0.10	3.58	0.38	0.65

^(c) See Eq. (4.11) and Eq. (4.12).

Table 4.7: Statistical calculations of the data set of AC-0.65

Temperature [°C]	Distribution	Checking for outliers		Distribution parameters			Anderson-Darling test ^(c)	
		Outliers	Sample size (<i>n</i>)	μ [MPa]	σ_R [MPa]	COV [%]	AD	AD*
-20	Normal	2	5	29.51	0.44	1.49	0.22	0.61
	Log-normal	2	5	3.38	0.01	0.30	0.21	0.61
-10	Normal	0	7	27.42	1.98	7.22	0.51	0.65
	Log-normal	0	7	3.31	0.07	2.11	0.55	0.65
0	Normal	0	7	27.13	1.21	4.46	0.37	0.65
	Log-normal	0	7	3.30	0.05	1.52	0.41	0.65
10	Normal	0	7	26.58	0.54	2.03	0.20	0.65
	Log-normal	0	7	3.28	0.02	0.61	0.20	0.65
20	Normal	0	6	21.50	1.08	5.02	0.37	0.63
	Log-normal	0	6	3.07	0.05	1.63	0.36	0.63
30	Normal	0	7	19.06	0.43	2.26	0.27	0.65
	Log-normal	0	7	2.95	0.02	0.68	0.28	0.65
40	Normal	1	6	16.72	0.58	3.47	0.22	0.63
	Log-normal	1	6	2.82	0.03	1.06	0.22	0.63

^(c) See Eq. (4.11) and Eq. (4.12).

Table 4.8: Statistical calculations of the data set of EP-0.35

Temperature [°C]	Distribution	Checking for outliers		Distribution parameters			Anderson-Darling test ^(c)	
		Outliers	Sample size (<i>n</i>)	μ [MPa]	σ_R [MPa]	COV [%]	AD	AD*
-20	Normal	0	7	29.36	2.04	6.95	0.45	0.65
	Log-normal	0	7	3.38	0.07	2.07	0.45	0.65
-10	Normal	0	7	29.69	1.86	6.26	0.53	0.65
	Log-normal	0	7	3.39	0.06	1.77	0.57	0.65
0	Normal	0	7	29.29	2.09	7.14	0.31	0.65
	Log-normal	0	7	3.38	0.07	2.07	0.32	0.65
10	Normal	1	6	29.68	0.17	0.57	0.59	0.63
	Log-normal	1	6	3.39	0.01	0.29	0.59	0.63
20	Normal	0	7	26.68	0.60	2.25	0.30	0.65
	Log-normal	0	7	3.28	0.02	0.61	0.31	0.65
30	Normal	0	7	22.43	0.86	3.83	0.34	0.65
	Log-normal	0	7	3.11	0.04	1.29	0.36	0.65
40	Normal	0	7	20.88	0.69	3.30	0.26	0.65
	Log-normal	0	7	3.04	0.03	0.99	0.27	0.65

^(c) See Eq. (4.11) and Eq. (4.12).

Table 4.9: Statistical calculations of the data set of EP-0.65

Temperature [°C]	Distribution	Checking for outliers		Distribution parameters			Anderson-Darling test ^(c)	
		Outliers	Sample size (<i>n</i>)	μ [MPa]	σ_R [MPa]	COV [%]	AD	AD*
-20	Normal	0	7	22.21	2.45	11.03	0.20	0.65
	Log-normal	1	6	3.25	0.02	0.46	0.32	0.63
-10	Normal	1	6	25.82	0.40	1.55	0.31	0.63
	Log-normal	1	6	3.25	0.02	0.62	0.32	0.63
0	Normal	0	7	23.62	2.77	11.73	0.34	0.65
	Log-normal	0	7	3.16	0.12	3.80	0.40	0.65
10	Normal	0	7	22.98	2.29	9.97	0.28	0.65
	Log-normal	0	7	3.13	0.10	3.19	0.31	0.65
20	Normal	0	7	23.89	0.76	3.18	0.33	0.65
	Log-normal	0	7	3.17	0.03	0.95	0.31	0.65
30	Normal	2	5	18.83	0.19	1.01	0.36	0.61
	Log-normal	2	5	2.94	0.01	0.34	0.36	0.61
40	Normal	0	7	18.90	1.01	5.34	0.42	0.65
	Log-normal	0	7	2.94	0.06	2.04	0.46	0.65

^(c) See Eq. (4.11) and Eq. (4.12).

Table 4.10 : Characteristic and design values R_k, R_d at each temperature for AC-0.35 and AC-0.65

Temperature [°C]	Distribution	AC-0.35		AC-0.65	
		R_k [MPa]	R_d [MPa]	R_k [MPa]	R_d [MPa]
-20	Normal	32.61	29.78	28.48	26.19
	Log-normal	32.62	30.02	28.50	26.39
-10	Normal	31.56	28.23	23.31	16.76
	Log-normal	31.60	28.62	23.45	18.38
0	Normal	27.52	23.56	24.62	20.63
	Log-normal	27.58	24.14	24.66	21.22
10	Normal	27.66	25.61	25.46	23.68
	Log-normal	27.69	25.82	25.48	23.83
20	Normal	25.46	23.68	19.15	14.88
	Log-normal	25.48	23.83	19.30	15.86
30	Normal	19.82	18.18	18.17	16.77
	Log-normal	19.85	18.34	18.19	16.89
40	Normal	12.67	6.87	15.45	13.15
	Log-normal	13.07	9.23	15.49	13.49

Table 4.11: Characteristic and design values R_k, R_d at each temperature for EP-0.35 and EP-0.65

Temperature [°C]	Distribution	EP-0.35		EP-0.65	
		R_k [MPa]	R_d [MPa]	R_k [MPa]	R_d [MPa]
-20	Normal	25.13	18.39	17.12	9.02
	Log-normal	25.33	20.09	24.95	23.48
-10	Normal	25.83	19.68	24.95	23.38
	Log-normal	25.15	20.93	24.95	23.48
0	Normal	24.95	18.03	17.87	8.72
	Log-normal	25.18	19.87	18.21	12.17
10	Normal	29.31	28.64	18.23	10.66
	Log-normal	29.31	28.65	18.50	13.18
20	Normal	25.44	23.46	22.31	19.80
	Log-normal	25.46	23.62	22.38	20.17
30	Normal	20.65	17.82	18.40	17.44
	Log-normal	20.68	18.21	18.39	17.48
40	Normal	19.14	17.14	16.80	13.45
	Log-normal	19.47	17.44	16.83	14.03

4.5.1 Determination of the partial factor

The partial factor at room temperature (at 20 °C) can be determined using equation (4.15) and its values are presented in Table 4.12.

$$\gamma_R = \frac{R_k}{R_d} \quad (4.15)$$

Table 4.12: Partial factors of the shear strength of the studied adhesives

AC-0.35		AC-0.65		EP-0.35		EP-0.65	
Normal	Log	Normal	Log	Normal	Log	Normal	Log
1.08	1.07	1.29	1.22	1.08	1.08	1.13	1.11

4.5.2 Determination of the conversion factor

In EN 1990:2002, the conversion factor (η) that takes the additional effects such as the moisture, the temperature effects, etc. is defined by equation (4.16):

$$R_d = \eta \frac{R_k}{\gamma_R} \quad (4.16)$$

The design value at any temperature can be related to the design value at room temperature by the conversion factor (η); therefore, (η) can be estimated by dividing the design value at each temperature by its value at the room temperature. To cover the temperature range studied, the minimum conversion factor η has to be considered. The proposed values of η are presented in Table 4.13.

Table 4.13: Values of the conversion factor (η)

AC-0.35		AC-0.65		EP-0.35		EP-0.65	
Normal	Log	Normal	Log	Normal	Log	Normal	Log
0.29	0.39	0.88	0.85	0.73	0.74	0.44	0.6

4.6 Evaluation of the maximum shear strength values on the basis of an analysis model

The above procedures were applied on small populations. Each one was considered at different temperature. The sample size, therefore, was of seven values as maximum (when no outliers detected). The risk of using such small sample size is when there is an extreme value relative to the rest values of the data set which is not detected by the “checking of outliers” tests. Hence, the parameters of the normal and log normal distributions used will be affected by these extreme values. This will normally result in getting a high scatterband that will surely affect the characteristic and design values as well as the partial factor accordingly calculated. To avoid having such problem, using a larger population that contains same features of the samples is recommended.

In our case, four larger populations are created by merging the data obtained for all temperatures. Each of them has the results of the specimens of the same adhesive material and the same thickness of the adhesive layer. These populations are: AC-0.35(M), AC-0.65(M), EP-0.35(M), and EP-0.65(M). The letter (M) indicates the merged data. Every population has now about 49 values.

One of the methods to evaluate the results of the tests is the analysis model-based method that can be implemented by the procedures explained in [57] and [62]. Van Straalen in his PhD-study has developed a systematic approach for reliable design rules for bonded joints [32].

The analysis models to describe these populations are formulated by considering that the shear strengths are functions of the temperature. i.e. $\tau_{max} = f(T)$; therefore, the mean values of (τ_{max}) at each temperature versus the corresponding temperature (T) were graphically plotted. The prediction models were then found by a regression analysis using Excel software as shown in Figure 4.14 (for AC-0.35(M) and AC-0.65(M)) and in Figure 4.15 (for EP-0.35(M) and EP-0.65(M)).

The uncertainties of the models can also be expressed by plotting the test results versus the results obtained from the models. It can be seen in Figure 4.16 which exhibits the models uncertainties that the proposed models fit well with the data sets.

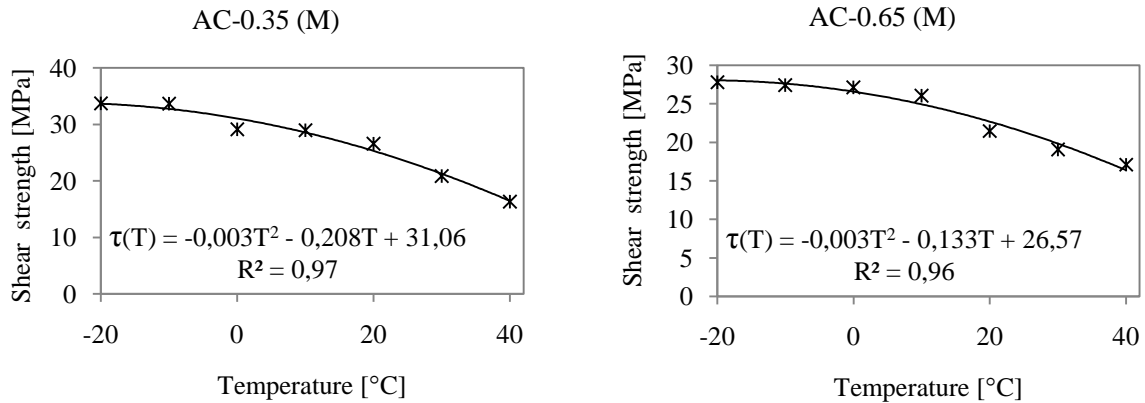


Figure 4.14: Shear strength vs. temperature for AC-0.35(M) and AC-0.65(M)

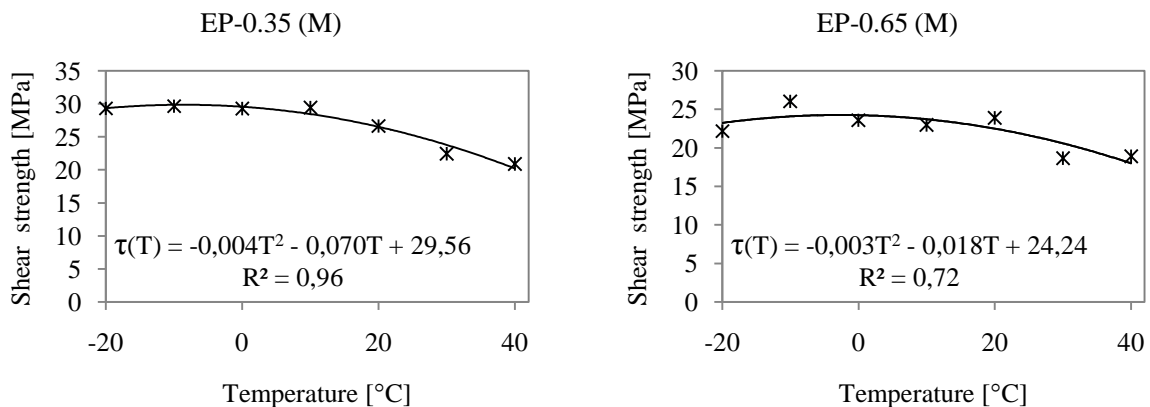


Figure 4.15: Shear strength vs. temperature for EP-0.35(M) and EP-0.65(M)

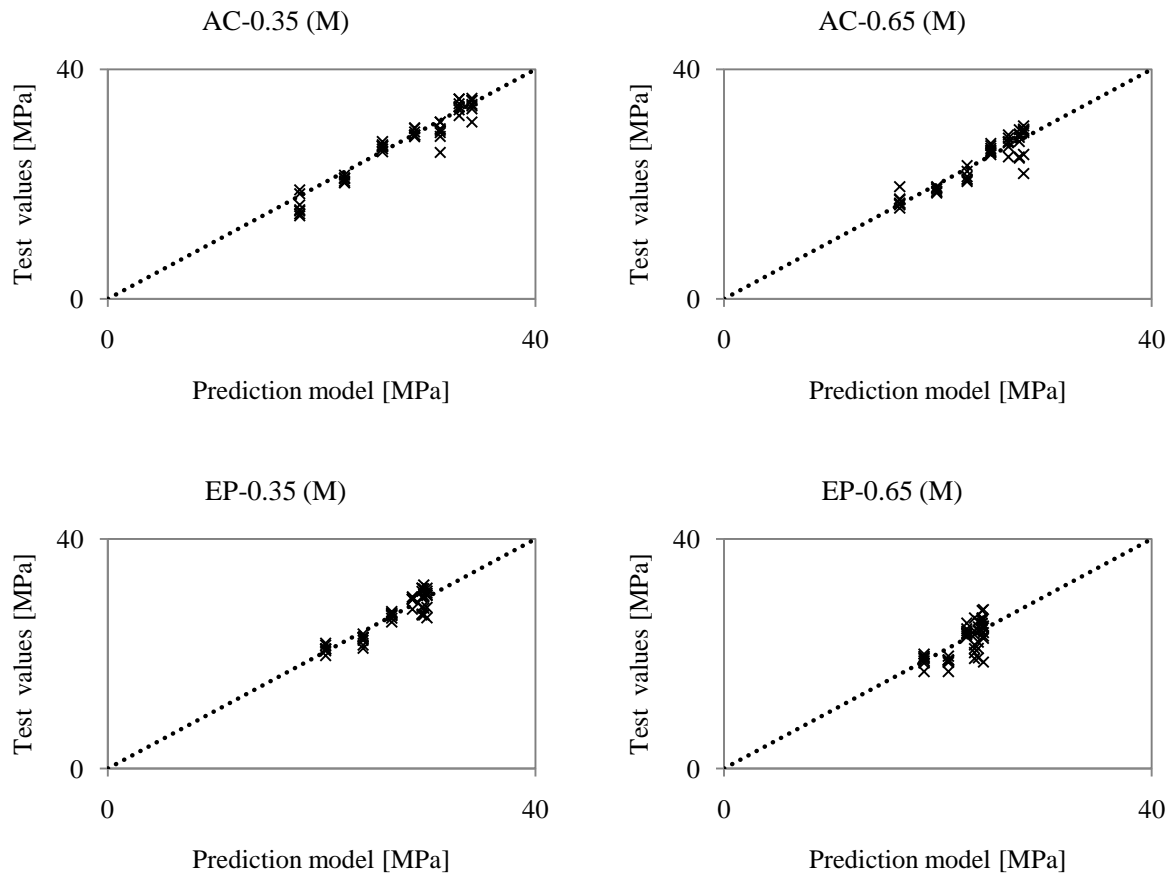


Figure 4.16: Comparison of test values with models values

To evaluate the test results by the proposed models, the methodology developed by Van Straalen, I. J. was used. The first step of the calibration process is to quantify the differences between the test values $R_{test,i}$ and the corresponding values calculated by the model $R_{model,i}$ for each data set by determining the multiplication factors K_i for all data points using equation (4.17):

$$K_i = \frac{R_{test,i}}{R_{model,i}} \quad (4.17)$$

New data sets of the calculated multiplication factors K_i will be obtained and can be statistically treated following the steps explained (in section 4.4.2 to section 4.4.4). To verify that these data sets are normally distributed, the Anderson-Darling test (AD test) was used. K_i sets of AC-0.65(M), EP-0.35(M), and EP-0.65(M) did not appear to be normally distributed; therefore, a simple procedure was done to transform the values to new values that fulfilled the normality test. The transformation procedure followed is:

Data set of:	Transformation formula
AC-0.65(M)	$(K_i)_{new} = [(K_i)_{old}]^2$
EP-0.35(M)	$(K_i)_{new} = [(K_i)_{old}]^4$

EP-0.65(M)

$$(K_i)_{new} = [(K_i)_{old}]^2$$

For checking of the outliers, the Z-test and Discordance test were applied. The statistical calculations including the estimated mean μ_K and standard deviation σ_K of the K_i sets are summarized in Table 4.14.

Applying the Bayesian method, the characteristic and design values of K_i can be determined. Once these values are obtained, a re-transformation process has to be done. Table 4.15 lists the re-transformed characteristic and design values of K_i for each population.

The characteristic and design values of the shear strength at each point can be calculated using the following equations (4.18) and (4.19). The results are summarized in Table 4.16.

$$R_{k,i} = K_K \cdot R_{model,i} \quad (4.18)$$

$$R_{d,i} = K_d \cdot R_{model,i} \quad (4.19)$$

Table 4.14: Statistical calculations of the data sets of K_i

K_i set of:	Distribution	Checking for outliers		Distribution Parameters		Anderson-Darling test ^(c)	
		Outliers	Sample size (n)	μ_K [-]	σ_K [-]	AD	AD*
AC-0.35(M)	Normal	3	46	0.99	0.05	0.73	0.74
AC-0.65(M)	Normal (transformed)	0	48	1.01	0.14	0.68	0.74
EP-0.35(M)	Normal (transformed)	0	49	1.01	0.21	0.71	0.74
EP-0.65(M)	Normal (transformed)	0	49	0.99	0.18	0.73	0.74

^(c) See Eq. (4.11) and Eq. (4.12).

Table 4.15: Characteristic and design values of K_i

	AC-0.35(M)	AC-0.65(M)	EP-0.35(M)	EP-0.65(M)
Characteristic value K_K [-]	0.9	0.88	0.9	0.83
Design value K_d [-]	0.82	0.75	0.76	0.63

4.6.1 Determination of the partial factor

By using equation (4.15), the partial factors at room temperature (at 20 °C) are determined. These values are presented in Table 4.17.

Table 4.16: Characteristic and design values R_k, R_d at each temperature for AC-0.35, AC-0.65, EP-0.35, and EP-0.65

Temperature [°C]	AC-0.35		AC-0.65		EP-0.35		EP-0.65	
	R_k [MPa]	R_d [MPa]	R_k [MPa]	R_d [MPa]	R_k [MPa]	R_d [MPa]	R_k [MPa]	R_d [MPa]
-20	30.62	27.90	24.67	21.02	26.42	22.31	19.42	14.74
-10	29.56	26.93	24.29	20.70	26.87	22.69	20.02	15.20
0	27.95	25.47	23.38	19.93	26.60	22.47	20.12	15.27
10	25.81	23.52	21.95	18.71	25.61	21.63	19.72	14.97
20	23.13	21.07	19.98	17.03	23.90	20.19	18.82	14.29
30	19.91	18.14	17.49	14.91	21.47	18.13	17.43	13.23
40	16.15	14.71	14.48	12.34	18.32	15.47	15.54	11.79

Table 4.17: Partial factors of the shear strength by calibrating the proposed models

AC-0.35	AC-0.65	EP-0.35	EP-0.65
1.10	1.17	1.18	1.32

4.6.2 Determination of the conversion factor

The conversion factor η is calculated by equation (4.16) which relates the design value at any temperature to the design value at room temperature. To cover the temperature range studied, the minimum conversion factor η has to be taken, see Table 4.18.

Table 4.18: Values of the conversion factor η

AC-0.35	AC-0.65	EP-0.35	EP-0.65
0.69	0.72	0.76	0.82

4.7 Conclusions

In this chapter, the investigation of lap shear galvanized steel joints bonded by two different structural adhesives from 3M Scotch-Weld™ (Epoxy DP 490 and toughened acrylic DP 810) is presented. Two thicknesses of the adhesive layer were used 0.35 mm and 0.65 mm.

The galvanized steel was tested in tension in order to obtain the mechanical properties of it. The effect of the temperature on the mechanical behaviour and shear properties of the adhesives when the joints are short-term-loaded was the main objective of the investigations.

The investigations were done over a temperature range from -20 °C to 40 °C with a step of 10 °C. The partial factors of the limit states as well as the conversion factors that cover the use conditions and circumstances, particularly the temperature influence, have been determined for the shear strengths of the adhesives. These factors were derived from the representative values (characteristic and design values) of the shear strength. The representative values were determined by evaluating the tests results data at each temperature using the direct evaluation

method according to ISO 2394:1998 and by using analysis models (prediction models) that describe the change of the shear strength of the studied adhesives due to the temperature change according to the standard procedure recommended by EN 1990:2002 together with the systematic approach developed by Van Straalen [32].

Based on the findings, the following conclusions can be made:

- Testing the adhesives with defined surfaces, i.e. in-situ samples, for determining their mechanical behaviour and the material properties is essential for obtaining more realistic illustration not only about the adhesive material, but also about the temperature effect on the adhesion of these materials with the surfaces.
- The maximum shear strength of the adhesive represents the carrying capacity of the joints, since all specimens failed either cohesively (CF) or special cohesively (SCF) with varying degrees due to the change of the temperature.
- The degradation of the shear strength and the shear modulus of the adhesives due to the increase of the temperature is still gradual. This is attributed to the fact that the studied temperature range is below the so-called glass transition temperature T_g after which the adhesive turns from a hard and relatively brittle state into a molten or rubber-like state. For DP 490, the glass transition temperature T_g , is 69 °C [63], while for DP 810, it has not been determined yet; however, it is thought that it is less than of the epoxy.
- The partial factors at room temperature, obtained by both evaluation methods, are relatively close; however, the values obtained by the analysis model method for AC-0.35, EP-0.35, and EP-0.65 are generally higher than the corresponding values obtained by the direct method. While for AC-0.65, the first method gives a higher value with a difference of about 10%.
- The differences between the conversion factors that cover the temperature range are relatively large especially for AC-0.35 and EP-0.65. This can be explained by the high coefficient of variation (COV) of the data points of the small samples (first method) at specific temperatures. For AC-0.35 at 40 °C, COV is equal to 10.73% while for EP-0.65 at 0 °C; COV is equal to 11.73%.
- Regardless of the adhesive kind or the bondline thickness investigated in this study, the maximum partial factor obtained by the direct evaluation method is 1.29 while from the model-based evaluation; the maximum partial factor is 1.32. It was also found that the minimum conversion factor of the temperature effect is 0.29 and 0.69 from the first and second methods respectively.
- The potential of the second method, the analysis model-based evaluation, is that most of the scattered points in the small samples (populations), which could not be detected as outliers to be excluded, will become points of a larger population which is less scattered because of the overlapping of the all data points when merging them. This will lead to obtain design values which are no longer sensitive to these points;

consequently, the results obtained by the second method appear to be more convenient and reliable than those obtained by the first one.

5 Shear creep behaviour of the adhesives used in the lap shear bonded steel joints

5.1 Introduction

In spite of the encouraging properties, by which the structural adhesives are characterized, the use of these materials in the structural engineering fields needs to be validated. This needs intensive test plans to assess both the short-term and long-term behaviours under defined conditions of mechanical and environmental loading. By demonstrating that bonded joints can carry predefined loads over the lifetime of the joint, the engineering industry would become convinced to use such a technique in its applications.

The bonded joint is generally subjected to different conditions such as static loads (short-term and long-term), dynamic (fatigue), and the environmental effects.

The assessment of a bonded joint is not simple when considering all conditions together, however, considering these conditions separately can facilitate the assessment process and gives acceptable results.

The durability of adhesive joints can be assessed by maintaining bonded joints for a specific period of time in a particular environment either dry environment (certain temperatures) or wet environment (humid air or submerging in water or other aggressive liquids) prior to testing. However, more realistic results are obtained when the joint is subjected to a combination of mechanical loading and environmental effects simultaneously.

Long-term assessment is more difficult than the short-term or the accelerated testing because especial techniques and equipments are needed for long time; therefore, the costs and especially when testing a large number of specimens to accommodate all conditions, might increase. However, the long-term testing results, under real conditions, are still more realistic.

The phenomenon of the increase in strain or deformation of a material with time is called creep. This phenomenon occurs when the material is subjected to a constant load over an extended period of time (i.e. time-dependent deformation). The time-dependent deformation increases as the applied load, temperature and relative humidity increase.

Adhesives, as being polymers, are viscoelastic materials that can deform over a period of time at relatively low stress levels and low temperatures. The durability of these materials, therefore, is expected to be reduced due to the loss of their strength that resulted from the creep phenomenon.

Due to the degradation of the adhesive material, the strengths of the bonded joints are prone to degradation with time. The degradation of the adhesive joints is resulted not only from the ageing of the adhesive and the environmental effect (mostly temperature and humidity), but also from the moisture penetrates the interfacial regions [20].

The degree of degradation under combined load and environmental effects can be assessed by two approaches [19]:

- **Rate of strength loss with time (residual strength):** by this approach the time taken for the strength of the joint to degrade to a design stress limit is determined. Below this stress limit, the joint is no longer considered safe.
- **Time-to-failure:** the average lifetime or the percentage of failures of a bonded joint at a specific stress level within a given exposure period is determined by this approach.

In this chapter, the time-dependent behaviour, shear creep behaviour, of double lap galvanized steel joints loaded in shear by tension, is investigated at different temperatures. The studied joints are assembled by bonding the galvanized steel adherends by a rigid structural adhesive (epoxy) and a flexible one (toughened acrylic). Two thicknesses of the bondline (0.65 mm and 0.35 mm) are used. The specimens are tested under different shear stress levels. Well-known rheological and empirical models are used to describe the behaviour of the adhesives. The relevant models parameters are experimentally estimated. The time-to-failure of the studied specimens is predicted for each case in accordance with short-term tests (rapid-loading tests) performed on similar specimens. The applied shear stress for particular lifetimes is proposed. An overview on the degradation of the adhesive shear strength for a specific case is given.

5.2 Viscoelasticity of materials

It is generally known that materials may behave elastically, i.e. they respond immediately to applied or removed stress, or viscously, i.e. they deform continuously when they are affected by stresses, they may also behave viscoelastically, which means that these materials exhibit both elastic and viscous behaviours.

When the viscoelastic material is being loaded and unloaded by constant levels of loads for a period of time, the material will respond and the time-dependent strains can be recorded. The behaviour of a viscoelastic material is considered linear, when the ratio between the applied stresses and the corresponding time-dependent strains at different particular times is constant, otherwise it is considered nonlinear.

Some viscoelastic materials, as polymers or adhesives, exhibit nonlinear behaviour with regard to the level of stress, to which the material is subjected [27].

5.3 Long-term behaviour of the bonded joints

The investigation of an adhesive-bonded joint under different mechanical conditions, different applied variable or constant stresses, and different environmental conditions over a relatively long time is recommended to determine the adhesive behaviour over the time and to estimate the time-to-failure or the loss in its capacity over the time.

The effects of the long-term loading on the deformation of the adhesives are of high importance and have to be accurately described.

In order to account for the long-term behaviour in the reliable design process, the time-dependent deformation has to be predicted over the time with the use of confidential prediction models that accurately describe the behaviour of the adhesives.

The investigations on the time-dependent behaviour of structural adhesives are still modest. Many researchers have focused on the creep behaviour of one of the available structural adhesives, which is the epoxy, and their investigations were set to study the creep behaviour of it in tension loading, see e.g. [30] and [27]. However, the shear creep of epoxy, used to connect fiber reinforced polymer (FRP) to the concrete, was studied and assessed in [64] and [65]. All of them described the long-term behaviour by using rheological models and empirical equations and found the relevant parameters of the used models. In stainless steel lap joints bonded by an epoxy adhesive, the time over which the adhesive resisted sustained loads was recorded and evaluated by [20].

The creep behaviour investigated by the above mentioned researches was obtained by functioning the joint under sustained loads. This kind of long-term tests will be illustrated here, while the other kinds of tests are illustrated in the respective standards.

The creep test of a bonded joint under sustained loads can be done similar to the procedure of (ETAG001-Part five, [66]). The principle of this test method is to maintain the applied load on the joint at a specific level (i.e. at predefined applied stresses, usually taken as ratios of the strength capacity of the same joint under short-term or rapid test). The deformation of the joint, mainly the adhesive, has to be measured until it appears to have stabilized or for at least three months. The frequency of monitoring the deformations (the displacements) has to be high initially in the early stages as the displacements are greatest in these stages and can be reduced with time.

The displacements measured in the tests have to be extrapolated according to a known model. The extrapolated displacements shall be less than the average value of the displacements obtained by reference tests (short-term or rapid tests).

The specimens have to be unloaded when the long-term test is finished and to be tested in the same procedure of the rapid test in order to check the remaining load capacity (joint strength).

To determine the temperature effect on the bonded joints, tests have to be performed at different temperatures, normal ambient temperature, increased temperature, and the maximum temperature of the service temperature range.

Also in ETAG-001(Part 5) for the bonded metal anchors in concrete, three temperature service ranges are defined; one of them is the range from -40 °C to +40 °C. For checking the long-term behaviour, the maximum temperature has to be taken at 0.6 times of +40 °C, i.e. the room temperature. It is known that the temperature in the room may vary by about ± 3 °C due to day/night and seasonal effects but the required test room temperature shall be achieved as an average over the test period.

It is also mentioned that in general, there is no need to check the long-term behaviour of the joints at negative temperatures because the bonded anchors are not affected by these temperatures.

Tests also have to be performed at different conditions such as freeze/thaw condition and changing temperature; for more details see [66].

5.4 Modelling of the creep behaviour of the adhesive

When the adhesive, as being a polymer, is under stress, the polymeric chains will move and over the time needed for the molecules to rearrange themselves under load into a new position, the adhesive will behave the so-called time-dependent behaviour. This behaviour can be described by empirical or mathematical equations and rheological models frequently used to describe this long-term behaviour of polymeric materials [28].

The creep behaviour of viscoelastic materials has been modelled by power-law equations like Bailey-Norton [27] that is given in equation (5.1):

$$\varepsilon(t) = A\sigma^q t^n \quad (5.1)$$

in which $\varepsilon(t)$ is the strain over the time t . The parameters A, q and n have to be found by best fitting the strain-time curve recorded for the applied stress σ .

Another empirical equation, which is frequently utilized to date to define the creep behaviour of polymeric materials, is Findley's approach which has been developed since 1956 [25] and many equations were derived from it till this time. The simplified Findley's model is given in equation (5.2):

$$\varepsilon(t) = \varepsilon_0 + at^b \quad (5.2)$$

where ε_0 is the instantaneous strain or the initial strain at $t = 0$ (measured directly after applying the load), and a and b are constants (tuning factors) evaluated by a regression analysis of the deformations measured during the creep test.

Due to the difficulties in measuring the exact instantaneous strain ε_0 , it can be determined separately by the short-term or rapid-loading test on a specimen of material identical to that used in the creep test being evaluated [25]. The instantaneous strain ε_0 by this way is defined in equation (5.3).

$$\varepsilon_0 = \frac{\sigma}{E_{t(0)}} \quad (5.3)$$

where σ is the applied stress in the creep test and $E_{t(0)}$ is the initial Young's modulus taken from rapid-loading test.

For relatively short-term data, the empirical power-law models seem to fit the viscoelastic behaviour of polymeric materials worthily. However, because of their unlimited retardation spectrum, these models are not able to describe the behaviour for long time [28].

To better understand the creep behaviour of viscoelastic materials, mechanical analogues are used to define this behaviour in terms of physical meaning.

Two well-known mechanical elements being used to create models to describe materials behaviours are: the spring and the dashpot. The first one is a linear elastic element with direct proportionality between stress and strain. While for the second one, the rate of straining is directly proportional to the applied stress.

The use of one spring and one dashpot in series yields the so-called Maxwell model, Figure 5.1(a), while using the two elements in parallel is called Kelvin-Voigt model, Figure 5.1(b).

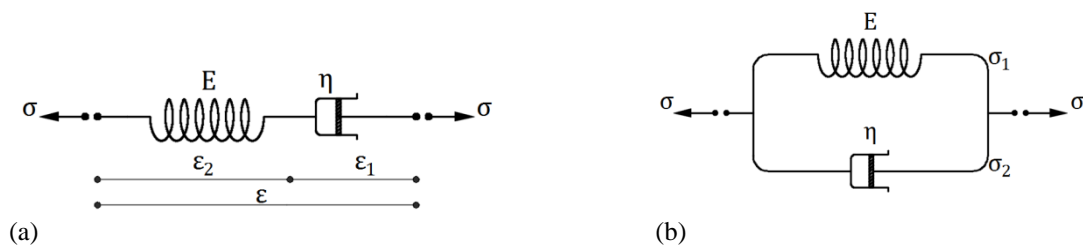


Figure 5.1: Combinations of mechanical analogues for creep behaviour (a) Maxwell model and (b) Kelvin-Voigt model, [24].

For Maxwell model [24], under a constant stress, the stress is identical in the spring and the dashpot. Therefore, the total strain is the sum of the strains of both spring and dashpot. The constitutive equation of this model can be set as given in equation (5.4):

$$\varepsilon(t) = \frac{\sigma}{E} + \frac{\sigma t}{\eta} \quad (5.4)$$

In Kelvin-Voigt model, the strain is identical in both branches and the total stress is the sum of both stresses in the spring and the dashpot. The constitutive equation of this model [24] can be expressed by equation (5.5):

$$\varepsilon(t) = \frac{\sigma}{E} \left(1 - e^{-\frac{E}{\eta}t} \right) \quad (5.5)$$

where E, η represent the elasticity and the viscosity of the spring and the dashpot respectively.

When the two previous models are attached in series, the mechanical Burger's model is created, Figure 5.2(a). This model can better describe the creep behaviour of polymers due to its ability to represent all stages that a loaded material passes through. Equation (5.6) presents the constitutive equation of this model:

$$\varepsilon(t) = \frac{\sigma}{E_M} + \frac{\sigma}{\eta_M} \cdot t + \frac{\sigma}{E_K} (1 - e^{-\frac{E_K}{\eta_K} t}) \quad (5.6)$$

where:

$\varepsilon(t)$ is the strain over the time t . σ is the constant applied stress. E_M, E_K, η_M and η_K represent the elasticity and the viscosity of Maxwell and Kelvin elements respectively. Figure 5.2(b) illustrates the comparison between the mentioned models responses.

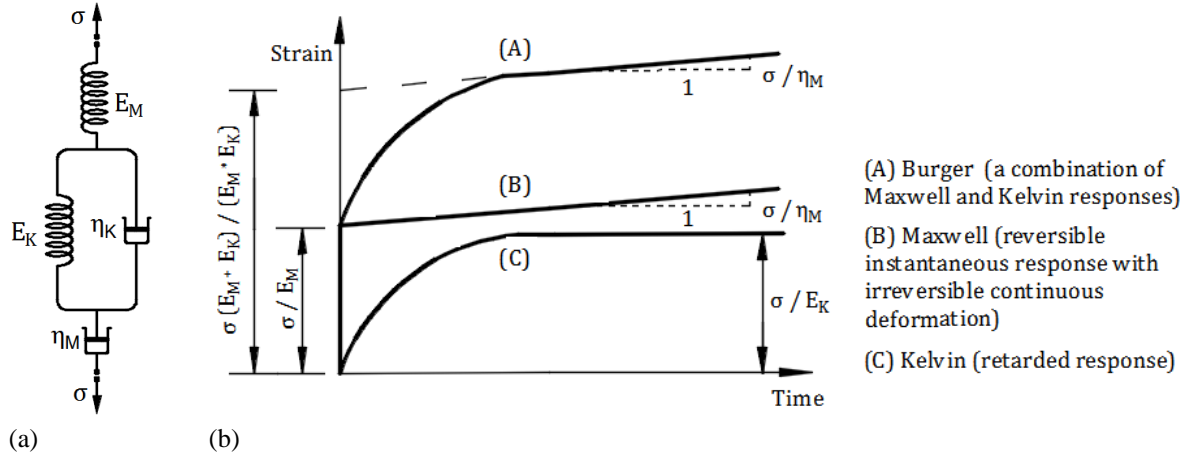


Figure 5.2: Mechanical models for the creep of polymers

(a) Mechanical Burger's model and (b) The comparison between Maxwell, Kelvin, and Burger responses.

It should be mentioned that all above equations are for the tension case. As for the shear case, the same relations can be used after replacing the definitions of the parameters with those being used in shear case, hence, the Findley's and Burger's models to be used in shear case become as written in equations (5.7) and (5.8) respectively:

$$\gamma(t) = \gamma_0 + At^B \quad (5.7)$$

where:

$\gamma(t)$ is the shear strain over the time t , γ_0 is the instantaneous shear strain when $t = 0$ and defined as $\gamma_0 = \frac{\tau}{G_{t(0)}}$, and A and B are constants (tuning factors in the shear case).

$$\gamma(t) = \frac{\tau}{G_M} + \frac{\tau}{\lambda_M} \cdot t + \frac{\tau}{G_K} (1 - e^{-\frac{G_K}{\lambda_K} t}) \quad (5.8)$$

in which τ is the constant applied shear stress; G_M, G_K, λ_M and λ_K represent the shear elasticity and the shear viscosity of Maxwell and Kelvin elements respectively. It is obvious that the first term in equation (5.8) represents the instantaneous shear strain (γ_0) when $t = 0$.

5.5 Creep tests of adhesively bonded joints

5.5.1 Studied joints

Double lap shear joints were selected for creep tests instead of single lap shear joints recommended in [67] and [68] for determining creep properties of metal-to-metal adhesive joints. The double lap joints recommended by (DIN EN ISO 9664-95 [51]) for fatigue tests was used with some adjustments. These adjustments had to be done due to the use of different testing machine and devices for measuring the creep strains of the joints for long time under sustained loads. Moreover, the adjusted joints have two advantages, the applied force will be centrally transferred from one side to the other through the adhesive layers and every specimen has four bonded areas to be tested instead of two. Figure 5.3 shows the proposed joint and its geometry.

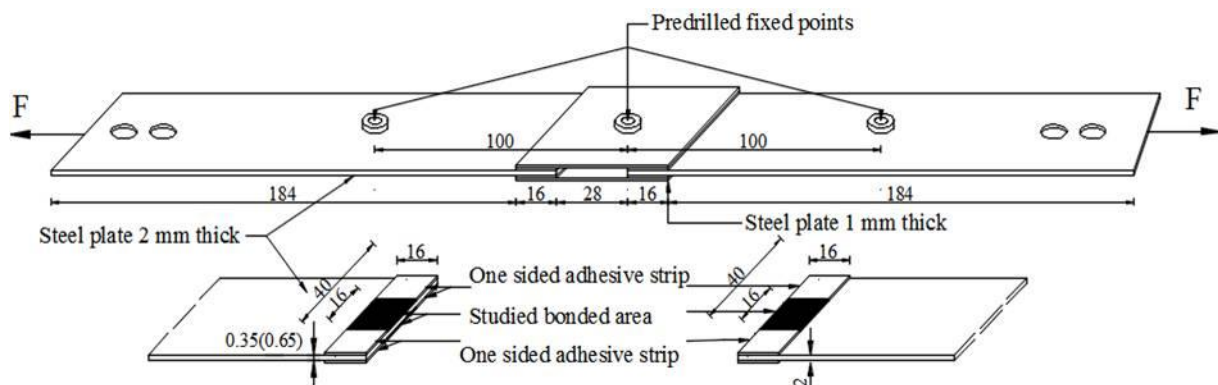


Figure 5.3: Double lap shear joint designed for the creep test (Black areas represent bonded areas)

The external and internal galvanized steel plates (of $D \times 51D + Z (275)$) are 1 mm and 2 mm thick, respectively. The studied adhesives are the structural epoxy and acrylic adhesives (DP 490 and DP 810 respectively). More details about the mechanical properties of materials and the curing process of the adhesives as well as the surface preparation are found in chapter 4.

Two thicknesses of the adhesive layer, 0.35 and 0.65 mm, were selected for testing at room temperature, while only 0.65 mm was chosen for testing at 0 °C and +40 °C.

The joints were made in a way similar to that one used for making the joints of short-term loading. The bonded areas, shown in black in Figure 5.3, are of the same size of the short-term joints, i.e. 16 mm \times 16 mm for each one.

Also the one-sided adhesive strips were used for achieving the adhesive thickness. Thus, pure adhesive layer is obtained.

Preventing the squeeze-out adhesive from participating in carrying a part of the shear stresses was also achieved with the use of transparent tapes after the overlap region on each side. The efficiency of using such tapes was proven during the tests, see Figure 5.4.



Figure 5.4: The efficiency of using the tapes during the tests

5.5.2 Test procedure at the room temperature

The specimens were installed into two creep machines each of them consists of six cantilever steel beams designed to amplify 5 times a given static load. The beams were placed by rollers on truss steel structures which are fixed to the ground of the laboratory; the creep machine is shown in Figure 5.5. These beams were designed to be rigid enough to avoid any possible deflection that may occur at the free ends of the shorter parts. Twelve specimens were able to be tested at once by using these machines.

Three constant shear stresses were used and applied to the specimens and they were chosen to be less than 50% of the maximum short-term shear strength [20] at 20 °C. To guarantee that the received forces at the shorter sides are accurate as possible, the used weights and all equipments were weighed and calibrated by using a tension sensor, attached to a digital screen Figure 5.6 installed where each specimen should be installed.

The temperature and the relative humidity were observed over the test period at different time intervals and found to be around 20 ± 3 °C and 40-50% of R.H. respectively.

The shear deformation was measured by observing the displacement of six gauge points (DEMECs predrilled gauge points) fixed at front and back faces on the specimens. The distances between the points were measured by using a movable digital strain device with 0.001 mm resolution, as shown in Figure 5.7. This procedure was followed by many researchers, e.g. [64], [65], and [69].

The test was repeated twice for a period of at least 3 months for each time (2182 h for the specimens bonded by acrylic adhesive and 2641 h for those bonded by epoxy adhesive) as recommended in ETAG001-part 5 [66]. However, some specimens failed earlier than the intended period as it will be explained later. In every test, four groups (AC-0.35, AC-0.65, EP-0.35, and EP-0.65) were investigated together. Each of them has three specimens loaded by three different shear stresses. The test setup is illustrated in Table 5.1. EP/AC represents the epoxy/acrylic adhesives and 0.35/0.65 indicates the thicknesses (in mm) of the adhesive layer.

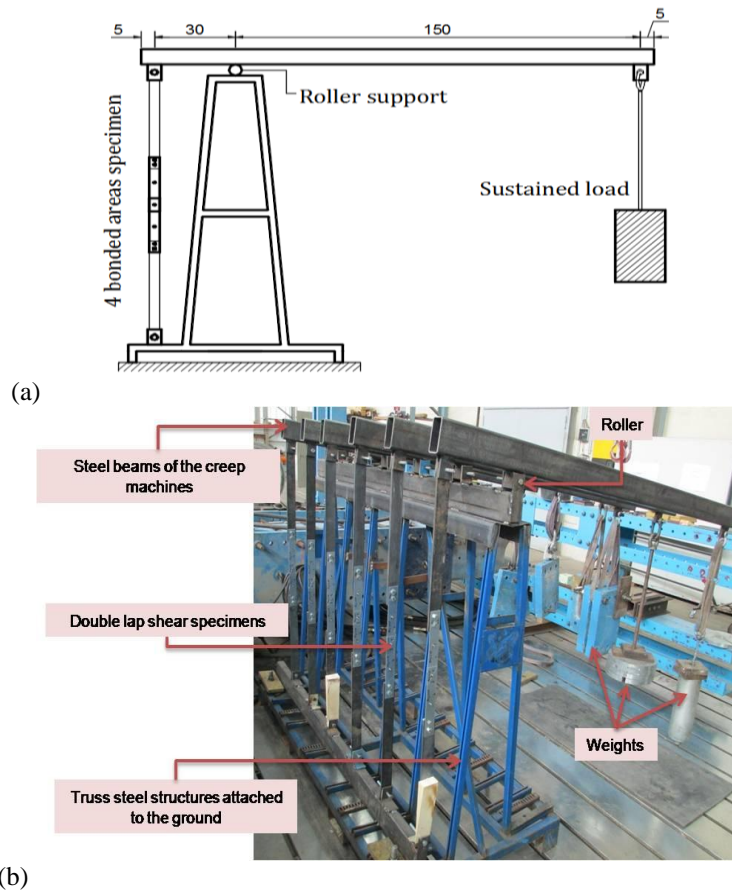


Figure 5.5: Creep machine
 (a) Schematic design of the creep machine (b) Specimens installed into the creep machine

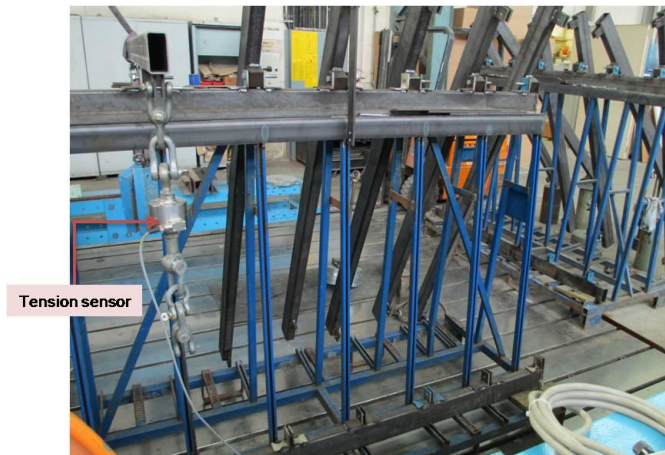


Figure 5.6: Tension sensor used to calibrate the applied loads

The shear stress was considered regularly distributed over the bondline and calculated by dividing the applied force by the two-sided bonded areas, i.e. $2 \times 16 \times 16 = 512 \text{ mm}^2$.

The frequency of measuring the displacements was high initially in the early stages and then it was reduced with time. The shear strain was calculated by taking the average value of the measured displacements (after excluding the normal strain of the steel adherends, see section 4.3.4) and divided by the relevant adhesive layer thickness. The shear strain-time curves were

plotted. Only for the cases of no failure recorded, the best-fitted curves of Findley's and Burger's models were found by the regression analysis provided in Excel software. Due to the fact that the data points are stabilized at the last stages of the curves, it was further suggested that the steady-state creep rate of the test results to be used together with the two other models.

It is well known that the creep strain of the adhesive after the steady-state stage is very rapid and occurs in a shorter time till the fracture (Figure 5.8); however, there is no model which can describe this short stage yet, thus, predicting the creep behaviour and then extrapolating the time-to-failure of an adhesive using the available models is usually based on omitting such a stage, this procedure is also recommended in [66].

Table 5.1: Experimental setup of the shear creep tests

		Adhesive-thickness [mm]	Applied shear stresses [MPa] Level I- Level II- Level III	Studied bonded areas
Test 1 or Test 2	Group 1	AC-0.35	5.74 - 7.66 - 9.57	4 - 4 - 4
	Group 2	AC-0.65	5.74 - 7.66 - 9.57	4 - 4 - 4
	Group 3	EP-0.35	5.74 - 7.66 - 9.57	4 - 4 - 4
	Group 4	EP-0.65	5.74 - 7.66 - 9.57	4 - 4 - 4



Figure 5.7: Long-term shear strain measurement

Six gauge points fixed on front and back surfaces (left). Movable device for measuring the displacements (right).

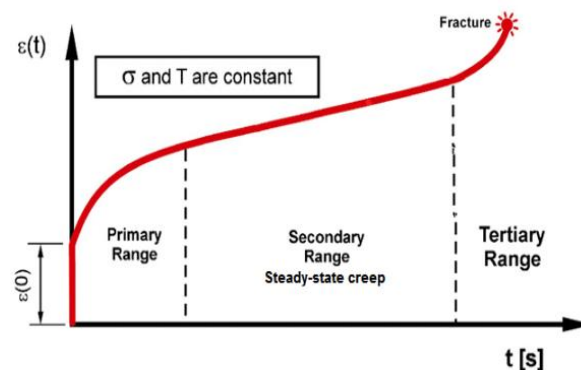


Figure 5.8: Three creep stages, [27]

5.5.2.1 Observations and discussions

During the tests, the following observations and notices were recorded:

- The specimens of AC-0.35 which were loaded by the highest level (level III) of the applied shear stress failed earlier than the intended time of the test (2182 h). The first specimen failed at 94 h and the second one failed at 406 h from the start of loading. It is thought that the reason behind these early failures might be that the specimens were over loaded by a shear stress equals to 36% of the maximum shear stress of the short-term test. In other words, the adhesive was loaded close to the so-called endurance limit.
- It was noticeable, that the adhesive of specimens AC-0.35 loaded by level II strained to an extent ($\gamma = 1.05$) which exceeds the average shear strain of the rapid test ($\gamma_{at\ Break} = 0.73$) with no failure recorded, this might be due to the nature of applying the loads to the specimens, i.e. the applied stress speed, which is in creep test considered completely static, while in rapid-loading test, it is considered quasi-static. The same notice was also recorded for the adhesive of AC-0.35 loaded by level III which strained to ($\gamma = 0.98$) that is higher than ($\gamma_{at\ Break} = 0.73$).
- The specimens of AC-0.65 which were loaded by the second and third levels (level II and level III) of the applied shear stress failed also earlier than the intended time of the test. For level II, the specimen failed at 648 h and the second one at 1416 h. However, for the level III the first specimen failed very soon after about 6.25 h while the second one failed at 360 h from the start of loading. This might also be attributed to that the specimens were over loaded by a shear stress equals to 35.6% (for level II) and 44.5% (for level III) of the corresponding maximum shear stresses of the short-term test.
- Noticeably, the measured displacements were scattered; consequently, the calculated shear strains were also scattered.

5.5.2.2 Creep results of adhesive-bonded joints

The plots of the obtained shear strains versus the time are presented in Figure 5.9, Figure 5.10, Figure 5.11, and Figure 5.12 for AC-0.35, AC-0.65, EP-0.35, and EP-0.65 respectively. It should be noted that where there is no failure recorded, the average shear strain values of the specimens tested were plotted, while for the other case, the shear strains of both specimens were plotted. Moreover, the average shear strains were best-fitted using Findley's and Burger's models (equations (5.7) and (5.8)) by regression analysis. The instantaneous shear strain γ_0 for both models was determined using the shear moduli (G) taken from the rapid-loading tests (in section 10.2.2, appendix B). After that, the parameters (λ_M, G_K , and λ_K) of Burger's model and those of Findley's model (A and B) were found.

The models parameters and the coefficient of determination R^2 of them are listed in Table 5.2 and Table 5.3. It is obvious, that both models well represent the shear creep of the used

adhesives. However, R^2 values generally indicate that Findley's model fits the data points better than Burger's model over the test period.

Table 5.2: Burger's model parameters of the shear creep strains

Applied shear stress	Burger's model parameters				R^2
	G_M [MPa]	λ_M [MPa h]	G_K [MPa]	λ_K [MPa h]	
AC-0.35					
Level I	191.33	3.225E+04	27.98	1537.63	0.964
Level II	191.50	2.652E+04	17.78	945.68	0.964
Level III	-	-	-	-	-
AC-0.65					
Level I	191.33	3.018E+04	24.85	1633.11	0.975
Level II	-	-	-	-	-
Level III	-	-	-	-	-
EP-0.35					
Level I	229.60	6.283E+05	646.33	2.418E+04	0.951
Level II	232.12	4.595E+05	427.75	3.283E+04	0.967
Level III	227.86	2.832E+05	222.53	2.340E+04	0.976
EP-0.65					
Level I	318.89	4.426E+05	367.63	433.36	0.921
Level II	306.40	5.170E+05	317.98	13641.12	0.983
Level III	308.71	3.019E+05	127.89	4593.32	0.887

Table 5.3: Findley's model parameters of the shear creep strains

Applied shear stress	Findley's model parameters			R^2
	γ_0	A	B	
AC-0.35				
Level I	0.030	0.029	0.382	0.994
Level II	0.040	0.070	0.343	0.997
Level III	-	-	-	-
AC-0.65				
Level I	0.030	0.028	0.400	0.998
Level II	-	-	-	-
Level III	-	-	-	-
EP-0.35				
Level I	0.025	0.001	0.476	0.947
Level II	0.033	0.001	0.493	0.966
Level III	0.042	0.003	0.472	0.991
EP-0.65				
Level I	0.018	0.005	0.270	0.923
Level II	0.025	0.004	0.352	0.988
Level III	0.031	0.021	0.243	0.964

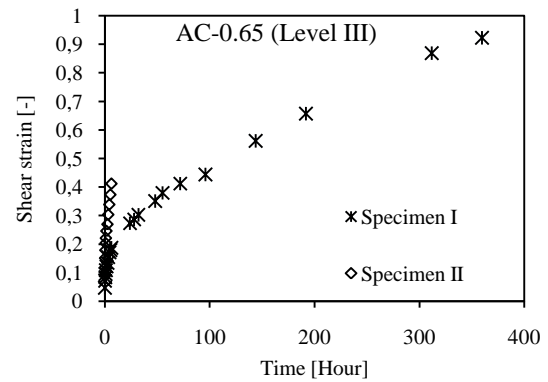
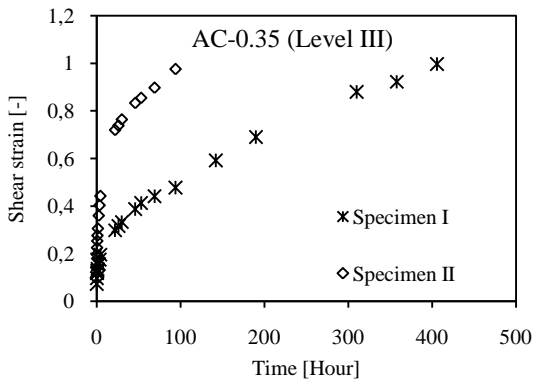
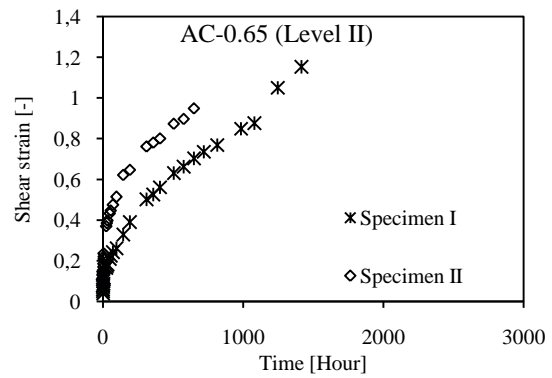
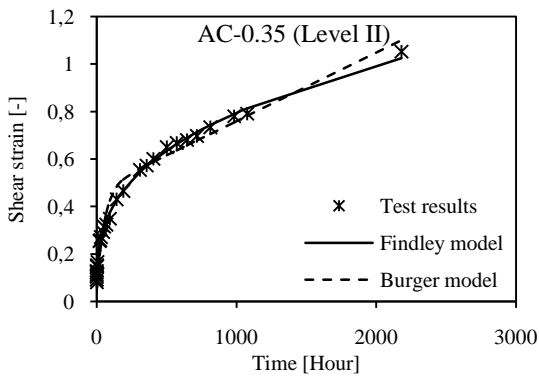
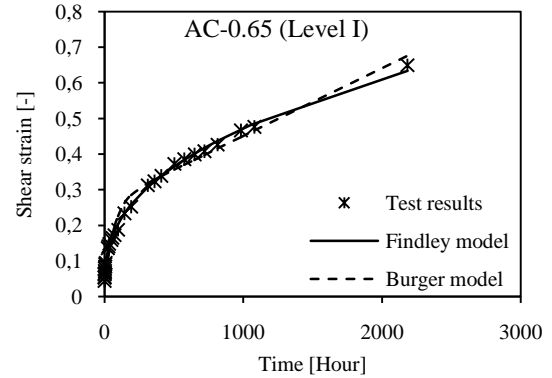
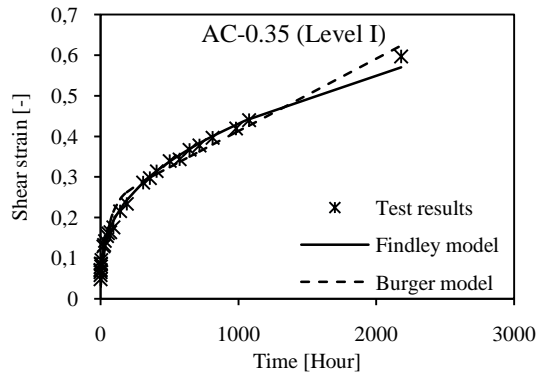


Figure 5.9: Shear creep strains of AC-0.35 at 20 °C Fitted Findley's and Burger's models for the first and second level.

Figure 5.10: Shear creep strains of AC-0.65 at 20 °C Fitted Findley's and Burger's models for the first level.

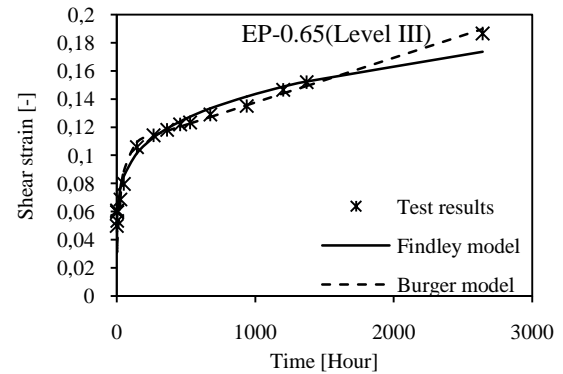
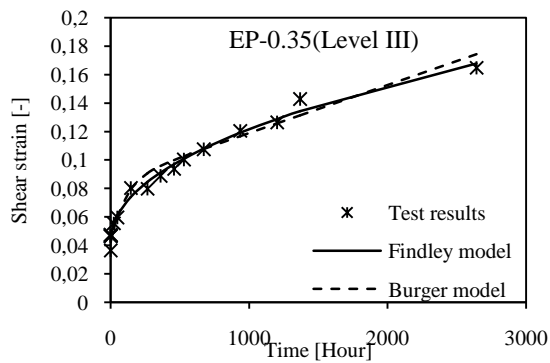
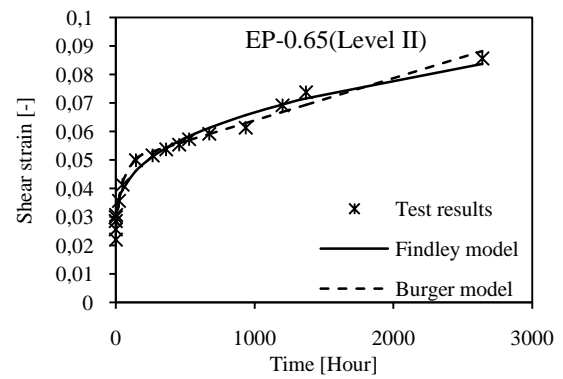
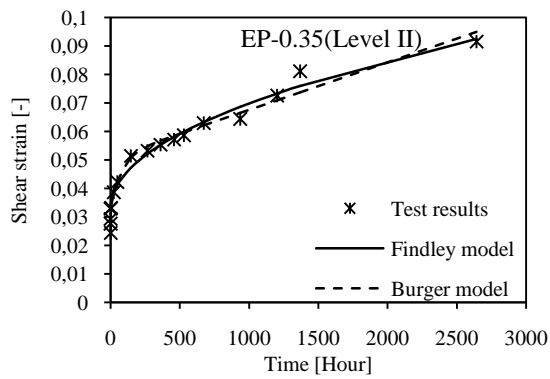
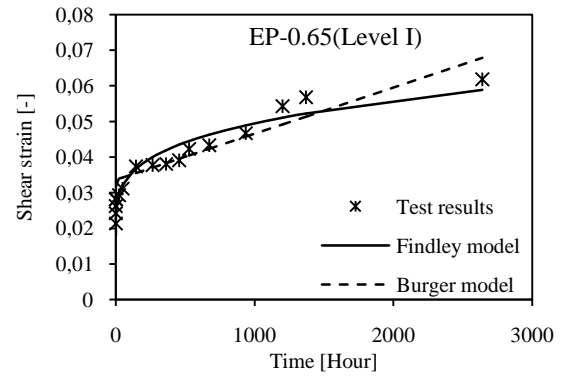
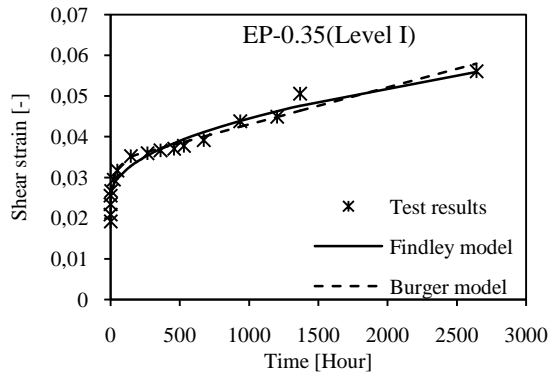


Figure 5.11: Shear creep strains of EP-0.35 at 20 °C and fitted Findley's and Burger's models.

Figure 5.12: Shear creep strains of EP-0.65 at 20 °C and fitted Findley's and Burger's models.

5.5.2.3 The lifetime expectancy of the bonded joints

For the specimens failed during the tests period, the time-to-failure is determined from the time at which the specimens failed, however, for the other specimens, and as recommended in [66], the time-to-failure was estimated using the fitted models, Findley's and Burger's models, assuming that the specimens will fail at the corresponding average shear strain obtained by the rapid-loading tests. However, as it is expected, the time-to-failure estimated by these approaches was associated with a noticeable variation. For this reason and for the sake of comparing the predicted (time-to-failure) obtained by these models with the corresponding one predicted by using another estimation, the principle of the steady-state creep rate is used, [70]. The principle of this method is that the creep rate has to be calculated over the secondary stage of the creep curve, Figure 5.13, where the data points are stabilized, and then the creep rate over this stage can be described by expression (5.9).

$$\gamma_s = \gamma^* \cdot t + a \quad (5.9)$$

in which γ_s is the shear strain of the adhesive at the steady-state stage, γ^* is the creep rate at this stage, and a is a parameter that expresses the intersection point at the shear strain axis.

The parameters of this expression can be estimated using the linear regression analysis of the points which are within the steady stage; therefore, the last three points of the shear creep strains has been taken in order to guarantee that they belong to this stage. This procedure was also done only for the cases where no failure recorded. Table 5.4 lists the parameters obtained by the regression analysis. The relevant short-term mechanical properties and predicted time-to-failure of studied bonded joints are shown in Table 5.5 in which values in brackets refer to the time-to-failure recorded from the test and values denoted by (a) refer to the average value between the real failure time recorded for one specimen and the failure time estimated by the relevant model for the other specimen.

As expected, the epoxy adhesive exhibited a creep strength that is much higher than the acrylic adhesive. It should be noted that an approximate estimation using the three methods was being made during the last month of the test. According to the steady-state creep rate and Burger's model, the second specimen bonded by EP-0.65 loaded by the highest level was supposed to fail at the end of intended test period; however, Findley's model gave much longer time to the failure. Therefore, this specimen was left till the failure happened, which was almost eight days after the last data recorded. This might verify the estimation by Burger's model. However, more tests should be performed for making good judgment. Table 5.6 shows the relative errors committed by using Burger's and Findley's models when compared with the steady-state creep rate approach. It is obvious that Findley's model gives very excessive time values especially for epoxy adhesive. It might, also, be evidence to the disability of Findley's model to describe creep behaviour for longer time due to its unlimited retardation spectrum of this model.

Estimation of the applied shear stress for particular lifetimes:

The normalized shear stresses (see Table 5.5) are plotted in Figure 5.14 as functions of the natural logarithm of the (time-to-failure). It should be noted that the Findley's predictions for epoxy adhesive are excluded. It is obvious, that the plots can be approximated by a straight line fit ([19], [71], and [70]) as follows:

$$\frac{\tau_{app}}{\tau_{max}} = -K \cdot \ln(t_f) + b \quad (5.10)$$

where τ_{app} is the applied shear stress, τ_{max} is the maximum short-term shear strength, K is the slope and t_f is the time-to-failure in hours, and b is a parameter that expresses the intersection point at the vertical axis.

The parameters K and b are found by a linear regression analysis and are shown in Table 5.7.

Using expression (5.10) with the estimated parameters (K, b), the lifetime of the studied adhesives and the applied shear stress can be estimated when one of them is given or assumed.

Table 5.8 gives the normalized shear stress ($\frac{\tau_{app}}{\tau_{max}}$), the minimum value according to all models used, which could be applied for 1, 5, 10, and 25 years. It was found that none of the joints are expected to remain for a lifetime of 50 years. The values of normalized shear stress, in fact, represent the conversion factors to be considered for the long-term loading of the studied joints; however, further work and more specimens are needed in order to ascertain this extrapolation and to satisfy the statistical considerations.

Table 5.4: Parameters of the steady-state creep rate approach

Applied shear stress	Steady-state creep rate approach parameters		
	γ^* [1/h]	a [-]	R^2
AC-0.35			
Level I	0.00015	0.28	0.99
Level II	0.00023	0.55	0.99
Level III	-	-	-
AC-0.65			
Level I	0.00015	0.31	0.99
Level II	-	-	-
Level III	-	-	-
EP-0.35			
Level I	0.000006	0.04	0.83
Level II	0.000011	0.06	0.88
Level III	0.000023	0.01	0.89
EP-0.65			
Level I	0.000005	0.05	0.95
Level II	0.000011	0.06	0.97
Level III	0.000028	0.11	0.99

Table 5.5: Short-term mechanical properties and predicted time-to-failure

Stress ratio	Short-term tests, rapid-loading tests*			Shear creep tests		
	G [MPa]	τ_{max} [MPa]	$\gamma_{at\ Break}$ [-]	Time to failure acc. to**		
				Findley [h]	Burger [h]	Creep rate [h]
AC-0.35						
I (21.6%)				4299	2780	3002
II (28.8%)	195.13	26.58	0.73	773	897	789
III (36.0%)				(250)	(250)	(250)
AC-0.65						
I (26.7%)				7331	3938	4654
II (35.6%)	196.23	21.50	1.01	(1032)	(1032)	(1032)
III (44.5%)				(183)	(183)	(183)
EP-0.35						
I (21.5%)				5.00E+5	4.0E+4	60120
II (28.7%)	233.97	26.68	0.4	1.06E+5	2.1E+4	30722
III (35.9%)				2.42E+4	9321	12857
EP-0.65						
I (24.0%)				1.39E+6	1.6E+4	38128
II (32.1%)	317.60	23.89	0.24	1.05E+5	1.3E+4	16551
III (40.1%)				7.80E+3(a)	3.5E+3(a)	3.7E+3(a)

* G is the shear elasticity modulus, τ_{max} is the maximum shear stress, and $\gamma_{at\ Break}$ is the average value of the shear strain at break.

** Values in brackets refer to the time-to-failure recorded from the test. While values denoted by (a) refer to the average value between the real failure time recorded for one specimen and the failure time estimated by the relevant model for the other specimen.

Table 5.6: Relative errors of the time-to-failure comparing with the steady-state creep rate approach

Stress level	Relative error of the time-to-failure [%]	
	Findley	Burger
AC-0.35		
I	43.20	7.39
II	2.03	13.68
III	-	-
AC-0.65		
I	57.52	15.38
II	-	-
III	-	-
EP-0.35		
I	731.67	33.46
II	245.02	31.64
III	88.22	27.50
EP-0.65		
I	3545.61	58.03
II	534.40	21.45
III	110.81	5.40

Table 5.7: Parameters of the normalized shear stress- $\ln(t_f)$ correlation

	Findley		Burger		Steady-state creep rate	
	K [1/ $\ln(h)$]	b [-]	K [1/ $\ln(h)$]	b [-]	K [1/ $\ln(h)$]	b [-]
AC-0.35	0.05	0.63	0.06	0.69	0.06	0.68
AC-0.65	0.05	0.69	0.06	0.75	0.05	0.73
EP-0.35	-	-	0.1	1.26	0.09	1.24
EP-0.65	-	-	0.09	1.15	0.07	0.95

Table 5.8: Normalized shear stress for 1, 5, 10, and 25 years

	$\left(\frac{\tau_{app}}{\tau_{max}}\right)$ [%]			
	1 year	5 years	10 years	25 years
AC-0.35	13.5	3.9	-	-
AC-0.65	20.5	10.9	6.7	1.2
EP-0.35	35.2	19.1	12.2	3.0
EP-0.65	31.5	18.8	12.6	4.3

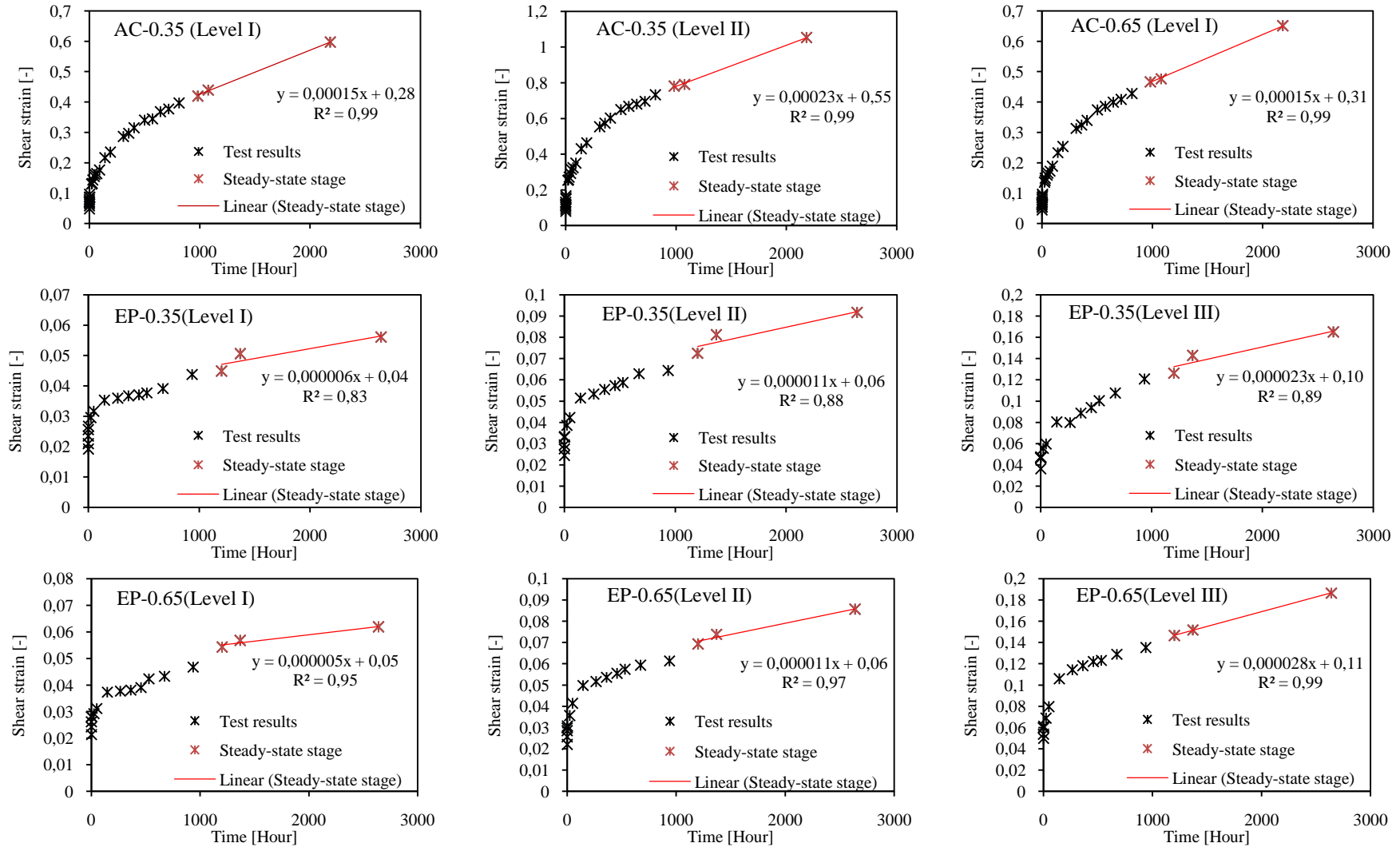


Figure 5.13: Determination of the steady-state creep rate at 20 °C

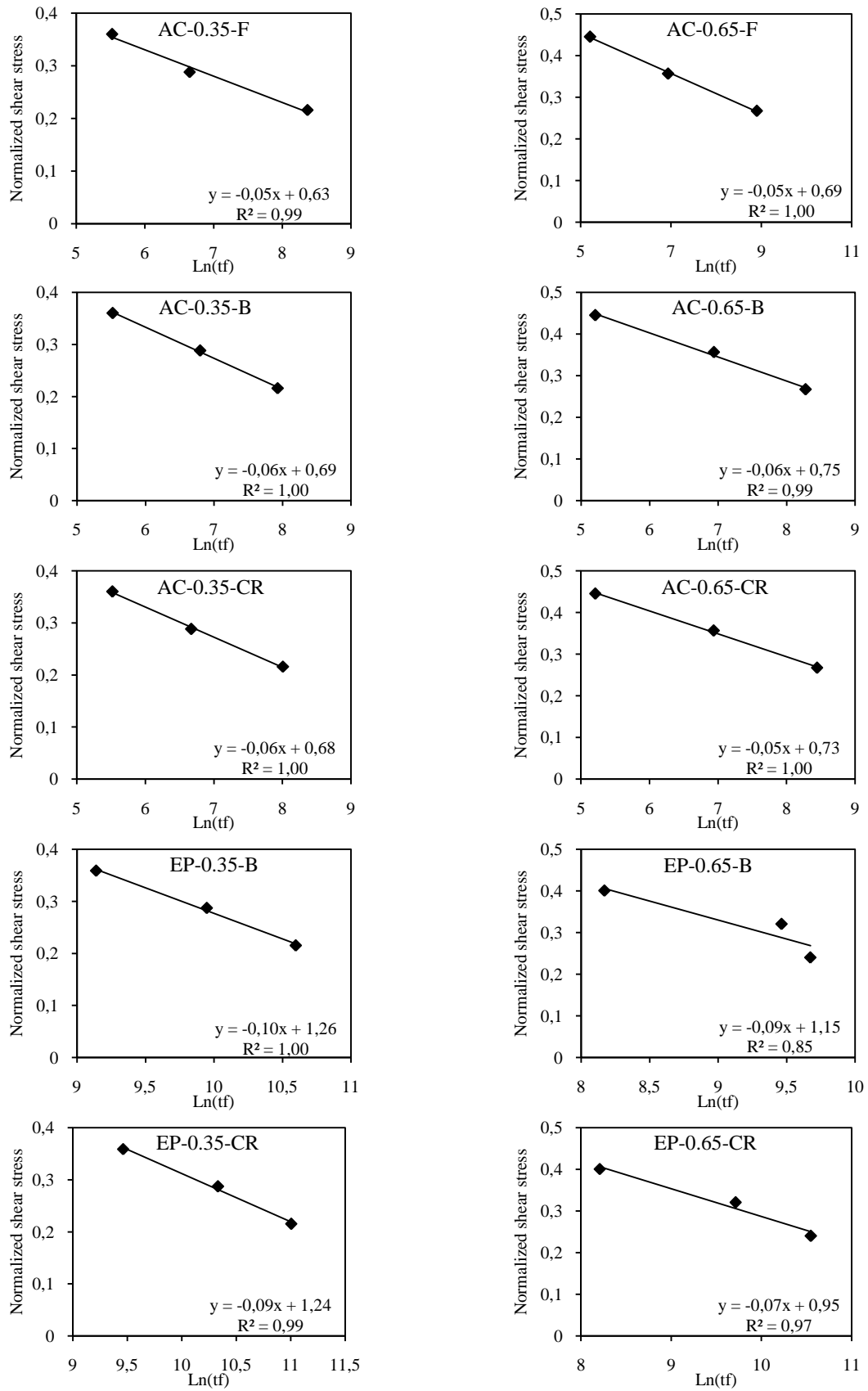


Figure 5.14: Normalized shear stress vs. $\ln(t_f)$.
(F, B, and CR) denote Findley, Burger, creep rate approaches respectively.

5.5.3 Test procedure at 40 °C and 0 °C

In order to gain some explanations about the shear creep behaviour of epoxy and acrylic adhesives at temperatures other than room temperature, the tests were conducted at +40 °C and 0 °C. It should be noted that in [66], whose recommendations are followed here, testing bonded joints for long time under sustained loads at the maximum temperature of the service temperature range (+40 °C) is not needed for a temperature range of (-40 °C to +40 °C) because the effect of the temperature, for long time, is tested under the normal ambient temperature. As for the negative temperatures, bonded joints (anchors) are not affected by service temperature down to -40 °C; however, if new bonding material is used, then this test is required.

In our case, and due to the difficulties associated with the test procedure and the equipments available in the laboratory, it was decided to conduct these tests at 40 °C and 0 °C.

Similar to the procedure followed in section 5.5.2, the specimens, Figure 5.3, were installed into the creep machine which was put inside a huge climate chamber of the laboratory of materials testing in BTU, Figure 5.15.

Because of the high expenses of using the climate chamber and knowing that a faster frequency will be needed to measure the shear strains because the specimens will creep at 40 °C faster than they do at room temperature, it was decided to test only one specimen (of 0.65 mm adhesive thickness) for each stress level. These considerations were applied for testing at 0 °C as well.

Three constant shear stresses were applied to three specimens, as listed in Table 5.9. The shear stress levels were chosen to be less than 50% of the short-term maximum shear strength corresponding to the temperature studied.



Figure 5.15: The creep machine and the calibration of the weights inside the climate chamber

The relative humidity (R.H.) was not controlled; however, it was ranging between 7% and 15%. During the test period which was 101 h for each temperature.

As for the tests at 0 °C, although the samples were subjected to higher shear stresses (see Table 5.9), no considerable displacements were recorded over the test period (101 h). This can be attributed to the fact that the material becomes more rigid at temperatures lower than the room temperature. The test at 0 °C, therefore, was stopped with no achieved results.

Table 5.9: Applied shear stresses in tests at 40 °C and 0 °C

	Temperature [°C]	Applied shear stress [MPa]	Stress ratio [%]
AC-0.65	40 °C	level I: 1.30	7.60
		level II: 1.91	11.17
		level III: 4.12	24.02
	0 °C	level I: 5.75	21.20
		level II: 7.65	28.20
		level III: 9.57	35.27
EP-0.65	40 °C	level I: 1.91	10.13
		level II: 4.12	21.79
		level III: 5.74	30.40
	0 °C	level I: 5.75	24.36
		level II: 7.65	32.41
		level III: 9.57	40.55

Creep results at 40 °C:

The calculated shear strain was plotted versus the time in hours for every stress level in Figure 5.16 for AC-0.65 and for EP-0.65.

It is obvious that the creep behaviour of the studied adhesives is affected by the shear stress that the joints are subjected to.

Despite that no failure occurred during the test, it was noticed that the shear strains of the joints AC-0.65 loaded by the highest shear stress (level III) and the joints EP-0.65 loaded by the level (II) and (III) reached extents which exceed the average shear strains of the rapid test at 40° C which are ($\gamma_{at\ Break} = 1.32$) for AC-0.65 and ($\gamma_{at\ Break} = 0.12$) for EP-0.65 as presented in Table 5.10. This might be attributed to the following:

- The nature of applying the loads to the specimens, i.e. the applied stress speed, which is considered completely static in the creep test, while in rapid-loading test, it is considered quasi-static.
- The temperature influences the behaviour of the adhesive over a long time and makes it more ductile.

To know how much shear strength of the adhesives was lost after the creep test under mechanical and thermal loading, the residual strength of these joints has to be determined. Therefore, the joints were unloaded (after 101 h of testing) and then tested at the room temperature in the tensile test machine. The speed rate of the crosshead was set to 1.27 mm/min. The residual shear strengths of the joints are listed in Table 5.11.

The estimated degradation of the shear strengths due to the static loads and temperature of 40 °C is about 60-65% of the shear strength at room temperature. The procedure of checking the residual strength may lead to a fact that taking the average shear strain of the short-term loading in order to predict the lifetime of the bonded joints using the prediction models, gives values of the lifetime which can be considered still on the safe side.

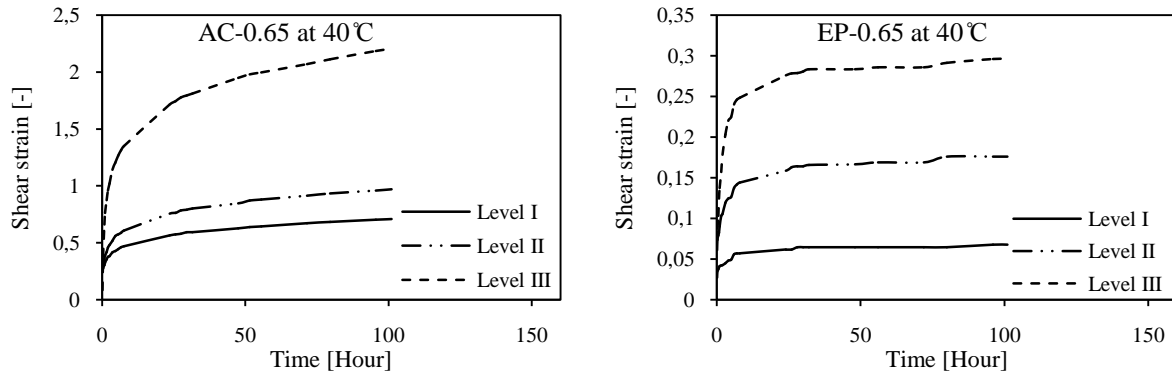


Figure 5.16: Shear creep strains of AC-0.65 and EP-0.65 at 40 °C

Table 5.10: Shear strains recorded at the end of the test for 40 °C

	Applied shear stress level	Shear strain recorded at 101 h	$\gamma_{at\ Break}$ [-]
AC-0.65	I	0.71	1.32
	II	0.97	
	III	2.20	
EP-0.65	I	0.07	0.12
	II	0.18	
	III	0.29	

Table 5.11: Degradation of the shear strength of the studied adhesives

	Applied shear stress level	Residual shear strength [MPa]	Shear strength at room temperature [MPa]	Degradation of the shear strength [%]
AC-0.65	I	8.46	21.50	60.65
	II	8.36		61.12
	III	7.47		65.26
EP-0.65	I	8.98	23.88	62.40
	II	8.50		64.41
	III	8.40		64.82

For developing the shear creep description of adhesively bonded steel joints at 40 °C, Findley's and Burger's model were fitted to the shear strain-time data. The fitted curves are exhibited in Figure 5.17 for the specimens studied; i.e. AC-0.65 and EP-0.65 at three applied shear stresses.

The models parameters were found and are listed in Table 5.12 and Table 5.13. It is clear that Findley's model fits the creep data better than Burger's model because the fitting process is done in this case for relatively short time period of testing (101 h).

It can also be seen that the transient stage of the creep data, which is the one just before the steady-state stage, is not accurately projected by Burger's model which adversely affects having a quite accurate projection for all data points.

The reason behind can be explained by the temperature effect and the moisture presence at the first few hours of the test. Feng et. al. [28], explained that the presence of the moisture facilitates the mobility of the molecular of the material and, therefore, decreases the energy amount needed for a material to be deformed. In consequence, the Burger's model was adapted by adding a new parameter (n) that accounts for this fact resulting equation (5.11) for the creep in tension, by which the projection can be more accurate.

$$\varepsilon(t) = \frac{\sigma}{E_M} + \frac{\sigma}{\eta_M} \cdot t + \frac{\sigma}{E_K} \left(1 - e^{-\left(\frac{E_K t}{\eta_M}\right)^{1-n}}\right) \quad (5.11)$$

This modified Burger's model might be used for giving much more accurate fitting; however, the problem is the presence of five parameters to be found which makes the convergence of the regression analysis quite hard. For this reason, the original model has been only used in this work.

Table 5.12: Findley's model parameters for the shear creep strains at 40 °C

Applied shear stress		γ_0	A	B	R^2
AC-0.65	Level I	0.011	0.325	0.166	0.98
	Level II	0.016	0.386	0.200	0.99
	Level III	0.034	0.752	0.240	0.97
EP-0.65	Level I	0.006	0.036	0.129	0.94
	Level II	0.014	0.084	0.156	0.94
	Level III	0.019	0.138	0.172	0.88

Table 5.13: Burger's model parameters for the shear creep strains at 40 °C

Applied shear stress		G_M [MPa]	λ_M [MPa h]	G_K [MPa]	λ_K [MPa h]	R^2
AC-0.65	Level I	118.18	372.04	3.16	1.06	0.86
	Level II	119.38	410.16	3.39	2.78	0.91
	Level III	121.18	455.29	2.98	5.25	0.97
EP-0.65	Level I	318.33	8978.18	42.70	15.00	0.77
	Level II	294.29	8330.33	33.60	30.30	0.86
	Level III	302.11	10239.60	24.90	37.50	0.95

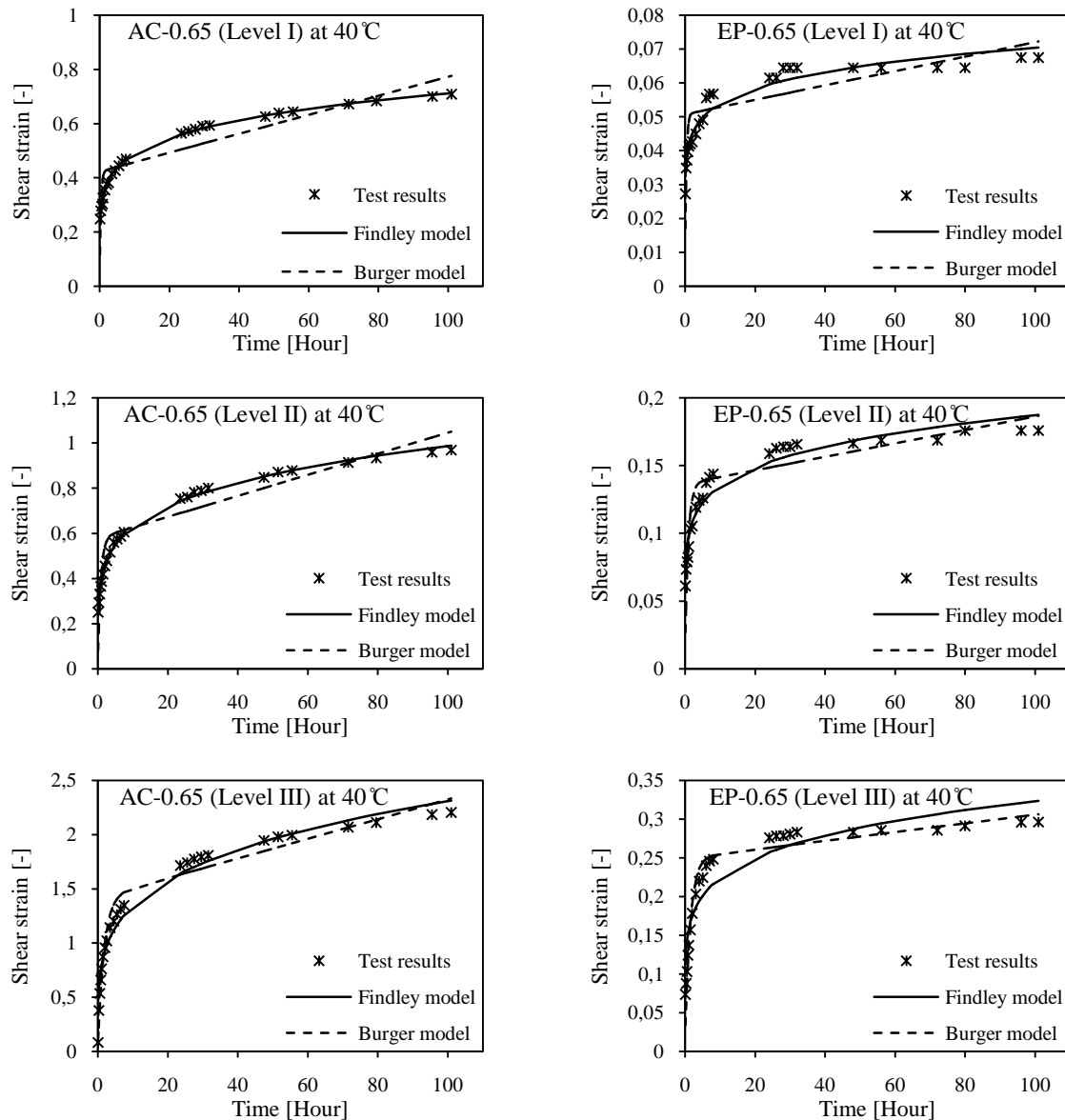


Figure 5.17: Fitted Findley's and Burger's models for shear creep strains at 40 °C

5.5.4 Conclusions

In this chapter two different kinds of structural adhesives, epoxy as a rigid material and toughened acrylic as a rather flexible one, were chosen to investigate the time-dependent behaviour (the shear creep behaviour). These adhesives were used to assemble double lap shear joints of galvanized steel sheets. The shear creep tests were performed under different conditions for relatively long time as follows:

- Tests at room conditions (≈ 20 °C and 40-50% R.H.) on specimens assembled by adhesives (0.35 mm and 0.65 mm-thick) under sustained loads generating three different shear stresses applied over the bonded areas for at least three months.

- Tests for a period of 101 h at (0 °C and 40 °C) and 7-15% R.H. on specimens assembled by 0.65 mm-thick adhesives. Three different shear stresses were also applied over the bonded areas.

The shear stresses used for each test were taken as ratios (less than 50%) of the maximum shear stress of the corresponding shear stress of the short-term tests (rapid tests).

The shear creep strains versus time (in hours) were plotted and described by Findley's and Burger's models, which were developed at 20 °C and 40 °C.

The time-to-failure of the joints was estimated by the prediction models which are mentioned above and by the steady-state creep rate prediction. This was done by assuming that the extrapolated shear strains have to be less than the average value in the corresponding short-term test. Afterward, the applied shear stresses for particular lifetimes of 1, 5, 10, and 25 years were proposed.

The remaining shear strength of the joints tested at 40 °C was checked so that the degradation of the strength has been determined.

Based on the findings, the following conclusions can be made:

- Creep test of the bonded joints under real conditions and for long time is essential and important because the long-term creep test can give more convincing evaluation of the behaviour of the bonded joints than the short-term creep test or accelerated test. However, it is associated with some problems such as the time required, the necessity of monitoring and recording the displacements, the method to measure the displacements over a long time, and the possible danger when a specimen fails while being measured; moreover, the cost of conditioning the specimens over a long time is quite high because it needs a huge climate chamber to accommodate the creep machine.
- Since the adhesive becomes more rigid at temperatures lower than the room temperature, performing creep test will need very long time to get sufficient data. Therefore, the short-term creep test using adapted testing machines might be more preferable.
- The measured displacements in all tests were noticeably scattered, therefore, increasing the number of the specimens is necessary for having representative descriptions of the creep behaviour of the adhesives by which reliable extrapolation can be made.
- Both Findley's and Burger's models well represented the shear creep of the used adhesives. However, generally, Findley's model fits the shear creep data points better than Burger's model over the test period. In this work it is seen that the long lifetime of the adhesives can be better predicted by Burger's model due to the unlimited retardation spectrum of Findley's model. This is proven when comparing the

predictions of these two models with the extrapolated lifetime using the steady-state creep rate approach.

- The epoxy adhesive exhibits a creep strength that is much higher than the acrylic adhesive; therefore, the use of epoxy adhesives in structural applications designed for long time is more recommended than the use of acrylic adhesive. Both of them are not able to resist the creep phenomenon for the intended lifetime of the structural applications of 50 years. As a contribution, this work expects that for applications designed for lifetimes up to 25 years, AC-0.65, EP-0.35, and EP-0.65 seem to be usable. While AC-0.35 may be used for applications designed for a period up to 5 years. However, further work and more specimens are needed in order to ascertain this extrapolation and to satisfy the statistical considerations.
- This work proposes the limits of the applied shear stresses over which the joints are expected to be failed earlier than a particular lifetime, for example, for the lifetime of 25 years, these limits are 1.2%, 3.0%, 4.3% of the maximum shear strengths of the adhesives AC-0.65, EP-0.35, and EP-0.65 respectively.
- The shear strains of the bonded joints can reach extents which exceed the strains of the rapid test due to the nature of applying the loads to the specimens which is fully static in the creep test; moreover, the temperature influences the behaviour of the adhesive over a long time and makes it more ductile.
- In this work, it is experimentally seen that taking the average shear strain of the short-term loading in order to predict the lifetime of the bonded joints using the prediction models, gives values of the lifetime which can be considered still on the safe side.
- Generally, it could be said that using structural adhesives for long time in structural applications still needs to be statistically ascertained by testing these materials with sufficient number of specimens and to consider all loading conditions that the bonded joint is supposed to resist. Until that time, the use of them with the help of a few rivets or bolts is recommended to construct a joint that is able to resist the creep by the rivets or bolts and also has high shear strength provided by the adhesive.

6 A practical application of adhesively bonded joints (Strengthening cold-formed thin-gauged galvanized steel girders)

6.1 Introduction

One of the procedures that are done for the purpose of maintenance and rehabilitation of the existed structures is strengthening the structural members that are suffering from design deficiencies, constructional errors, or changing the use conditions that the structure or the member is designed for; for example, increasing the loads which have to be carried by the member. Providing additional steel reinforcement is one of the methods that are frequently used in the structural engineering to strengthen a structural member. This technique was used for strengthening concrete structures by externally bonded plates in 1960. The bonded plate reinforcement technique has also been applied to timber and masonry structures [33].

In a bonded plate/strengthened member joint, the connection between the plate and the member will be provided by the adhesive which will be mainly loaded in shear.

In steel structures, studies have been made to introduce externally bonded plate reinforcement as a way to strengthen thin-gauged steel members. Experimental investigations were conducted on a knee joint [34] and on a box girder [72] strengthened by additional bonded plates. The tests, conducted on both structures clearly confirmed that this method of strengthening is effective and that the carrying capacity of the structures can be increased by this method to a higher level than other methods of strengthening [4].

The effect of the reinforcement by additional bonded metallic sheets on cold-formed light gauge members was examined on a channel section ("C" section) under bending loading [37]; the ultimate load was increased by approximately 22% in the reinforced section with no failure of the bondline. Using this technique was also tested on mullion-transom facades strengthened by bonding additional steel plate inside the profile; satisfactory results were achieved when an increase of the stiffness of the strengthened profile of about 50% could be achieved [73].

The efficiency of bonding additional plate to a strengthened member is that a joint mostly loaded in shear is structured. In such a joint, the shear stress that will be developed over the adhesive layer will be much less than the shear strength of the adhesive because a large area of bonding is used.

In this chapter, the efficiency of applying this technique to strengthen a cold-formed thin-gauged galvanized steel girder of channel section (C section) is presented as an example of practical applications of adhesively bonded joints in structural engineering. Tests are performed on the girders strengthened by adding additional plates (galvanized steel plates) bonded by two structural adhesives (acrylic and epoxy) on the flanges at room temperature. A comparison of the increase in the capacity of the strengthened girders with non-strengthened one is made.

The temperature effect on the capacity of the strengthened girders at the minimum and maximum temperatures of the temperature range considered (i.e. at -20 °C and 40 °C) is numerically investigated by the finite elements method (FEM) using the commercial software ABAQUS making use of the mechanical properties obtained from the tests on small scale specimens (double lap shear tests).

The stress distribution over the adhesive layers as well as the collapse of the girders for all cases is presented and discussed.

6.2 Studied girders

The girders studied are cold-formed from the galvanized steel sheets of 2 mm thick and manufactured as channel section (“C” section) with a length of one meter. Seven girders were made; the width of the flanges equals to 39.6 ± 0.7 mm and a height of the section is 78 ± 0.8 mm. The radius of the corners is (2 ~ 3 mm). For strengthening the girders, 500 mm long steel plates of a section area 35 x 2 mm were cut from a galvanized steel sheet of 2 mm thick.

Four patterns of the girders to be investigated were made (see Figure 6.1):

- The first one is a non-strengthened girder which is tested and used as a reference one.
- The second pattern is the girders in which upper flanges are strengthened by bonding an additional plate using the acrylic adhesive DP 810 (denoted later as AC-U) and the epoxy adhesive DP 490 (denoted as EP-U). The plates are bonded on the external surface of the upper flanges.
- The third pattern is the girders in which bottom flanges are strengthened by bonding an additional plate under the bottom flanges. This pattern is denoted as AC-B and EP-B for the acrylic and epoxy adhesives respectively.
- The last one is the girders that their upper and bottom flanges are strengthened by externally bonded plates. The girders of this pattern are named as AC-U-B and EP-U-B.

The bonding process followed here is similar to the one used for the small scale specimens in the previous tests. Figure 6.2(a) shows the application of the adhesive on the prepared surfaces with a thickness of 0.65 mm achieved by the red one-sided adhesive strips, while in Figure 6.2(b) the weights put on the bonded plates for 24 h are shown.

Twenty-four hours after bonding, 50 x 75 x 5-angles with 30 mm long were bonded at the middle of the upper flanges of each girder. Bonding these angles was directly on the upper flange of those which are strengthened at the bottom and on the upper bonded plates for the other girders as shown in Figure 6.2(c).

These angles were suggested to be used for distributing the applied load over the area under each of them, since the load will be transferred to the girder by the adhesive used for bonding these angles. The girders were left 5 days for AC and 7 days for EP at room temperature (the curing time needed for each adhesive to be fully cured) and then tested.

6 A practical application of adhesively bonded joints (Strengthening cold-formed thin-gauged galvanized steel girders)

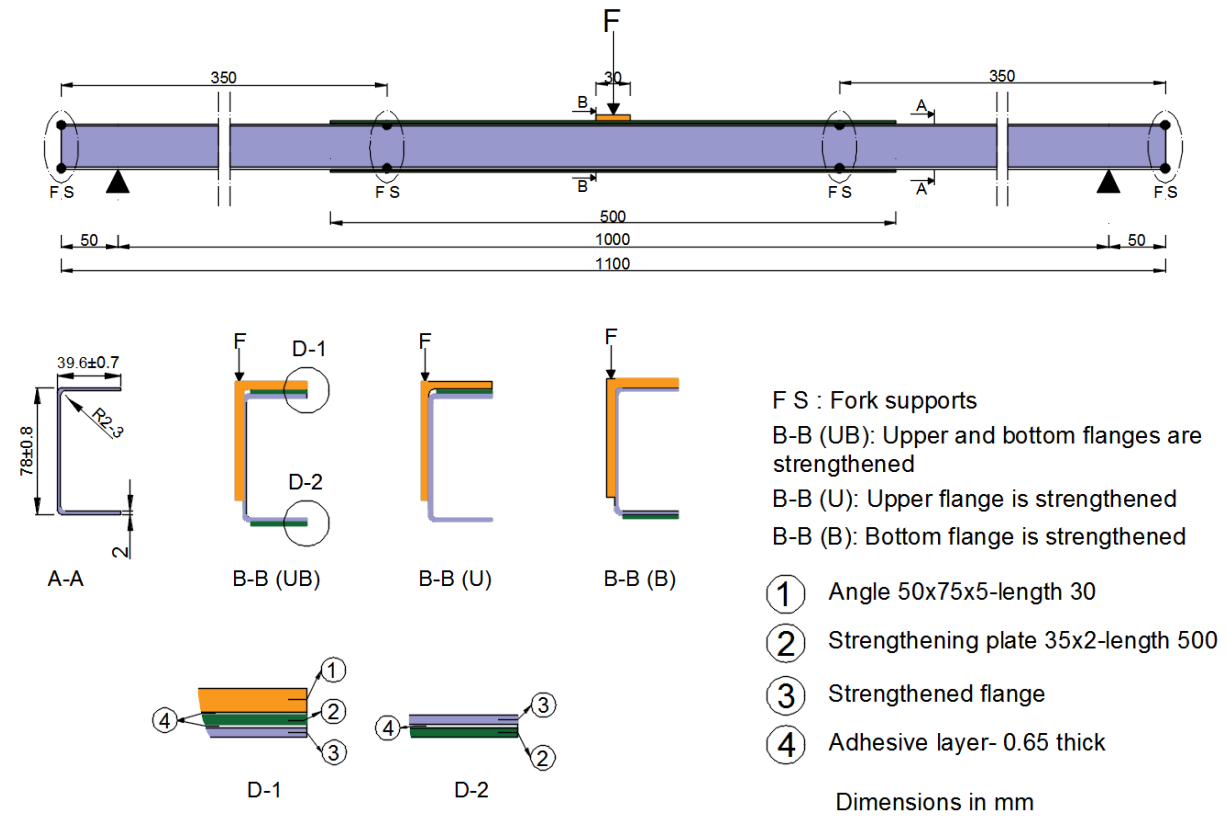


Figure 6.1: Geometries and types of the girders

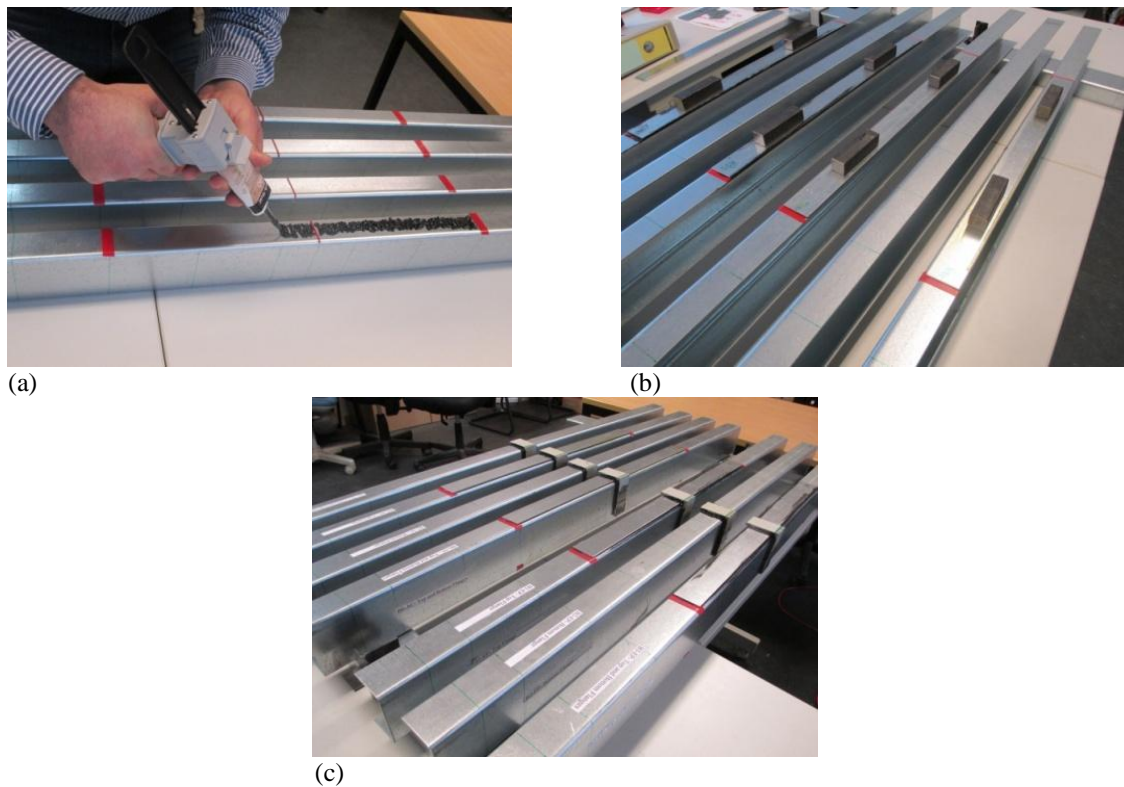


Figure 6.2: Strengthened girders manufacturing
 (a) Applying the adhesive (b) Weights used on the bonded plates for 24 h (c) Bonding the angles for loading

6.3 Test set-up

3-points bending test was used for testing the seven girders (one girder for each case) at room temperature. The girders were simply supported during the test. To prevent the lateral torsional buckling of the unsymmetrical sections, fork supports at four positions over the length of the tested girders were used. The load was applied on the top of the vertical legs of the angles. The speed rate of the crosshead of the compressor was 7.5 mm/min. The deflection at the mid-span was measured using linear displacement sensors. The test set-up is shown in Figure 6.3.

6.4 Test results and observations

During and after the tests, the following points were remarked:

1. As expected, the reference pattern (non-strengthened girder) failed because of the local buckling occurred close to the mid-span of it (exactly after the bonded angle) where there is the maximum moment, Figure 6.4. A slight curvature in the girder was noticed. The maximum force carried by the girder was 10.48 kN.
2. The girders of the second pattern, i.e. AC-U and EP-U, started bowing noticeably and then a lateral torsional buckling at the middle region of the girders between the middle fork supports occurred, Figure 6.5(a). In consequence, the regions just after the strengthening plates started rotating with local buckling-like. No local buckling at the mid-span happened as well as no separation of the strengthening bonded plates was noticed for AC-U (Figure 6.5(b)), however for EP-U, the bonded plate started to separate at the farthest edges near to the rotated regions (Figure 6.5(c)). The maximum forces recorded for the girders were 13.70 kN and 13.76 kN for AC-U and EP-U respectively.
3. Girders strengthened only at the bottom flanges, AC-B and EP-B, behaved like the non-strengthened one; they failed because of the local buckling occurred close to the mid-span. The deformation of AC-B and EP-B with the non-strengthened girder is shown in Figure 6.6(a). However, a larger curvature in the girders was noticed without a separation of the bonded plates, see Figure 6.6 (b,c) . The maximum forces recorded were 12.60 kN and 12.56 kN for AC-B and EP-B respectively.
4. The girders of the forth pattern, i.e. AC-U-B and EP-U-B, had the same behaviour of the second pattern; however, the curvature was larger. The lateral torsional buckling between the middle fork supports occurred, and then the regions just after the strengthening plates started rotating with local buckling-like, Figure 6.7(a). No local buckling at the mid-span happened. The bonded plates of EP-U-B separated from the flanges (Figure 6.7(b)), while for AC-U-B; no separation of the strengthening plates was to be noticed (Figure 6.7(c)). The maximum forces recorded for the girders were 16.11 kN and 15.70 kN for AC-U-B and EP-U-B respectively.



Figure 6.3: Test set-up
(a) 3-points bending test (b) Fork supports used (c) Applying the load on the top edge of the vertical leg of the angle.

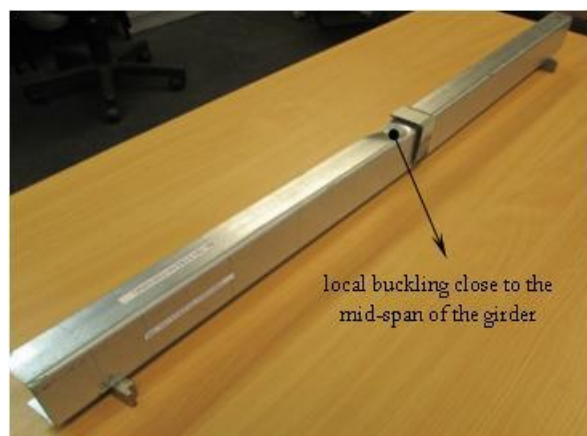
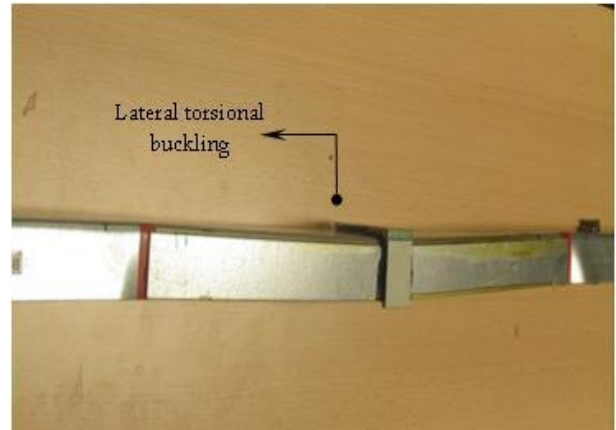
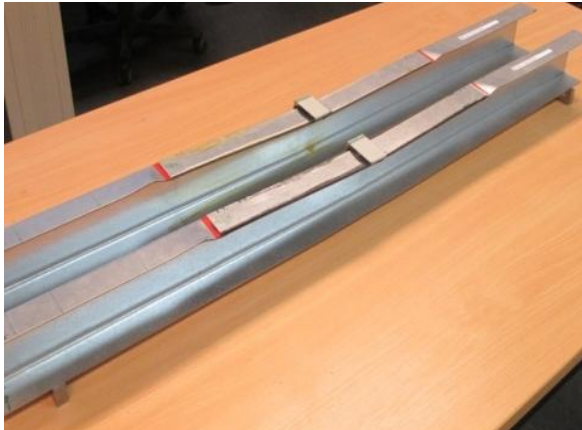
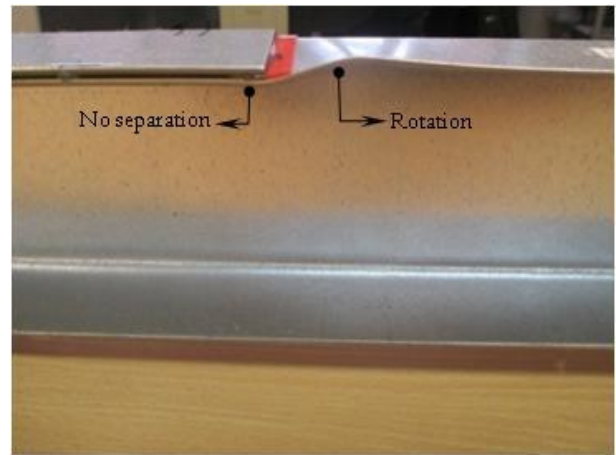
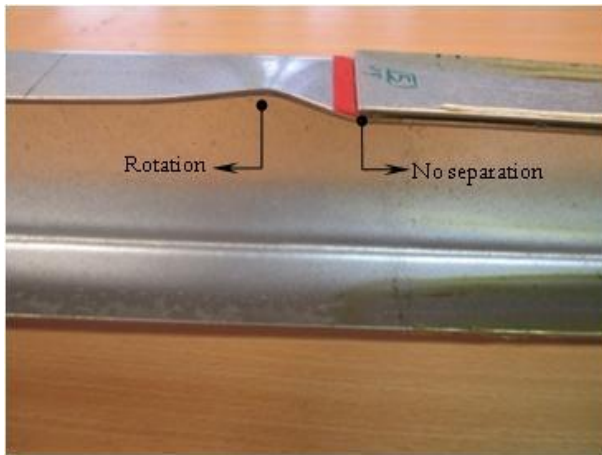


Figure 6.4: Deformation of the non-strengthened girder

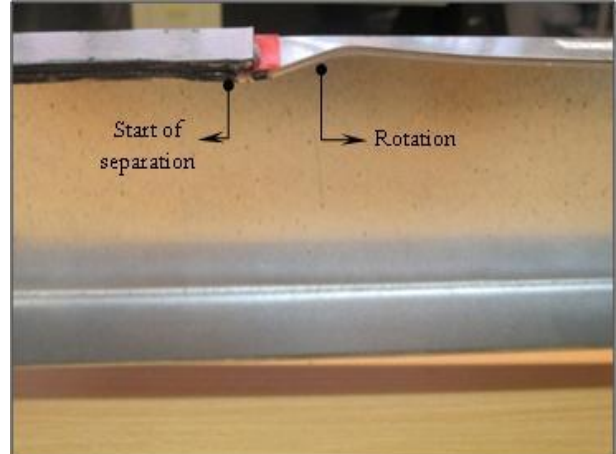
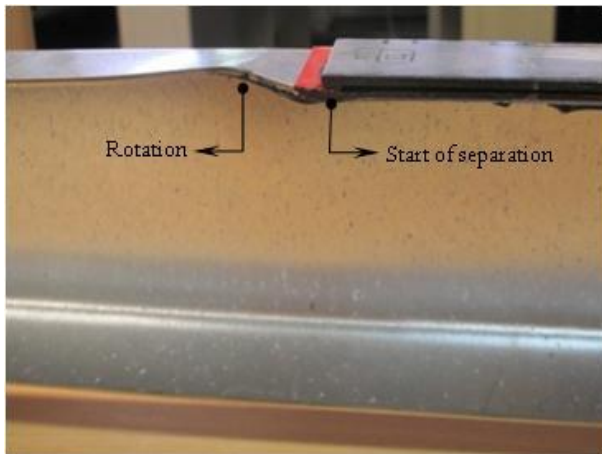
6 A practical application of adhesively bonded joints (Strengthening cold-formed thin-gauged galvanized steel girders)



(a) Deformed girders of AC-U and EP-U (left)
lateral torsional buckling at the middle region (right)

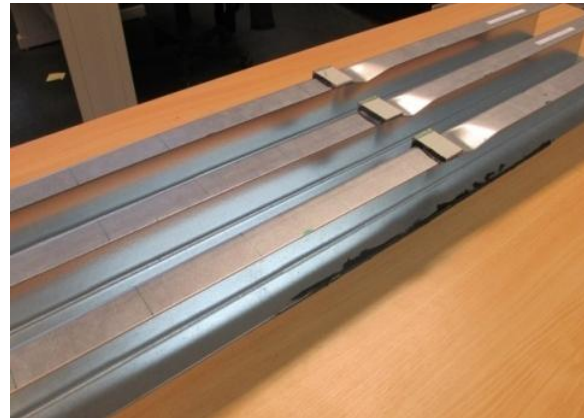


(b) Left and right rotated regions of AC-U

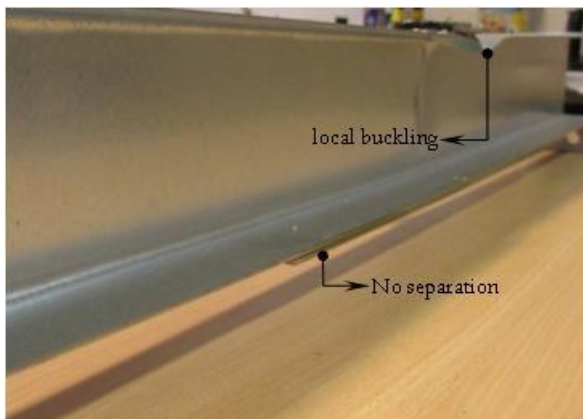


(c) Left and right rotated regions of EP-U

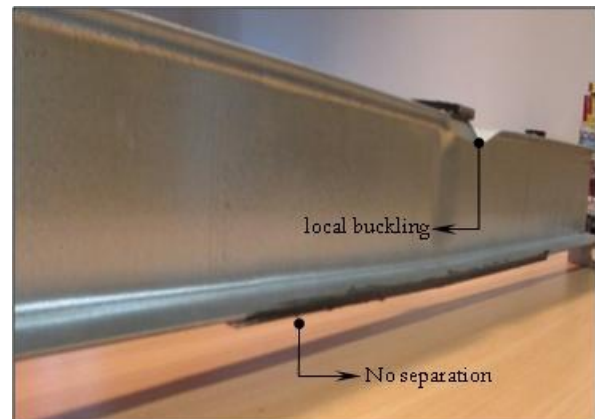
Figure 6.5: Deformations of AC-U and EP-U



(a)



(b)



(c)

Figure 6.6: Deformations of AC-B and EP-B

(a) Deformations of AC-B, EP-B and the non-strengthened girder (b) AC-B (c) EP-B

6.5 Stress distribution within the adhesive layers

Better understanding of the behaviours of the bonded strengthening joints can be obtained by knowing the stress distributions developing within the adhesive layers. This can be done through numerical investigations by finite element method-based models.

6.5.1 FEM-models (at the room temperature)

6.5.1.1 Models building

When modelling by the use of the finite element method, great attention has to be given to represent the structure including its geometry, mechanical properties of the materials, loading and boundary conditions; hence, getting results which are identical to those obtained from the test is possible [74]. Analysis type selected as well as tolerances made to facilitate the modelling process and to save the time needed for the completion of the analysis have to be judged and then to be determined.

The finite element method using ABAQUS software [75] is used in the present work. Six models represent the six strengthened girders tested at room temperature (AC-U, AC-B, AC-

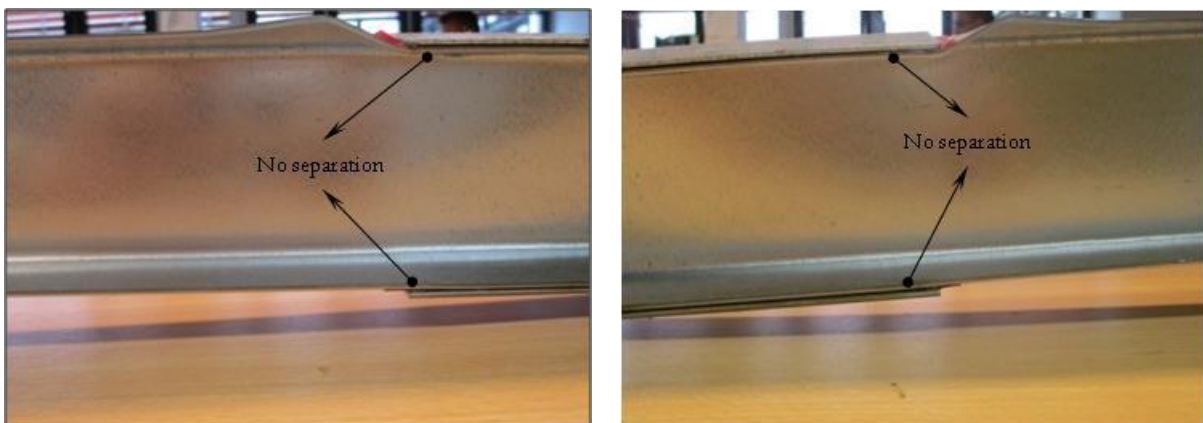
U-B, EP-U, EP-B, and EP-U-B) were built. The geometries of the models are presented in Figure 6.1.



(a) Deformed girders of AC-U-B and EP-U-B (left)
The curvature of the girders (right)



(b) The separation of the bonded plates in EP-U-B



(c) No separation of the bonded plates in AC-U-B

Figure 6.7: Deformations of AC-U-B and EP-U-B

The selection of the element type and the mesh size has a great importance to represent the models accurately. The steel structures (“C” section and the strengthening plates) were modeled with use of the 4-node linear quadrilateral shell elements of type S4R; the “C”

section was meshed into 7700 elements while the strengthening plate was meshed into 700 elements. The layer of adhesive was modeled with use of the 8-node linear hexahedral solid elements of type C3D8R and it was meshed into 800 elements.

Similar to the boundary conditions applied during the tests, the models of the girders are simply supported, and prevented to move horizontally at the four locations of the fork supports over the length of the girders. Figure 6.8. displays the mesh and the boundary conditions used in the models. Using the definitions of the constraints available in ABAQUS, the angles were represented by defining the areas under them as rigid bodies, while the force was applied to a defined reference point attached to the rigid body of the angle using the definition of coupling. Based on the fact that the joint fails cohesively, i.e. the failure happens in the adhesive layer not at the interfacial surfaces, the layers of the adhesive were connected with the steel adherends (the flange and the strengthening plate) by an appropriate definition of contacts based on the theory of the so-called slave and master surfaces. A specific tie constraint, which connects two surfaces together so that there is no relative motion between them, was used [75], [74], and [4]. The advantage of this type of constraint is that it allows connecting two regions together even if the meshes between the surfaces are different. In Figure 6.9, the representation of the angles used as well as the tie constraints between the contacting surfaces is illustrated.

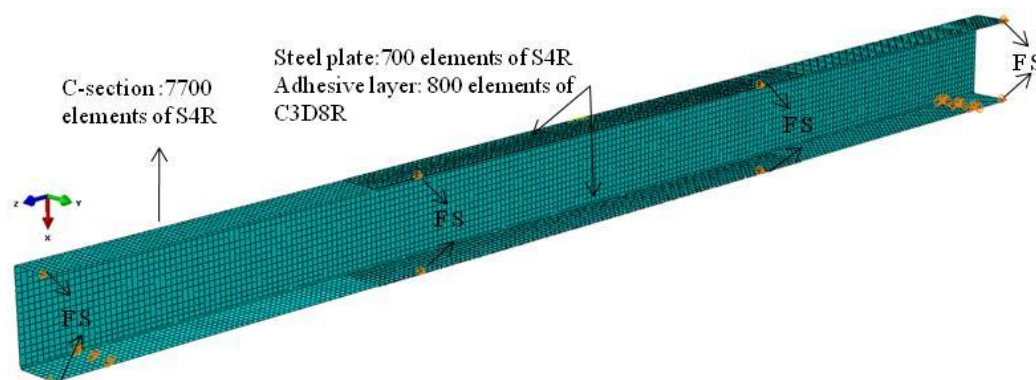


Figure 6.8: The mesh and the boundary conditions used in the models

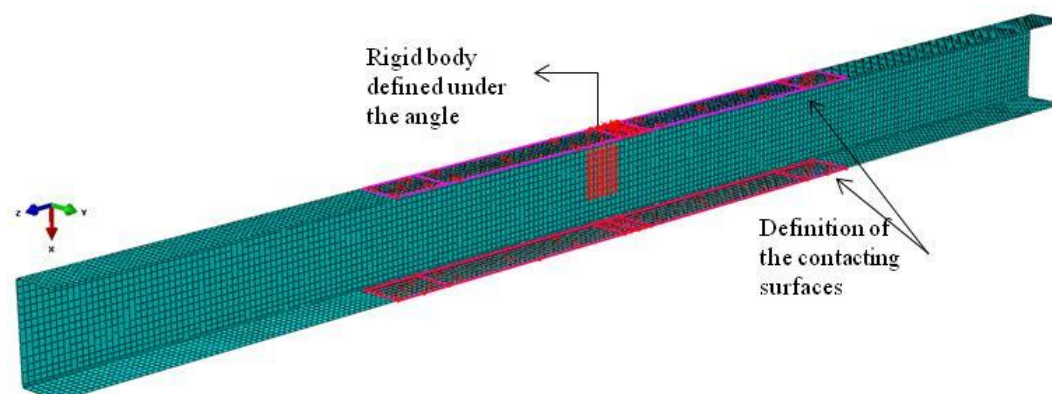


Figure 6.9: The rigid body under the angle and the contacting surfaces definitions

Based on EN 1993-1-5: 2006 [76], geometrical imperfections have to be introduced into the numerical models and carefully analyzed. The introduction of imperfections is based on the linear solution of the buckling analysis resulting in several local buckling modes. Afterwards, linear combinations of the chosen buckling (local) modes should be created after scaling them by adequate factors. This procedure provides the models with the new geometries; therefore, new configurations of the models will be achieved. The combinations of the chosen modes of the buckling analysis of each model are listed in Table 6.1. After introducing these combinations, the nonlinear post-buckling analysis using the Riks method was carried out on the newly created models.

Table 6.1: Combinations of the chosen modes obtained from the buckling analysis

The girder	The combination of the chosen modes *
AC-U and EP-U	-1.25 x (mode 2 + mode 16)
AC-B and EP-B	0.8 x (mode 1)
AC-U-B and EP-U-B	-1.5 x (mode 3 + mode 25)

* see Figure 10.7 to Figure 10.9 in appendix C , sections (10.3.1 to 10.3.3)

6.5.1.2 Materials description

Defining the materials of the steel members in the models was done by the use of the true stress-strain curves given in Figure 4.3 (chapter 4). The adhesive material was considered as a linear elastic isotropic material; therefore, the elasticity modulus (E), the Poisson's ratio (ν), and the yield strength (σ_y) should be determined.

The determination of these properties can be done by many test methods. Basically, they can be divided into two main categories[9]: tests on bulk specimens and tests in a joint or in-situ. Although tests in the bulk form are easy to carry out, however, the thickness of the samples should represent the thin adhesive layer used in adhesive joints; therefore, the thickness should be as small as possible. Tests conducted on in-situ joints are more preferred due to the fact that they more closely represent reality. However, these tests are characterized by the difficulty of measuring the very small adhesive displacements of thin adhesive layers. Great care has to be given when preparing the samples of both test methods in order to avoid the voids within the adhesive layer that affect the strength. Since there has been intense debate about the most appropriate method [9], a special strategy was applied here to obtain the required mechanical properties of the adhesive materials.

This strategy is to conduct the tests in joints (i.e. butt joints) by which the so-called apparent elasticity modulus E^* and the yield strength (σ_y) can be obtained, then the real elasticity modulus E and the Poisson's ratio (ν) of the adhesive can be determined using the equations (6.1) and (6.2), [77] :

$$\nu \approx \frac{2G - E^*}{2(G - E^*)} \quad (6.1)$$

$$E \approx E^* \cdot \frac{(1 + \nu)(1 - 2\nu)}{(1 - \nu)} \quad (6.2)$$

where G is the shear elasticity modulus of the adhesive.

The tests on the butt joints were conducted according to ISO 6922-1987. The steel adherends used were made as circular sections with a diameter of 25 ± 0.1 mm. The adhesive layer investigated was 0.65 mm. The speed rate of the crosshead of the testing machine was 1.27 mm/min.

Five samples were tested for the acrylic adhesive and three samples for the epoxy one. Unfortunately, the tensile strength results of the adhesives were not satisfactory because of the voids found within the adhesive layers; therefore, only the apparent elasticity modulus E^* was considered from these tests. As for the tensile strength of the adhesives, it was estimated using the von Mises formula given in equation (6.3). This assumption was used by [78], too. It was also found by Da Silva, L.M. *et al.* [16] that although the von Mises criterion is not strictly valid for polymers, but it can give a reasonable estimate of both the shear stress and strain, from test results in tension.

$$\sigma_y = \sqrt{3} \cdot \tau_y \quad (6.3)$$

Applying the previous equations using the corresponding shear properties (obtained in chapter 4) gives the required properties of the adhesives to be introduced to ABAQUS. These properties are listed in Table 6.2.

Table 6.2: Material properties of the adhesives used in Abaqus

	E^* [MPa]	ν	E [MPa]	σ_y [MPa]
AC-0.65	1819	0.44	565	36.90
EP-0.65	1618	0.378	875.21	41.37

6.5.1.3 Models validation

Calibration of the models was carefully done on the basis of the results of the experimental investigations performed.

The external load (F) and deflection (u) at the middle of the span were measured. The validation of the models was done by comparing the numerical and experimental results quantitatively and qualitatively. Figure 6.10 presents the quantitative comparison of the numerical and experimental (F - u) diagrams for the investigated girders. The high conformity of the stiffness of all models and relatively high agreement between the ultimate capacities can be observed. The qualitative validation of the numerical results is shown in Figure 6.11.

6.5.2 Investigations on the temperature effect

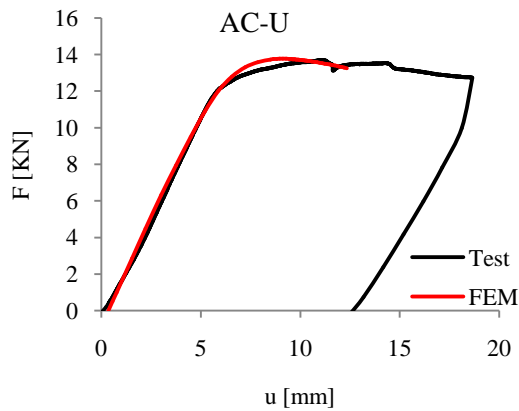
To experimentally investigate the temperature effect on large scale specimens (girders), a special testing machine inside a climate chamber is needed. Using such machine will

guarantee that no loose of the studied temperature occurs. However, this machine is not available at the materials testing-laboratory of BTU.

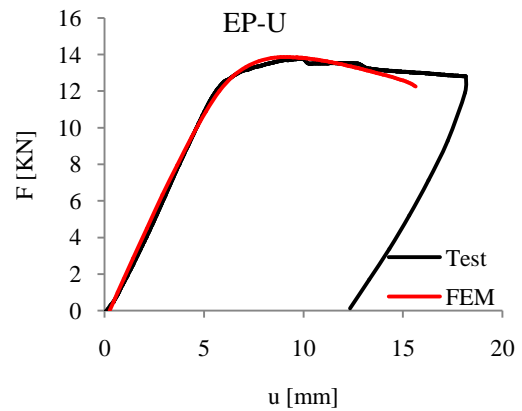
Two alternative methods were possible; the first one is to condition the girders in a big climate chamber and then to transfer them to the testing machine (out of the climate chamber) to test them very fast, but this procedure does not guarantee the temperature due to the time needed for installing the girders and the measuring devices as well as calibrating the fork supports. The second method is to do the investigations numerically by the FEM-models created for the room temperature tests and validated to be utilized for a parametric study. The temperature effect can be introduced to the models by making use of the mechanical properties obtained from the small scale specimens at the required temperatures. Applying such procedure has an advantage which is, there is no need to introduce the thermal properties (such as thermal expansion and thermal conductivity coefficients) of the materials because the mechanical properties of the adhesives were obtained using the same adherends (the galvanized steel) and subjected to the temperatures; therefore, these coefficients are already considered.

The temperature effect investigations were done at the maximum and minimum temperatures of the service temperature range considered in this research, i.e. at $-20\text{ }^{\circ}\text{C}$ and $+40\text{ }^{\circ}\text{C}$. Applying equations (6.1), (6.2), and (6.3) using the corresponding shear properties (obtained in chapter 4) gives the required properties of the adhesives to be introduced to ABAQUS. Table 6.3 lists the obtained properties at $-20\text{ }^{\circ}\text{C}$ and $+40\text{ }^{\circ}\text{C}$.

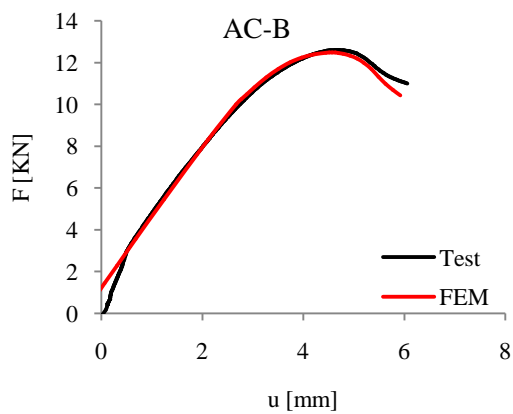
The Poisson's ratio of the steel was taken as 0.3 and assumed to remain unchanged over the temperature range studied, [79]. Similarly and for simplicity sake, this assumption was made for the adhesives although the Poisson's ratios of them slightly vary over the temperature range considered which is less than the glass transition temperature T_g of the adhesives. The slight variation of Poisson's ratios of some epoxy adhesives over a temperature range from ($-173\text{ }^{\circ}\text{C}$ to $+22\text{ }^{\circ}\text{C}$) is given in [80].



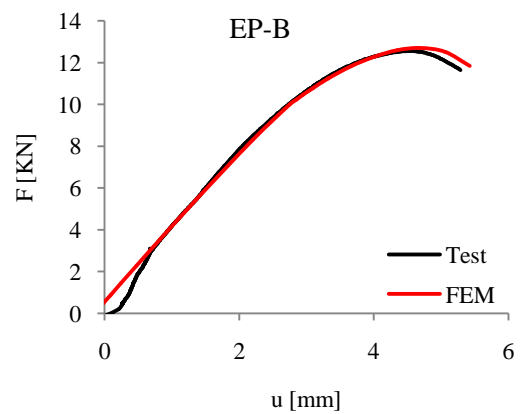
Comparison of AC-U: $F_{\max}(\text{test}) = 13.70 \text{ kN}$,
 $F_{\max}(\text{FEM}) = 13.76 \text{ kN}$



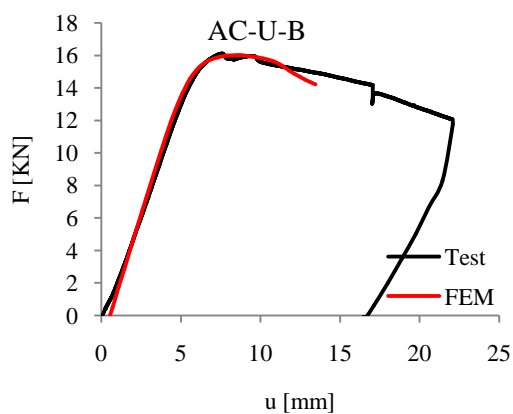
Comparison of EP-U: $F_{\max}(\text{test}) = 13.76 \text{ kN}$,
 $F_{\max}(\text{FEM}) = 13.86 \text{ kN}$



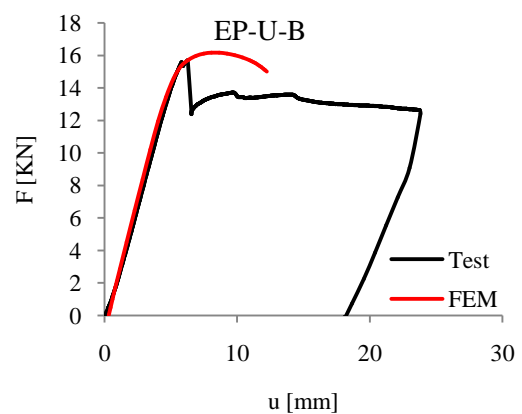
Comparison of AC-B: $F_{\max}(\text{test}) = 12.60 \text{ kN}$,
 $F_{\max}(\text{FEM}) = 12.48 \text{ kN}$



Comparison of EP-B: $F_{\max}(\text{test}) = 12.56 \text{ kN}$,
 $F_{\max}(\text{FEM}) = 12.69 \text{ kN}$



Comparison of AC-U-B: $F_{\max}(\text{test}) = 16.11 \text{ kN}$,
 $F_{\max}(\text{FEM}) = 16.00 \text{ kN}$



Comparison of EP-U-B: $F_{\max}(\text{test}) = 15.70 \text{ kN}$,
 $F_{\max}(\text{FEM}) = 16.16 \text{ kN}$

Figure 6.10: Quantitative comparisons between test results and FEM results

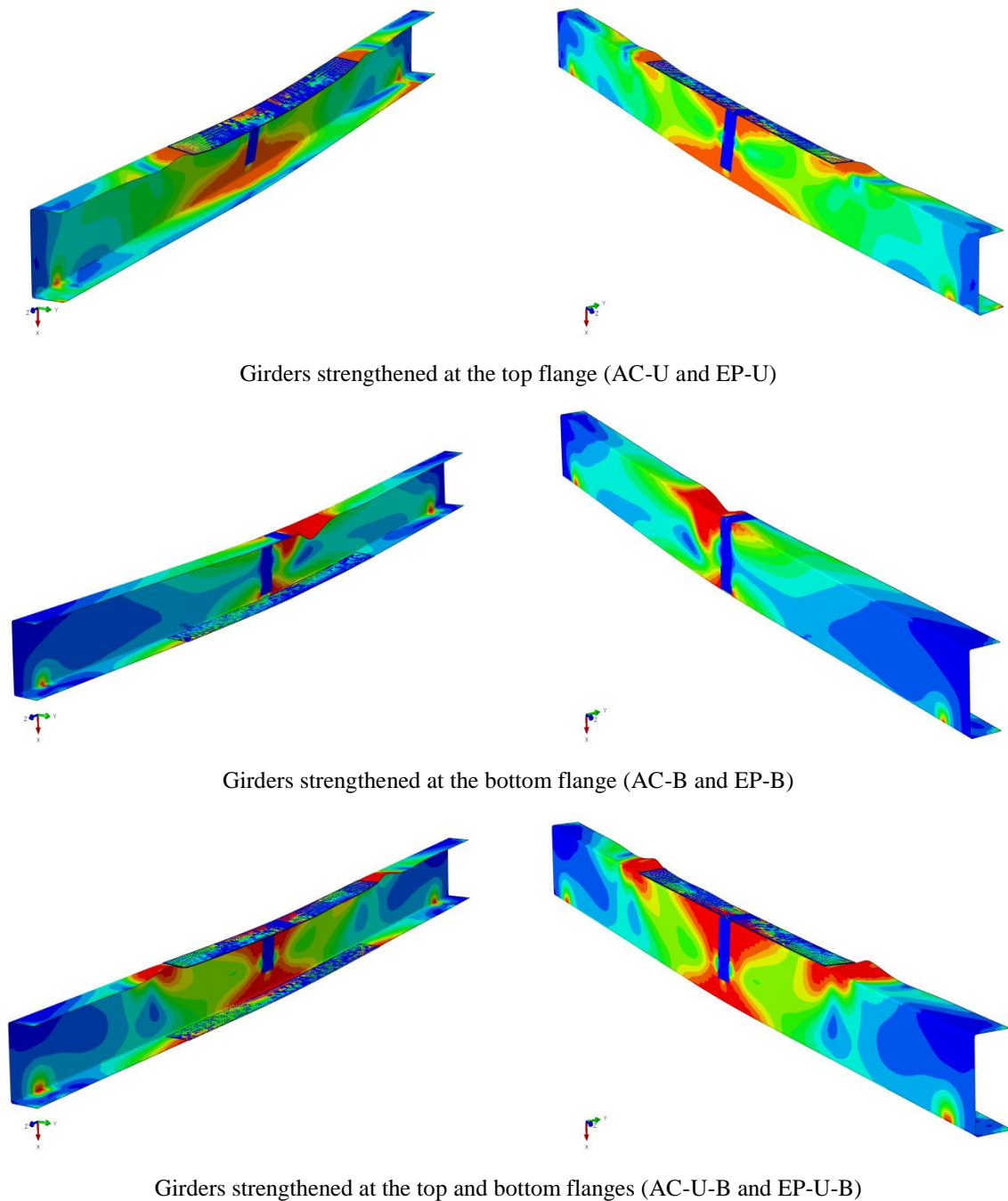


Figure 6.11: Qualitative validation of the models
Front view (left), back view (right)

Table 6.3: Material properties of the adhesives used in Abaqus for -20 °C and +40 °C

	Temperature [°C]	E [MPa]	σ_y [MPa]
AC-0.65	-20	1053	51.11
	+40	303	28.96
EP-0.65	-20	1023	38.47
	+40	812	32.74

6.5.3 Observations and results of the numerical investigations

It was noticed that the ($F-u$) diagrams for the investigated girders at the temperatures studied (-20 °C, and +40 °C) are identical to those obtained at the room temperature (shown in Figure 6.10); therefore they will not be presented again. In consequence, the capacities of the girders have not varied from those reached at room temperature, see section 6.4. Moreover, the stresses developing over the adhesive layers are distributed in the same form but having different values according to the temperature.

The von Mises stress distributions at the room temperature (RT), corresponding to the maximum force (F_{max}) recorded in FEM- calculations, are presented in Figure 6.12 for the girders strengthened by AC-bonded plates and in Figure 6.13 for those strengthened by EP-bonded plates.

It is clear that the farthest corners of the adhesive layers are the most stressed and that the high stresses are concentrated at the regions of (5-10 mm) wide which are very close to the edges while the stresses acting between these regions are relatively small.

It is well-understood that in lap bonded joints, the peel stresses (S_{11}) and shear stresses developing parallel to the adhesive layer (S_{13}) are concentrated at the ends of the adhesive layers; however, the concentration of all normal stresses (S_{11} , S_{22} , and S_{33}) have been increased in the layers used at the top due to the rotations occurred in the top flanges beside the strengthening plate, see Figure 6.14(a,c) for AC-bonded girders and Figure 6.15(a,c) for EP-bonded girders. This is obvious when these stresses are compared with the corresponding stresses developing over the bottom adhesive layers, Figure 6.14(b,d) and Figure 6.15(b,d) for AC-bonded girders and EP-bonded girders respectively.

Interestingly, it was found that the maximum von Mises values for the AC-bonded girders at the three temperatures studied are still lower than the yield strengths of the AC adhesive. This explains why no separation of the bonded plates occurred during the test at room temperature and also indicates the efficiency of these materials to be used over the temperature range considered. The same conclusion can be drawn to the girders bonded by epoxy at the bottom flange (EP-B), it can be seen that the yield strength at -20 °C and at room temperature has not been reached where no separation of the bonded plates was recorded. However, at +40 °C, the yielding of the adhesive is reached, and therefore, the separation is probable at this temperature as shown in Figure 6.15(b).

For the remaining cases (EP-U and EP-U-B), the separation is probable at the three temperatures since the yielding strength of epoxy has been reached. This also explains the separations of the bonded plates occurred during the test at room temperature.

6 A practical application of adhesively bonded joints (Strengthening cold-formed thin-gauged galvanized steel girders)

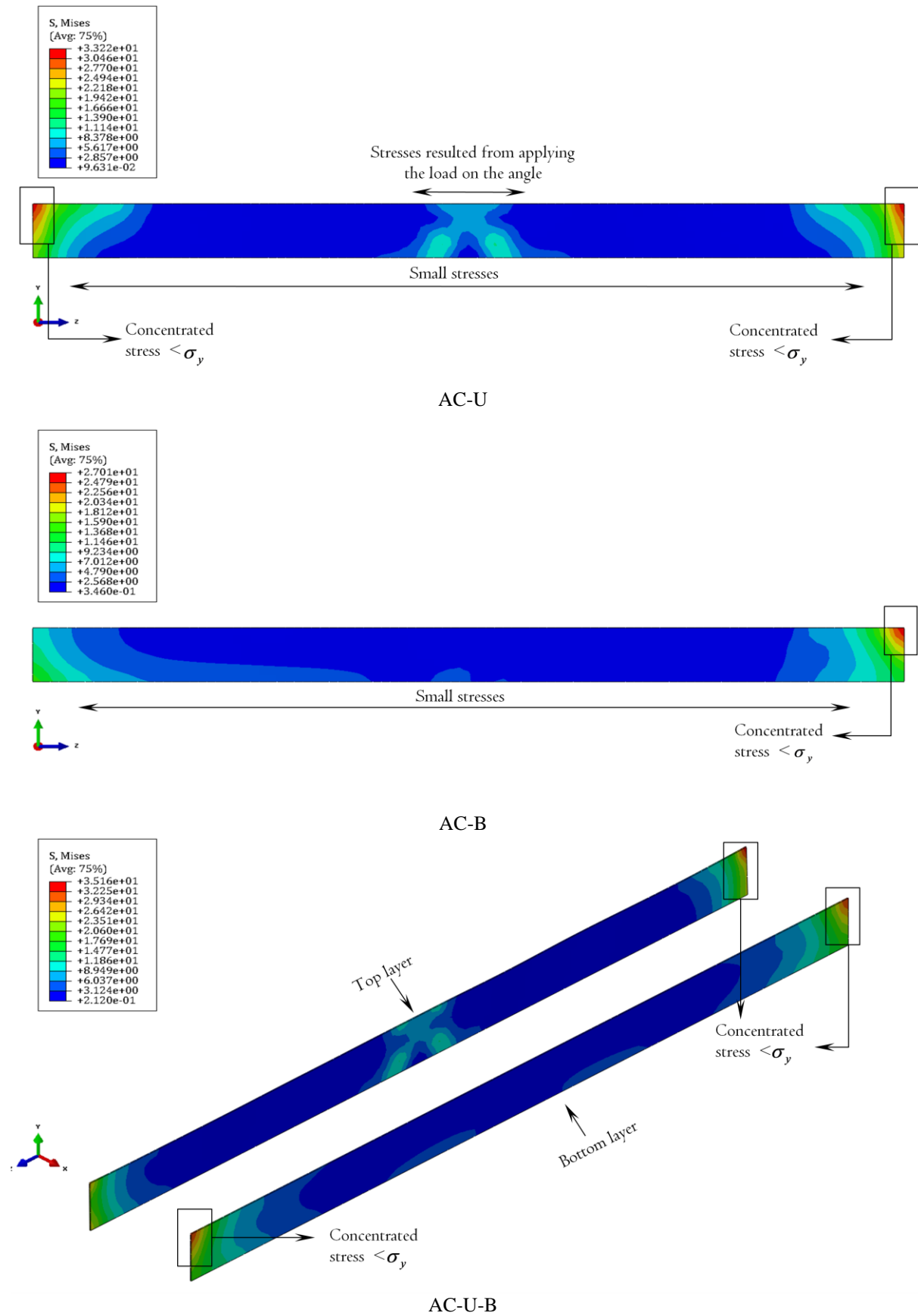


Figure 6.12: Von Mises stress distributions over the adhesive layers in AC-bonded girders

6 A practical application of adhesively bonded joints (Strengthening cold-formed thin-gauged galvanized steel girders)

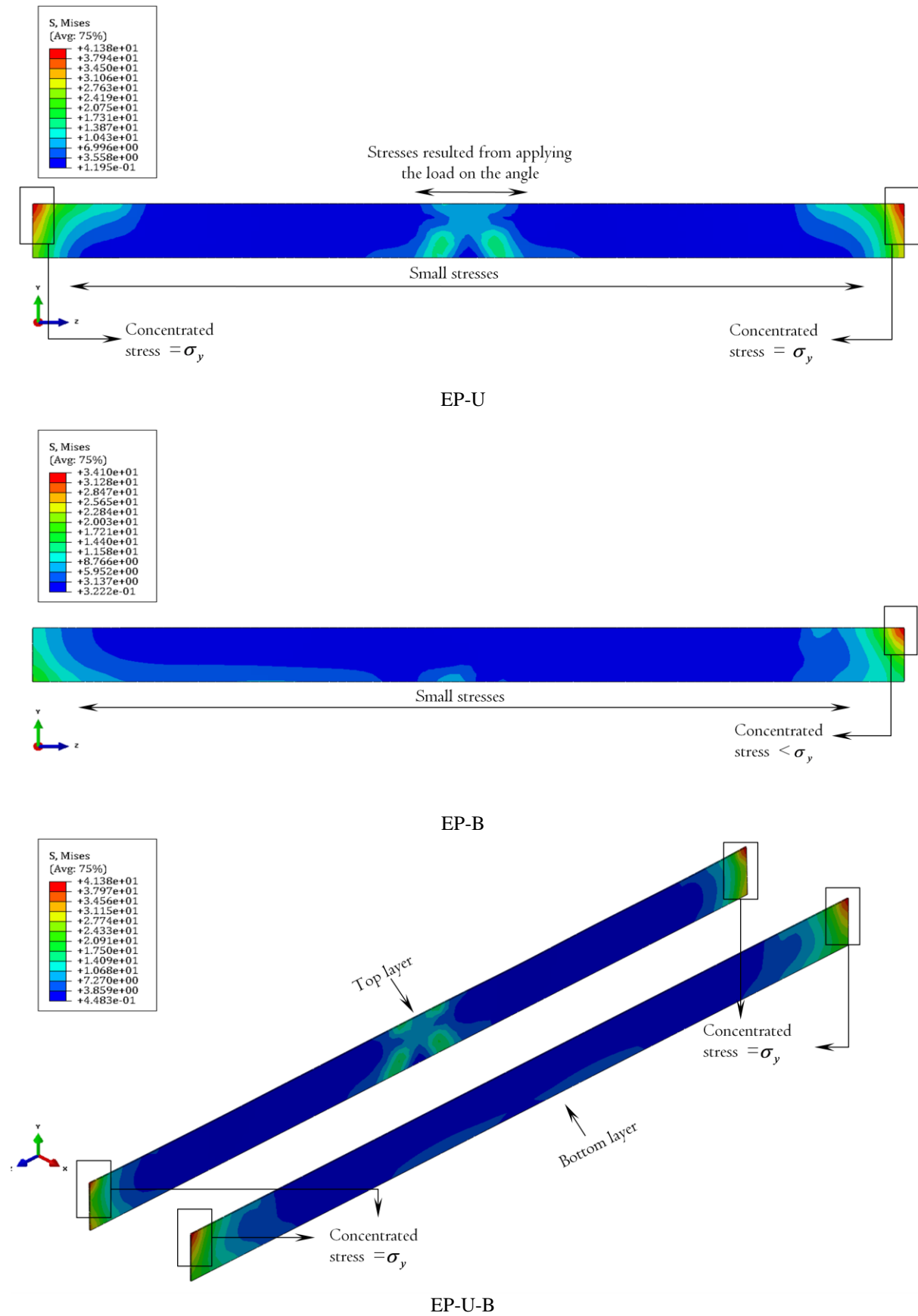


Figure 6.13: Von Mises stress distributions over the adhesive layers in EP-bonded girders

6 A practical application of adhesively bonded joints (Strengthening cold-formed thin-gauged galvanized steel girders)

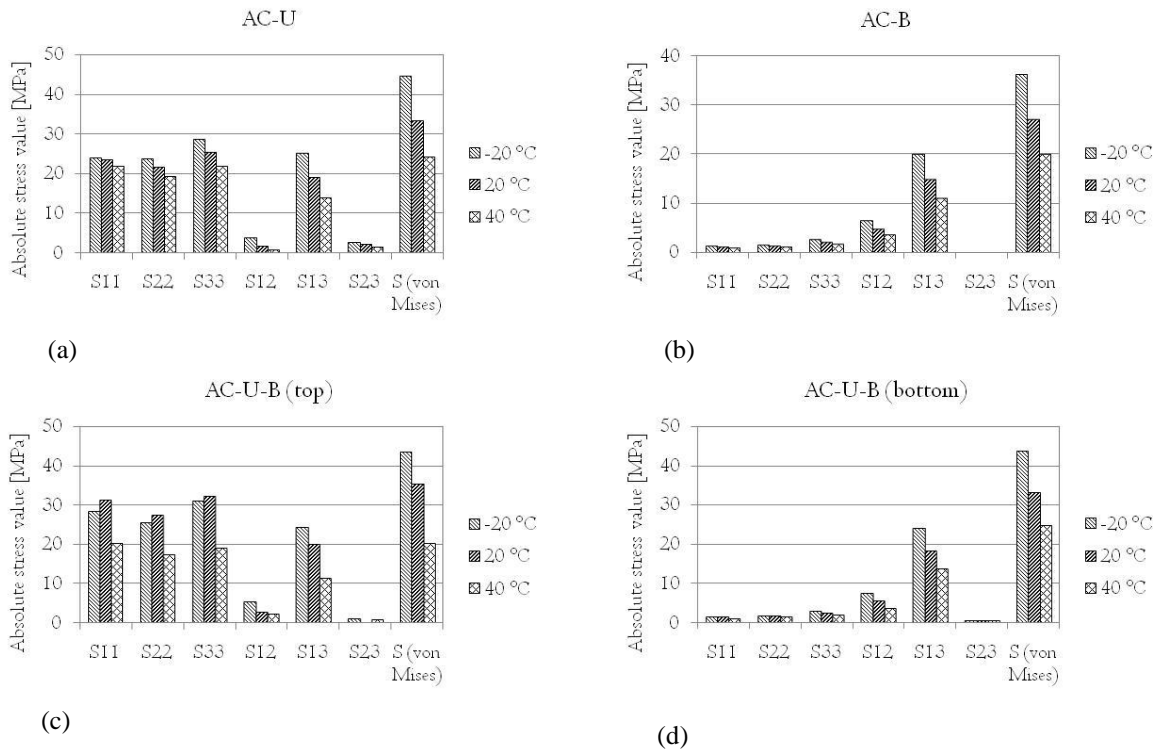


Figure 6.14: Absolute stress values in [MPa] for AC-bonded girders Corresponding to F_{max} , at the most stressed corner of adhesive layers at temperatures studied. σ_y values at (-20 °C, 20 °C, and 40 °C) are: (51.11 MPa, 36.96 MPa, and 28.96 MPa) respectively.

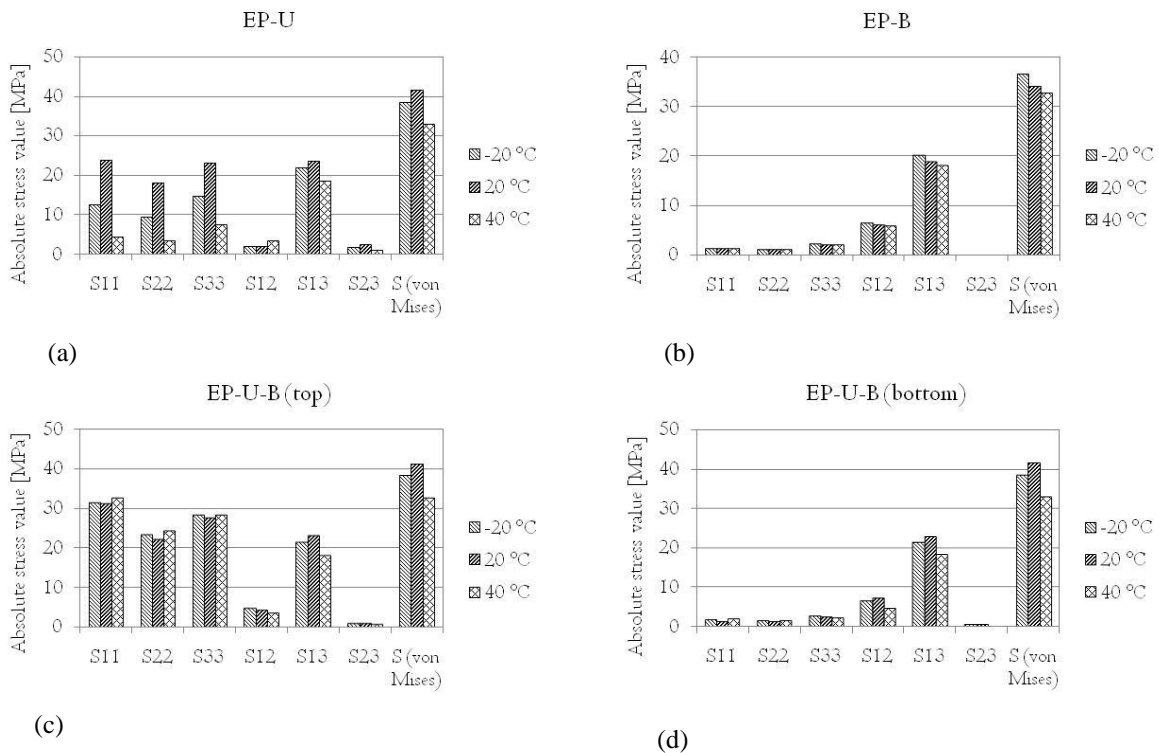


Figure 6.15: Absolute stress values in [MPa] for EP-bonded girders Corresponding to F_{max} , at the most stressed corner of adhesive layers at temperatures studied. σ_y values at (-20 °C, 20 °C, and 40 °C) are: (38.47 MPa, 41.38 MPa, and 32.74 MPa) respectively.

6.6 Conclusions

From the experimental results at the room temperature (RT) and the numerical results at (-20 °C, RT, and +40 °C) as well as the observations recorded during and after the tests, the following conclusions can be made:

- Strengthening the “C” section girders by bonding additional plates on their flanges could increase the capacity of the girders by about 31% for those which are strengthened at the top, 20% for those strengthened at the bottom, and 50-54% when girders are strengthened on both flanges. It should be noted that the increase of the capacity of the girders is not only dependent on the efficiency of the bonded joints, but also on the geometry of the plates used.
- Comparing with the deformation of the reference girder, the local buckling problem in the compressed flanges can be solved by strengthening these flanges using bonded joints to increase the thickness of the flange by an additional plate, which can be bonded not only externally, but also inside the profile.
- Comparing the girders bonded by EP at top flange (EP-U) with the corresponding girders bonded by AC, reveals that although the bonded plates started to separate (for EP girders), the increase of the capacity was the same because the collapse of the strengthened girders was due to the collapse of the “C” sections, out of the strengthened regions, which was earlier than the separation of the bonded plates.
- Comparing the girders bonded on both top and bottom flanges EP-U-B with AC-U-B, reveals that the bonded plates separated (for EP girders) a little before reaching the maximum capacity achieved by using AC adhesive (15.70 kN for EP and 16.11 kN for AC) making only 4% as a difference in the increase of the capacity. This is also because the separation of the bonded plates was approximately at the same time of the collapse of the “C” sections out of the strengthened regions.
- The temperature-dependent properties of the adhesives materials do not play any effective role in changing the behaviour of the strengthened girders nor their capacities. This is because the separation of the strengthening plates happens almost at the same time of the occurrence of the dominating collapses of the “C” girders.
- To absorb the deformations of the ductile steel sheets, the preferable adhesive to be used in their joints is the ductile one (acrylic adhesive AC) since it is easier to deform without breaking it.
- The efficiency of using bonded joints comes from the fact that relatively large bonded areas are used because most of these areas are subjected to very small stresses comparing with the stresses at the edges of them.
- Within the temperature range studied, the use of the bonded joints to strengthen the light-weight steel girders by additional plates might be considered more efficient as a strengthening method when the ends of these bonded plates are fixed to the strengthened structure by the use of one rivet (or bolt) at each end to reduce the

normal stresses at the edges of the adhesive layer. This idea might help not only for reducing the mentioned normal stresses, but also for resisting the creep phenomenon of the adhesives; however, further work has to be done on such combined joining methods.

7 General conclusions

This work presents a contribution to investigate the temperature effect on lap shear galvanized steel joints bonded by two different structural adhesives (Epoxy DP 490 and toughened acrylic DP 810) for short and long-term loading; in addition, a practical application of strengthening cold-formed lightweight steel girders of “C” section by bonding additional plates at their flanges is also given.

The investigations in the first experimental part, chapter 4, have focused on the effect of the temperature on the mechanical behaviour and shear properties of the adhesives when the joints are short-term-loaded. Two thicknesses of the adhesive layers are investigated (0.35 and 0.65 mm). The temperature range considered is from -20 °C to 40 °C.

The partial factors of the limit states as well as the conversion factors that cover the use conditions and circumstances, particularly the temperature influence, have been determined for the shear strengths of the adhesives. These factors were derived from the representative values (characteristic and design values) of the shear strength using the direct evaluation method according to ISO 2394:1998 and analysis model-based evaluation following the standard procedure recommended by EN 1990:2002 together with the systematic approach developed by Van Straalen. The proposed models describe the change of the shear strength of the studied adhesives due to the temperature change.

It was found that within the temperature range, the failure modes of the galvanized steel joints bonded by both acrylic and epoxy adhesives are mostly cohesive or special cohesive failures which necessarily means that the maximum shear strength of the adhesives represent the carrying capacity of the joints.

The degradation of the shear strength and the shear modulus of the adhesives due to the increase of the temperature are gradual because the studied temperature range is below the glass transition temperature T_g of both adhesives investigated.

Regardless of the adhesive kind or the bondline thickness investigated in this study, the maximum partial factor obtained by the direct evaluation method is 1.29 while from the model-based evaluation; the maximum partial factor is 1.32.

It was also found that the minimum conversion factor of the temperature effect is 0.29 and 0.69 from the first and second methods respectively. It is thought that the results obtained by the second method appear to be more convenient and reliable than those obtained by the first one because the direct evaluation method is strongly affected by the extreme values of the data sample within each statistical population considered; therefore, it is recommended to use the direct evaluation method only when the sample size of the results is big enough and the data obtained is not scattered.

In the chapter 5, the time-dependent behaviour (the shear creep behaviour), of both adhesives systems was investigated by performing realistic (non-accelerated) creep tests under different shear stress levels and temperatures.

Based on the findings of these investigations, it was concluded that:

Both Findley's and Burger's models well represent the shear creep of the used adhesives. However, generally, Findley's model fits the shear creep data points better than Burger's model over the test period. In this work it is seen that the long lifetime of the adhesives can be better predicted by Burger's model due to the unlimited retardation spectrum of Findley's model. This has been proven when comparing the predictions of these two models with the extrapolated lifetime using the steady-state creep rate approach.

The epoxy adhesive exhibits a creep strength that is much higher than the acrylic adhesive; therefore, the use of epoxy adhesives in structural applications designed for long time is more recommended than the use of acrylic adhesive. Both of them are not able to resist the creep phenomenon for the intended lifetime of the structural applications of 50 years. As a contribution, this work expects that for applications designed for 25 years lifetime, AC-0.65, EP-0.35, and EP-0.65 seem to be usable. While AC-0.35 may be used for applications designed for a period up to 5 years.

The limits of the applied shear stresses over which the joints are expected to be failed earlier than a particular lifetime are estimated throughout these investigations. It was found, for example, for the lifetime of up to 25 years, these limits are 1.2%, 3.0%, 4.3% of the maximum shear strengths of the adhesives AC-0.65, EP-0.35, and EP-0.65 respectively.

The shear strains of the bonded joints can reach extents which exceed the average shear strains of the rapid test due to the static nature of applying the loads; moreover, the high temperature influences the behaviour of the adhesive over a long time and makes it more ductile while the low temperature makes it more rigid.

It is also seen that taking the average shear strain of the short-term loading in order to predict the lifetime of the bonded joints using the prediction models, gives values of the lifetime which can be considered still on the safe side.

Generally, it could be said that using structural adhesives for long time in structural applications still needs to be statistically ascertained by testing these materials with sufficient number of specimens and to consider all loading conditions that the bonded joint is supposed to resist. Until that time, the use of them with the help of a few rivets or bolts is recommended to construct a joint that is able to resist the creep by the rivets or bolts and also has high strength provided by the adhesive.

The last part of the investigations on the strengthened cold-formed "C" section girders by bonding additional plates at their flanges (chapter 6) at the room temperature (RT) and at (-20 °C and +40 °C) showed that:

Strengthening the "C" section girders by bonding additional plates at their flanges can increase the capacity of the girders by about 31% for those which are strengthened on the top,

20% for those strengthened at the bottom, and 50-54% when girders are strengthened on both flanges.

The local buckling problem in the compressed flanges can be solved by strengthening these flanges using bonded joints to increase the thickness of the flange by an additional plate, which can be bonded not only externally, but also inside the profile.

The collapse of the strengthened girders is due to the collapse of the “C” sections, out of the strengthened regions, which is earlier than the separation of the bonded plates.

The temperature-dependent properties of the adhesives materials do not play any effective role in changing the behaviour of the strengthened girders nor their capacities.

To absorb the deformations of the ductile steel sheets, the preferable adhesive to be used in their joints is the ductile one (acrylic adhesive AC) since it is easier to deform without breaking it.

The efficiency of using bonded joints comes from the fact that relatively large bonded areas are used because most of these areas are subjected to very small stresses comparing with the stresses at the edges of them.

Within the temperature range studied, the use of the bonded joints to strengthen the light-weight steel girders by additional plates might be considered more efficient as a strengthening method when the ends of these bonded plates are fixed to the strengthened structure by the use of one rivet (or bolt) at each end to reduce the normal stresses at the edges of the adhesive layer.

8 Future works

This work has shown a great efficiency of the adhesive bonding technique for joining and strengthening lightweight steel structures. The potential of using the bonded joints comes basically from two facts: the first is the improved properties of the structural adhesives and the second is that large bonded areas are used in such joints. So, for developing this technique and making it applicable by the structural designers in the field of steel constructions, it is recommended as future research activities and works to standardize this technique by extending the study field to accommodate different bondline thicknesses and all possible loading and environmental conditions into account, such as the effect of varying loading cases (cyclic and impact loading), constant and varying humidity, the humidity with temperature together, and different combinations of mechanical and environmental loading.

This procedure will provide the designers with the reliable representative values of the capacities of bonded steel joints and partial safety factors suitable for all possible conditions to which these joints are subjected over the designed lifetime of the structure.

The need to perform the long-term tests with a larger number of specimens is of great importance in order to verify the predicted time-to-failure presented in this research. Moreover, it is necessary to realize the influence of changing environmental conditions in the creep tests.

It is also advised to investigate the adhesively bonded steel joints with a few rivets or bolts at the ends of the bonded strengthening plates.

9 References

- [1] **Hart-Smith L. j.:** *Adhesive-bonded double-lap joints*: National Aeronautics and Space Administration, Technical Report NASA CR-112235, 1973.
- [2] **Tasi M. Y.; Oplinger D. W.; Morton J.:** *Improved theoretical solutions for adhesive lap joints*: Int. J. Solids Structures, vol. 35, Nr. 12, pp. 1163-1185, 1998.
- [3] **Kim H. ; Kedward K.:** *Stress analysis of in-plane, shear-loaded, adhesively bonded composites and assemblies*: University of California Santa Barbara, Final Report Nr. DOT/FAA/AR-01/7, 2001.
- [4] **Pasternak H.; Piekarczyk M.; Kubieniec G.:** *Adhesives in strengthening of steel structures*: Statybinės Konstrukcijos ir Technologijos, vol. 2, Nr. 2, pp. 45-50, 2010.
- [5] **Da Silva L. F.; Carbas R. J.; Critchlow G. W.; Figueiredo M. A.; Brown K. :** *Effect of material, geometry, surface treatment and environment on the shear strength of single lap joints (steel joints with epoxy)*: International Journal of Adhesion & Adhesives, vol. 29, Nr. 6, pp. 621-632, 2009.
- [6] **Eskandarian M.; Rousseau N.; Hamel F.:** *On the influence of joint geometry and adhesive bulk properties on quasistatic performance of lap-shear joints*: Proceedings of the 34th Annual Meeting of the Adhesion Society, Canada, 2011.
- [7] **Müller M.; Herák D.:** *Dimensioning of the bonded lap joint*: Res. Agr. Eng., vol. 56, Nr. 2, pp. 59-68, 2010.
- [8] *Guide to the structural use of adhesive*: The Institution of Structural Engineers SETO ISBN 1 874266 43 3, London, 1999.
- [9] **Da Silva L. F.; Dillard D. A.; Blackman B.; Adams R. D.:** *Testing Adhesive Joints_ Best Practices*: Wiley-VCH Verlag & Co. KGaA, ePDF ISBN: 978-3-527-64705-7, 2012.
- [10] **San Román J. D. C.:** *Experiments on Epoxy, Polyurethane and ADP Adhesives*: Composite construction laboratory, Technical Report Nr. CCLab2000.1b/1, 2005.
- [11] *Adhesive Material Characterisation-Enforce EP structural adhesives (Standard & Winter Grade)*: Joining Technology Research Centre, Oxford BROOKES University, Report Nr. JTRC/Wsbd/01, 2002.
- [12] **Czarnocki P.; Piekarski K.:** *Yielding of adhesives*: Journal of materials science, vol. 21, pp. 4296-4298, Chapman & Hall Ltd.,1986.
- [13] **Huveners E. M.; Van Herwijnen F.; Soetens F.; Hofmeyer H.:** *Mechanical shear properties of adhesives*: Glass Performance Days, Proceedings of the 10th International conference in Tampere, pp.367-370, Finland, 2007.
- [14] **Tomblin J.; Seneviratne W.; Escobar P.; Yoon-Khian Y.:** *Shear Stress-Strain Data for Structural Adhesives*: U.S. Department of Transportation, Office of Aviation Research, Final report DOT/FAA/AR-02/97, Washington, 2002.
- [15] **Ojeda C. E.; Oakes E. J.; Aldi D.; Forsberg G. A.:** *Temperature effects on adhesive bond strengths and modulus for commonly used spacecraft structural adhesives*: Jet Propulsion Laboratory, California Institute of Technology, 2011.

- [16] **Da Silva L. F.; Adams R. D.:** *Measurement of the mechanical properties of structural adhesives in tension and shear over a wide range of temperatures:* J. Adhesion Sci. Technol., vol. 19, Nr. 2, pp. 109–141, 2005.
- [17] **Osanai K. R.; Reis M. L.:** *Temperature effect on the strength of adhesively bonded single lap joints:* Engenharia Térmica (Thermal Engineering), vol. 11, Nr. 1-2, pp. 03-06, 2012.
- [18] **Sahellie S.; Pasternak H.:** *Temperature Effect on Mechanical Behaviour of Adhesive Bonded Steel Joints under Short and Long-Term Loading:* 13th International Scientific Conference, vol. II, pp. 7-12, Sofia, 2013.
- [19] **Broughton W. R.:** *Creep Testing of Adhesive Joints Analysis of Creep Rupture Data:* NPL Report CMMT(A) 195 Nr.14, UK, 1999.
- [20] **Boyes R.:** *Adhesive bonding of stainless steel: strength and durability:* Ph.D. Thesis, Sheffield Hallam University, 1998.
- [21] **Broughton B.:** *Durability performance of adhesive joints:* Measurement good practice guide Nr.28, National physical laboratory NPL,ISSN 1368-6550, UK, 2000.
- [22] **Willams M. L.; Landel R. F.; Ferry J. D.:** *The temperature dependence of relaxation mechanisms in amorphous polymers and other glass forming liquids:* Journal of American Chemical Society, vol. 77, pp. 3701-3707, 1955.
- [23] **Dealy J.; Plazek D.:** *Time-Temperature Superposition- A user Guide:* Rheology Bulletin, vol. 78, Nr. 2, pp. 16-31, 2009.
- [24] **Dasappa P.:** *Constitutive Modelling of Creep in a Long Fiber Random Glass Mat Thermoplastic Composite:* Ph.D. thesis in Mechanical Engineering, University of Waterloo, Canada, 2008.
- [25] **Horvath J. S.:** *Mathematical Modelling of the Stress-Strain-Time Behaviour of Geosynthetics Using the Findley Equation: General Theory and Application to EPS-Block Geofoam:* Manhattan College Research Report Nr. CE/GE-98-3, USA, 1998.
- [26] **Dean G. D.; Broughton W. R.:** *A Review of Creep Modelling for Toughened Adhesives and Thermoplastics:* NPL Report DEPC-MPR 011, ISSN 1744-0270, UK, 2005.
- [27] **Majda P.; Skrodzewicz J.:** *A modified creep model of epoxy adhesive at ambient temperature:* International Journal of Adhesion & Adhesives, vol. 29, pp. 396–404, 2009.
- [28] **Feng C. -W.; C. Keong -W.; Hsueh Y. -P.; Wang Y. -Y.; Sue H. -J.:** *Modeling of long-term creep behaviour of structural epoxy adhesives:* International Journal of Adhesion & Adhesives, vol. 25, pp. 427–436, 2005.
- [29] **Costa I. G.; Barros A. O.:** *Prestressed NSM-FRP laminates – assessing the creep behaviour of the bonding agent:* Semana da Escola de Engenharia, Minho, 2011.
- [30] **Costa I. G.; Barros A. O.:** *Assessment of the long term behaviour of structural adhesives in the context of NSM flexural strengthening technique with prestressed CFRP laminates:* FRPRCS11- Joaquim Barros & José Sena-Cruz (Eds) / UM, Guimarães, 2013.
- [31] **Van Straalen I. J.; Van Tooren M. L.:** *Development of design rules for adhesive bonded joints:* HERON, vol. 47, Nr. 4, 2002.

- [32] **Van Straalen I. J.:** *Development of design rules for structural adhesive bonded joints- A systematic approach*: Ph.D. thesis, Delft University of Technology, ISBN 90-9014507-9, the Netherlands, 2001.
- [33] **Davies C.:** *The use of adhesive bonding in steel-framed buildings and structures*: ISSN 1018-5593, European Commission, Directorate-General of Science, Research and Development, UK, 1997.
- [34] **Pasternak H.; Meinz J.:** *Versuche zu geklebten Verstärkungen im Stahlhochbau*: Bauingenieur , vol. 81, pp. 212-217, 2006.
- [35] **Pasternak H.; Schwarzlos A. :** *Kleben von Stahl- Stahlbaukalender 2005*,: Ernst & Sohn Verlag, vol. 7, pp. 785-818, 2005.
- [36] **Pasternak H.; Schwarzlos A.; Schimmack N.:** *The application of adhesives to connect steel members*: Journal of Constructional Steel Research, vol. 60, pp. 649–658, 2004.
- [37] **Pasternak H.; Meinz J.:** *Adhering in steel construction- advantages and possibilities*: 9th International Conference Proceedings: Modern Building Materials, Structures and Techniques, Vilnius (Litauen), 2007.
- [38] **Pasternak H.; Meinz J.:** *Adhesive bonding- a promising joining technique also in steel construction*: Fifth International Conference on Thin-Walled Structures, vol. 1, pp. 67-74, Brisbane, Australia, 2008.
- [39] *History of adhesives*: BSA-Educational Services Committee ESC, ESC report, vol. 1, Nr. 2, pp. 1-4, 1991.
- [40] **Habenicht G.:** *Applied Adhesive Bonding- A Practical Guide for Flawless Results*: ISBN: 978-3-527-32014-1, WILEY-VCH Verlag GmbH & Co. KGaA, Weinheim, 2009.
- [41] Adhesives.org/Sealants.org: Adhesive and Sealant Council (ASC), 2008. [Online]. Available: <http://www.adhesives.org/adhesives-sealants/market-overview-applications/transportation>.
- [42] **Meinz J.:** *Kleben im Stahlbau- Betrachtungen zum Trag- und Verformungsverhalten und zum Nachweis geklebter Trapezprofilanschlüsse und verstärkter Hohlprofile in Pfosten-Riegel-Fassaden*: Ph.D. thesis at BTU-Cottbus, ISBN 978-3-89998-184-1, Weißensee Verlag, Berlin, 2010.
- [43] **Pasternak H.; Meinz J.; Feldmann M.; Völling B.; Abeln B.; Dilger K.; Böhm S.; Ullmann M.; Ummenhofer T.; Medgenberg J.; Geiß L.; Wagner A. :** *Neue Konstruktionen durch Einsatz von Klebverbindungen im Stahlbau: Forschung für die Praxis*, Projekt P 654 , Deutschland, 2008.
- [44] **Habenicht G.:** *Kleben: Grundlagen, Technologien, Anwendungen*: Technical University of München, expanded and updated edition 5, Germany, 2005.
- [45] DIN EN 10327-2004: *Continuously hot-dip coated strip and sheet of low carbon steels for cold forming*.
- [46] DIN 50125-2009: *Testing of metallic materials –Tensile test pieces*.
- [47] ISO 6892-1- 2009(E): *Metallic materials — Tensile testing — Part 1: Method of test at room temperature*.
- [48] **Ciupack Y.; Pasternak H.:** *Calibration of Design Rules in Accordance with Eurocode Using the Example of Adhesive Joints*: Bauingenieur, Nr. 87, pp. 116-123, 2012.

- [49] ASTM: D 3528 – 96: reapproved 2002: *Standard Test Method for Strength Properties of Double Lap Shear Adhesive Joints by Tension Loading*.
- [50] DIN EN 14869-2- 2011: *Structural adhesives – Determination of shear behaviour of structural bonds – Part 2: Thick adherends shear test*.
- [51] DIN EN ISO 9664- 1995: *Test methods for fatigue properties of structural adhesives in tensile shear*.
- [52] **Sahellie S.; Pasternak H.:** *Concentration of the normal stresses in the adherends of adhesively bonded double lap steel joints due to reducing the width of the bonded area: 14th international scientific conference VSU'2014, Sofia, 2014*.
- [53] **Klamer E.-L.:** *Influence of temperature on concrete beams strengthened in flexure with CFRP: Ph.D. thesis-ISBN 978-90-6814-619-6, Technische Universiteit Eindhoven, 2009*.
- [54] EN ISO 10365- 1995: *Adhesives - Designation of main failure patterns*.
- [55] ASTM: D 5573- 1999: *Standard Practice for Classifying Failure Modes in Fiber-Reinforced-Plastic (FRP) Joints*.
- [56] **Pasternak H.; Ciupack Y.; Dilger K.; Hanssen E.:** *Entwicklung eines Eurocode-basierten Bemessungskonzepts für Klebverbindungen im Stahlbau (in Anlehnung an DIN EN 1990), IGF-Vorhaben: 16494 BG-FOSTA P 827, Final report, Germany, 2012*.
- [57] EN 1990 - 2002: *Eurocode — Basis of structural design*.
- [58] **Romeu J. L.:** Anderson – Darling: *A goodness of fit test for small samples assumptions: Selected topics in Assurance Related Technologies (START), Reliability Analysis Center (RAC), vol. 10, Nr. 5, 2005*.
- [59] *Guidance for data quality assessment-Practical methods for data analysis: EPA QA/600/R-96/084 (QA 97 version), United States Environmental Protection Agency, USA, 1998*.
- [60] **Dixon W. J.:** *Ratios involving extreme values*, University of Oregon: contract N6-onr-218/IV with the office of Naval Research, 1950.
- [61] **Rorabacher D.:** *Statistical Treatment for Rejection of Deviant Values Critical Values of Dixon's "Q" Parameter and Related Subrange Ratios at the 95% Confidence Level: analytical chemistry, vol. 63, Nr. 2, 1991*.
- [62] ISO 2394- 1998: *General principles on reliability for structures*.
- [63] **Pap J.-S.; Kästner M.; Müller S.; Jansen I.:** *Experimental characterization and simulation of the mechanical behaviour of an epoxy adhesive: Procedia Materials Science, vol. 2, pp. 234-242, 2013*.
- [64] **Meshgin P.; Choi K.; Taha M.:** *Shear creep of epoxy at the concrete–FRP interfaces: ScienceDirect, vol. Part B 38, pp. 772–780, 2007*.
- [65] **Meshgin P.; Choi K.; Taha M.:** *Experimental and analytical investigations of creep of epoxy adhesive at the concrete–FRP interfaces: International Journal of Adhesion & Adhesives, vol. 29, pp. 56–66, 2009*.
- [66] ETAG 001- 2008: *Guideline for European Technical Approval of metal anchors for use in concrete-Part five: Bonded Anchors*.
- [67] ASTM: D 2294–96 - reapproved 2008: *Standard Test Method for Creep Properties of Adhesives in Shear by Tension Loading (Metal-to-Metal)*.

- [68] ASTM:D 1780-99 - 1999: *Standard Practice for Conducting Creep Tests of Metal-to-Metal Adhesives*.
- [69] **Yanni V. Y. G.:** *Multi-scale investigation of tensile creep of ultrahigh performance concrete for bridge applications: A Doctoral Thesis Dissertation*, Georgia Institute of Technology, 2009.
- [70] **Queiroz R. A.; Sampaio E. M.; Cortines V. J.; Rohem N. R.:** *Study on the creep behaviour of bonded metallic joints*: Applied Adhesion Science, vol. 8, Nr. 2, 2014.
- [71] **Cook R. A.; Douglas E. P.; Davis T. M.:** *Adhesive Anchors in Concrete under sustained loading conditions*: NCHRP, Report 639, ISSN 0077-5614, ISBN 978-0-309-11788-3, university of Florida, Transportation Research Board, Washington, 2009.
- [72] **Kubieniec G.; Piekarczyk M.:** *Thin-Walled Steel Girders Reinforced With Use of Adhesives- Experimental and Numerical Investigation*: 5th European Conference on Steel and Composites Structures Eurosteel, pp. 1611-1616., Graz, Austria, 2008.
- [73] **Pasternak H.; Mainz J.:** *Kleben im Stahlbau – zwei Beispiele aus dem Fassadenbau*: Bauingenieur, vol. 82, Nr. 3, 2007.
- [74] **Albakhali E. A.:** *Finite element modelling for thermal stresses developed in riveted and riveted-bonded joints*: International Journal of Engineering & Technology, vols. IJET-IJENS11-6, pp. 106-112, 2011.
- [75] Abaqus, user's manual, version 6.11-3, 2011.
- [76] EN 1993-1-5 - 2006: *Eurocode 3 - Design of steel structures - Part 1-5: Plated structural elements*.
- [77] **Öchsner A.; Stasiak M.; Mishuris G.; Gracio J.:** *A new evaluation procedure for the butt-joint test of adhesive technology: Determination of the complete set of linear elastic constants*: International Journal of Adhesion & Adhesive, vol. 27, pp. 703–711, 2007.
- [78] **Suhir E.:** *Interfacial thermal stresses in a bi-material assembly with a low-yield-stress bonding layer*: Modelling and Simulation in Materials Science and Engineering, vol. 14, pp. 1421–1432, 2006.
- [79] **Nirosha N. B.:** *Structural behaviour and design of cold-formed steel beams at elevated temperatures*: Ph.D. Thesis, school of urban developments, Queensland University of Technology, 2010.
- [80] **Cease H.; Derwent P.; Diehl H.; Fast J.; Finley D.:** *Measurement of mechanical properties of three epoxy adhesives at cryogenic temperatures for CCD construction*: Fermi National Accelerator Laboratory, Fermilab-TM-2366-A, Batavia, 2006.

10 Appendices

10.1 Appendix A

The reported failure modes with respect to the environmental conditions of film and paste adhesives used to bond aluminum lap shear joints according to [14].

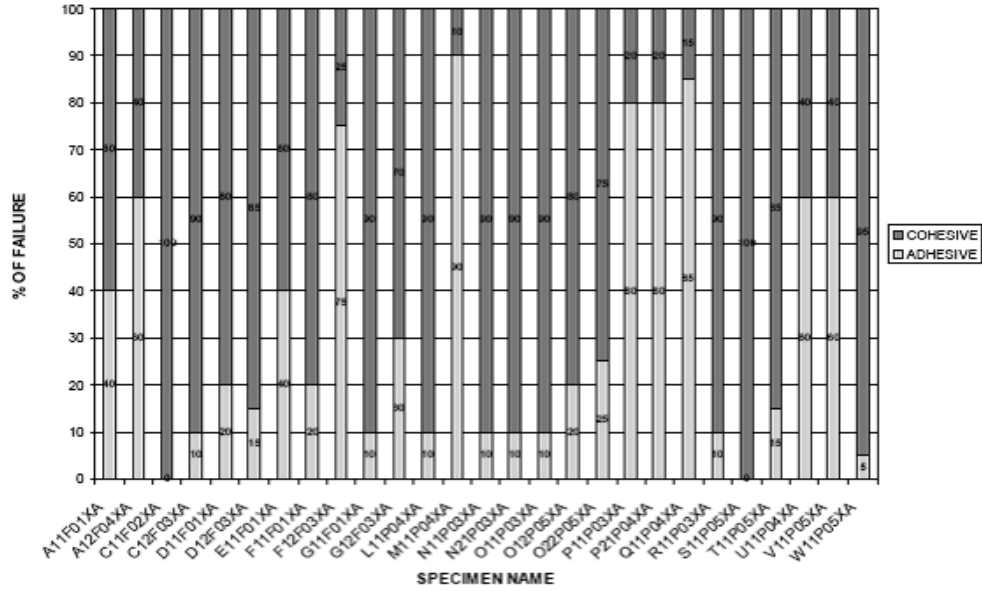


Figure 10.1: Failure modes of (RTD) specimens

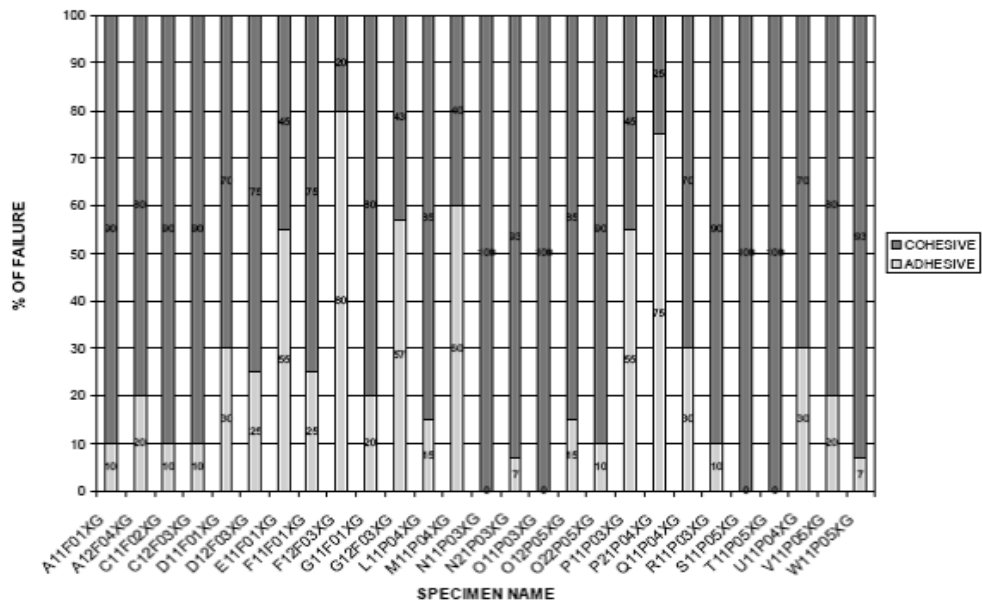


Figure 10.2: Failure modes of (ETD) specimens

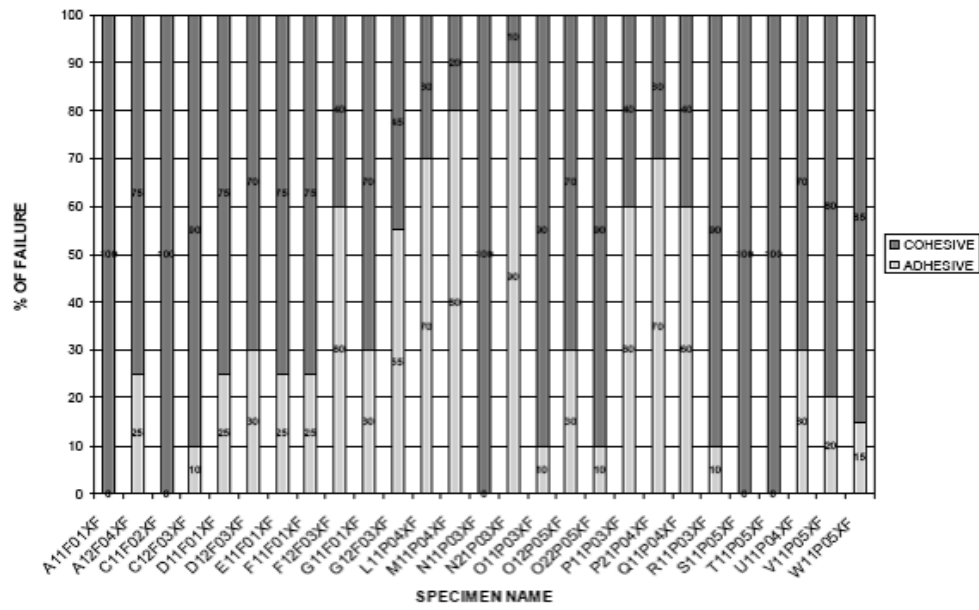


Figure 10.3: Failure modes of (ETW) specimens

10.2 Appendix B

10.2.1 Failure modes designations







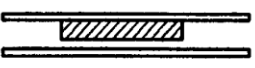
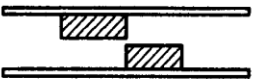
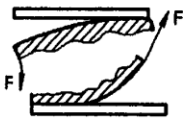
	Failure patterns	Designation
Substrate	 <p>Failure of one or both adherends (Substrate failure)</p>	SF
	 <p>Failure of an adherend (Cohesive substrate failure)</p>	CSF
	 <p>Failure through delamination (Delamination failure)</p>	DF
Adhesive	<p>Types of cohesion failure</p>  <p>Cohesion failure</p>	CF
	  <p>Special cohesion failure</p>	SCF
	  <p>Adhesion failure</p>	AF
	 <p>Adhesion and cohesion failure with peel</p>	ACFP

Figure 10.4: Designations of the failure patterns acc. to EN ISO 10365:1995

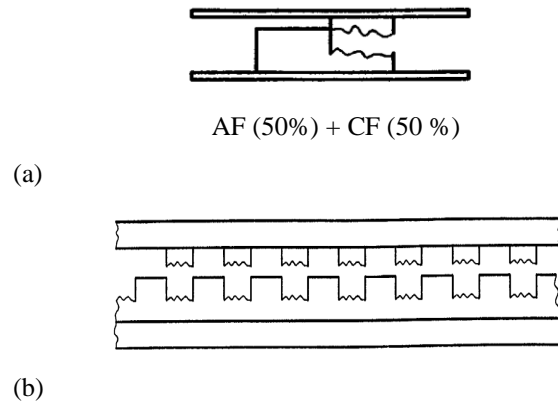


Figure 10.5: Examples of (a) the mixed failure and (b) the oscillating rupture acc. to EN ISO 10365:1995

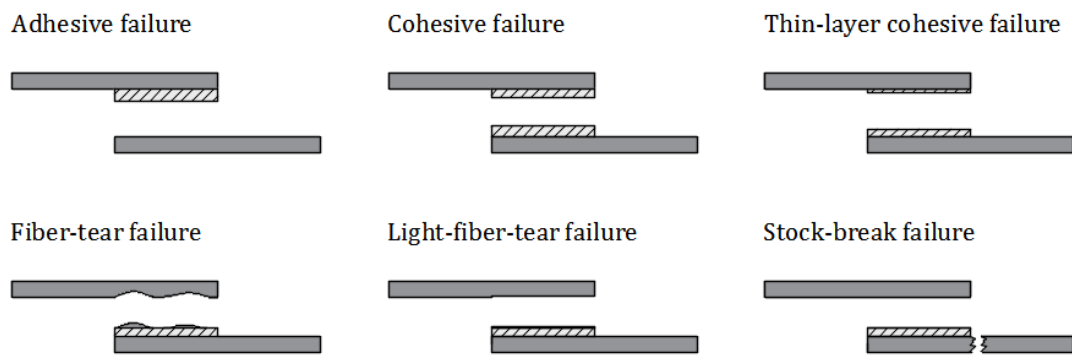


Figure 10.6: Sketches representing the failure modes acc. to ASTM 5573-99

10.2.2 Mean values and standard deviations of the mechanical properties of the acrylic and epoxy adhesives

For AC-0.35:

	Temperature [°C]						
G [MPa]	-20	-10	0	10	20	30	40
Mean	279.58	234.73	236.91	254.09	195.13	118.84	79.49
S.D.	56.63	17.66	69.71	52.22	32.45	5.87	7.26

	Temperature [°C]						
τ_{max} [MPa]	-20	-10	0	10	20	30	40
Mean	33.70	33.66	29.11	28.95	26.58	20.85	16.31
S.D.	1.40	1.01	1.81	0.62	0.54	0.50	1.75

	Temperature [°C]						
$\tau_{at Break}$ [MPa]	-20	-10	0	10	20	30	40
Mean	33.45	33.36	28.40	27.96	25.37	17.56	12.02
S.D.	1.44	0.99	2.27	0.76	0.59	4.82	3.97

	Temperature [°C]						
$\gamma_{at \tau_{max}}$ [-]	-20	-10	0	10	20	30	40
Mean	0.41	0.43	0.49	0.52	0.69	0.75	0.86
S.D.	0.03	0.02	0.10	0.04	0.04	0.04	0.13

	Temperature [°C]						
$\gamma_{at Break}$ [-]	-20	-10	0	10	20	30	40
Mean	0.45	0.47	0.57	0.62	0.73	0.87	1.31
S.D.	0.05	0.03	0.13	0.06	0.05	0.04	0.13

For AC-0.65:

	Temperature [°C]						
G [MPa]	-20	-10	0	10	20	30	40
Mean	365.79	321.33	382.89	301.20	196.23	157.36	119.68
S.D.	38.45	25.11	46.50	20.11	39.94	10.74	39.55

	Temperature [°C]						
τ_{max} [MPa]	-20	-10	0	10	20	30	40
Mean	27.80	27.42	27.13	26.04	21.50	19.06	17.13
S.D.	3.09	1.98	1.21	0.70	1.08	0.43	1.22

	Temperature [°C]						
$\tau_{at Break}$ [MPa]	-20	-10	0	10	20	30	40
Mean	27.69	27.26	26.16	25.03	15.42	12.84	11.38
S.D.	3.02	1.97	1.20	1.18	3.30	4.63	3.43

	Temperature [°C]						
$\gamma_{at \tau_{max}}$ [-]	-20	-10	0	10	20	30	40
Mean	0.27	0.23	0.37	0.42	0.64	0.69	0.98
S.D.	0.09	0.09	0.07	0.07	0.09	0.05	0.20

	Temperature [°C]						
$\gamma_{at Break}$ [-]	-20	-10	0	10	20	30	40
Mean	0.29	0.24	0.46	0.50	1.01	0.97	1.32
S.D.	0.11	0.10	0.10	0.12	0.19	0.13	0.27

For EP-0.35:

	Temperature [°C]						
G [MPa]	-20	-10	0	10	20	30	40
Mean	224.08	287.84	254.79	214.91	233.97	195.23	205.96
S.D.	55.76	14.76	61.17	13.29	50.81	12.79	11.24

	Temperature [°C]						
τ_{max} [MPa]	-20	-10	0	10	20	30	40
Mean	29.36	29.69	29.29	29.41	26.68	22.43	20.88
S.D.	2.04	1.86	2.09	0.72	0.60	0.86	0.69

	Temperature [°C]						
$\tau_{at Break}$ [MPa]	-20	-10	0	10	20	30	40
Mean	29.36	28.90	28.30	28.37	24.72	21.40	19.95
S.D.	2.04	3.08	1.88	1.07	2.12	1.11	0.59

	Temperature [°C]						
$\gamma_{at \tau_{max}}$ [-]	-20	-10	0	10	20	30	40
Mean	0.16	0.18	0.24	0.24	0.25	0.23	0.23
S.D.	0.03	0.05	0.08	0.04	0.04	0.10	0.04

	Temperature [°C]						
$\gamma_{at Break}$ [-]	-20	-10	0	10	20	30	40
Mean	0.16	0.26	0.33	0.29	0.40	0.28	0.33
S.D.	0.03	0.13	0.17	0.05	0.16	0.14	0.03

For EP-0.65:

	Temperature [°C]						
G [MPa]	-20	-10	0	10	20	30	40
Mean	371.05	348.60	336.32	296.87	317.59	262.92	294.53
S.D.	36.66	15.46	24.22	33.84	14.66	20.45	22.24

	Temperature [°C]						
τ_{max} [MPa]	-20	-10	0	10	20	30	40
Mean	22.21	26.07	23.62	22.98	23.89	18.66	18.90
S.D.	2.45	0.76	2.77	2.29	0.76	0.84	1.01

	Temperature [°C]						
$\tau_{at Break}$ [MPa]	-20	-10	0	10	20	30	40
Mean	22.21	26.05	23.62	22.97	21.32	14.80	18.79
S.D.	2.45	0.75	2.77	2.28	1.28	6.94	0.96

	Temperature [°C]						
$\gamma_{at \tau_{max}}$ [-]	-20	-10	0	10	20	30	40
Mean	0.07	0.13	0.08	0.11	0.14	0.17	0.11
S.D.	0.02	0.03	0.02	0.02	0.02	0.05	0.02

	Temperature [°C]						
$\gamma_{at Break}$ [-]	-20	-10	0	10	20	30	40
Mean	0.07	0.13	0.08	0.11	0.24	0.19	0.12
S.D.	0.02	0.03	0.02	0.02	0.07	0.05	0.02

10.2.3 Critical values ($D_{critical}$) for discordance test, acc. to [59]

n	Level of significance α		n	Level of significance α	
	0.01	0.05		0.01	0.05
3	1.155	1.153	27	3.049	2.698
4	1.492	1.463	28	3.068	2.714
5	1.749	1.672	29	3.085	2.73
6	1.944	1.822	30	3.103	2.745
7	2.097	1.938			
8	2.221	2.032	31	3.119	2.759
9	2.323	2.11	32	3.135	2.773
10	2.410	2.176	33	3.150	2.786
			34	3.164	2.799
11	2.485	2.234	35	3.178	2.811
12	2.550	2.285	36	3.191	2.823
13	2.607	2.331	37	3.204	2.835
14	2.659	2.371	38	3.216	2.846
15	2.705	2.409	39	3.228	2.857
16	2.747	2.443	40	3.240	2.866
17	2.785	2.475			
18	2.821	2.504	41	3.251	2.877
19	2.854	2.532	42	3.261	2.887
20	2.884	2.557	43	3.271	2.896
			44	3.282	2.905
21	2.912	2.58	45	3.292	2.914
22	2.939	2.603	46	3.302	2.923
23	2.963	2.624	47	3.310	2.931
24	2.987	2.644	48	3.319	2.94
25	3.009	2.663	49	3.329	2.948
26	3.029	2.681	50	3.336	2.956

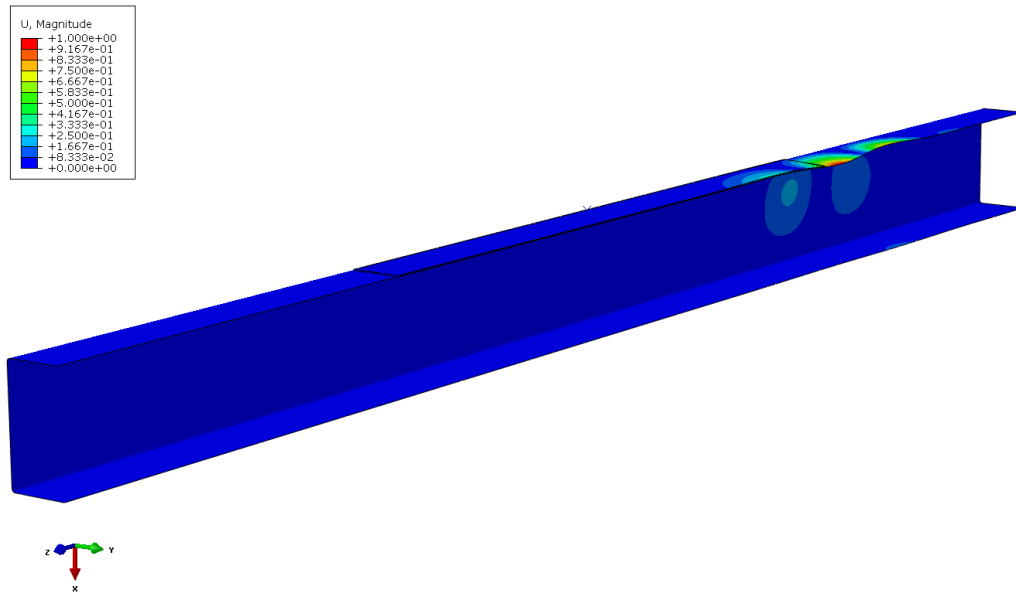
10.2.4 Critical values of Dixon's $r_{1,0}$ acc. to [61]Table I. Critical Values of Dixon's r_{10} (Q) Parameter As Applied to a Two-Tailed Test at Various Confidence Levels, Including the 95% Confidence Level^a

N^b	confidence level					
	80% ($\alpha = 0.20$)	90% ($\alpha = 0.10$)	95% ($\alpha = 0.05$)	96% ($\alpha = 0.04$)	98% ($\alpha = 0.02$)	99% ($\alpha = 0.01$)
3	0.886	0.941	0.970	0.976	0.988	0.994
4	0.679	0.765	0.829	0.846	0.889	0.926
5	0.557	0.642	0.710	0.729	0.780	0.821
6	0.482	0.560	0.625	0.644	0.698	0.740
7	0.434	0.507	0.568	0.586	0.637	0.680
8	0.399	0.468	0.526	0.543	0.590	0.634
9	0.370	0.437	0.493	0.510	0.555	0.598
10	0.349	0.412	0.466	0.483	0.527	0.568
11	0.332	0.392	0.444	0.460	0.502	0.542
12	0.318	0.376	0.426	0.441	0.482	0.522
13	0.305	0.361	0.410	0.425	0.465	0.503
14	0.294	0.349	0.396	0.411	0.450	0.488
15	0.285	0.338	0.384	0.399	0.438	0.475
16	0.277	0.329	0.374	0.388	0.426	0.463
17	0.269	0.320	0.365	0.379	0.416	0.452
18	0.263	0.313	0.356	0.370	0.407	0.442
19	0.258	0.306	0.349	0.363	0.398	0.433
20	0.252	0.300	0.342	0.356	0.391	0.425
21	0.247	0.295	0.337	0.350	0.384	0.418
22	0.242	0.290	0.331	0.344	0.378	0.411
23	0.238	0.285	0.326	0.338	0.372	0.404
24	0.234	0.281	0.321	0.333	0.367	0.399
25	0.230	0.277	0.317	0.329	0.362	0.393
29	0.227	0.273	0.312	0.324	0.357	0.388
27	0.224	0.269	0.308	0.320	0.353	0.384
28	0.220	0.266	0.305	0.316	0.349	0.380
29	0.218	0.263	0.301	0.312	0.345	0.376
30	0.215	0.260	0.298	0.309	0.341	0.372

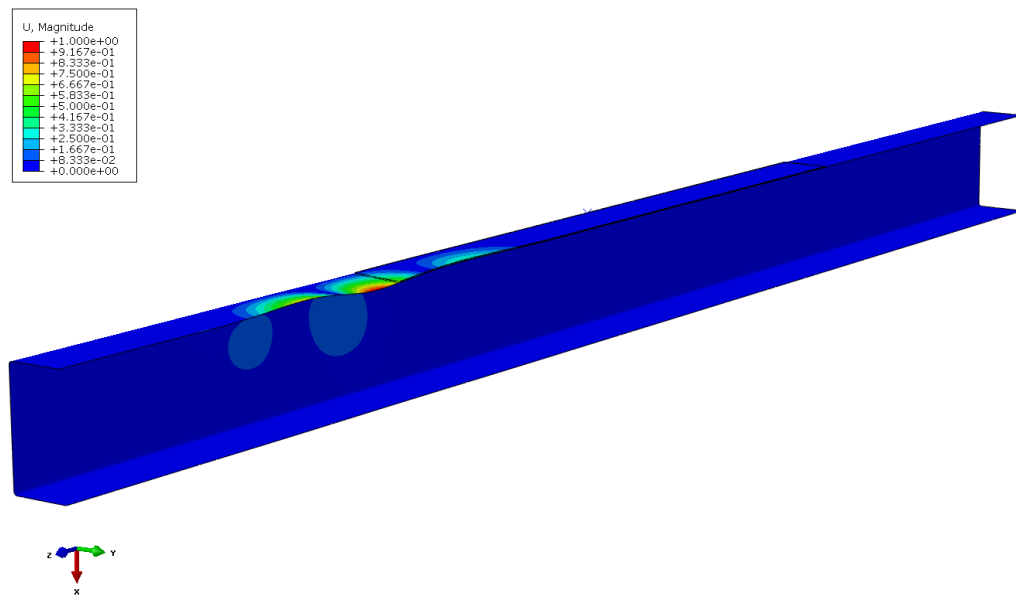
^aIn this and the other accompanying tables, the newly generated or corrected values are indicated in boldface. ^bSample size.

10.3 Appendix C

10.3.1 Chosen buckling modes obtained from buckling analysis of girders strengthened at the top flange AC-U and EP-U:



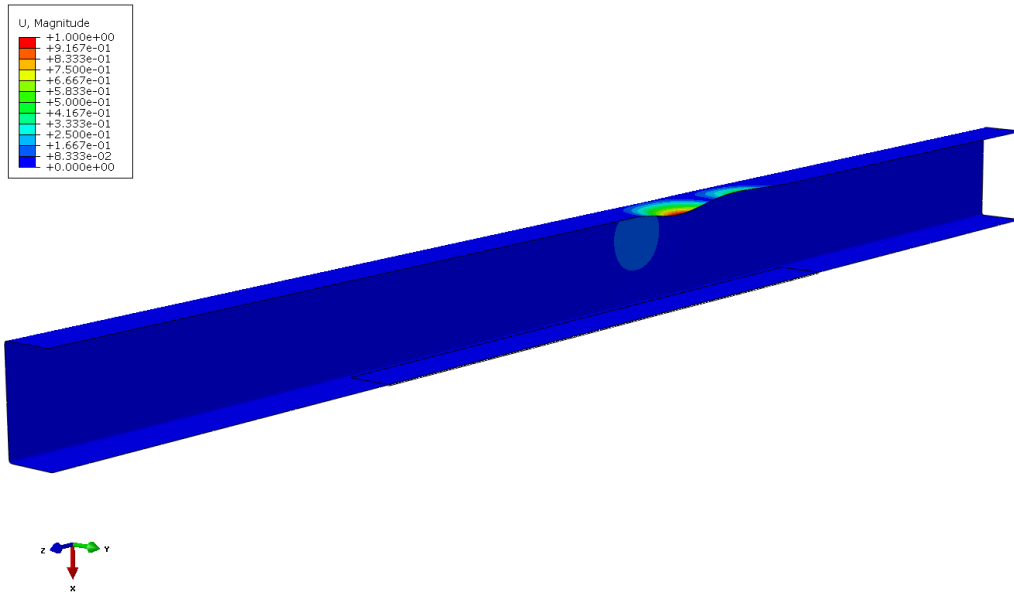
Second buckling mode



Sixteenth buckling mode

Figure 10.7: Buckling modes used for AC-U and EP-U girders

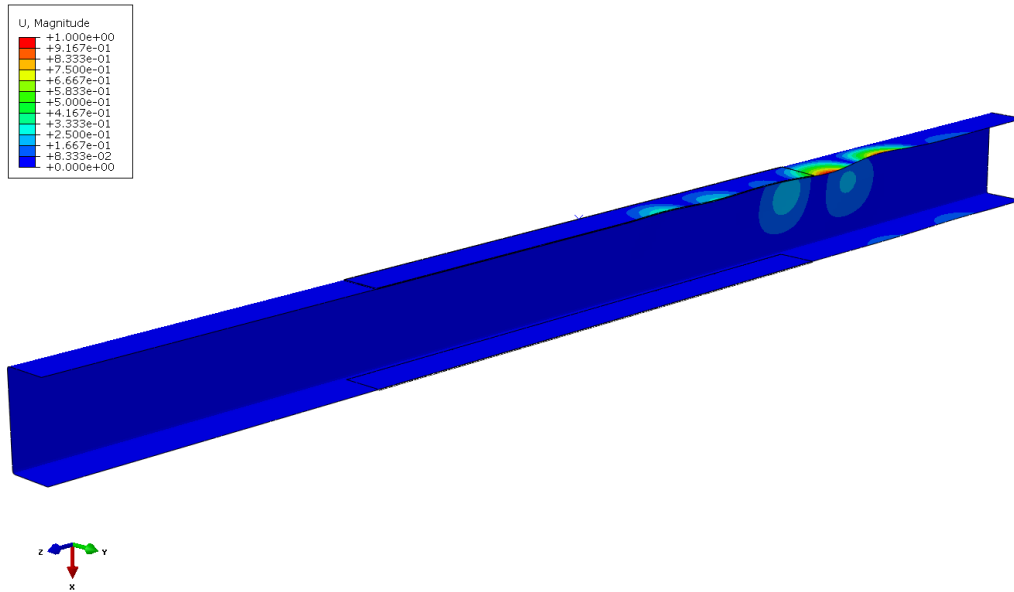
10.3.2 Chosen buckling modes obtained from buckling analysis of girders strengthened at the bottom flange AC-B and EP-B:



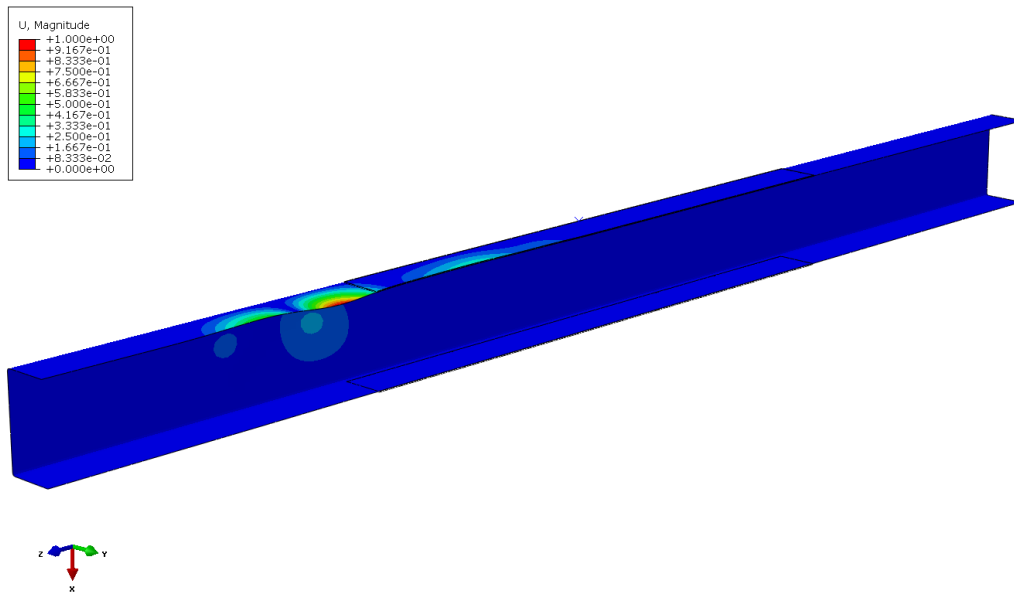
First buckling mode

Figure 10.8: Buckling mode used for AC-B and EP-B girders

10.3.3 Chosen buckling modes obtained from buckling analysis of girders strengthened at the top and bottom flanges AC-U-B and EP-U-B:



Third buckling mode



Twenty-fifth buckling mode

Figure 10.9: Buckling modes used for AC-U-B and EP-U-B girders